

**Research on the mechanisms of  
temperature-dependent sex determination in  
American alligator (*Alligator mississippiensis*)**

**Yatsu, Ryohei**

**SOKENDAI**

**(The Graduate University for Advanced Studies)**

**School of Life Science**

**Department of Basic Biology**

## Table of Contents

<b>I.</b>	<b>General Introduction</b>	<b>3</b>
<b>II.</b>	<b>Chapters</b>	<b>6</b>
	<b>1. TRPV4 associates environmental temperature and sex determination in the American alligator</b>	
	<b>2. RNA-seq analysis of the gonadal transcriptome during <i>Alligator mississippiensis</i> temperature-dependent sex determination and differentiation</b>	
<b>III.</b>	<b>General Discussion</b>	<b>101</b>
<b>IV.</b>	<b>References</b>	<b>105</b>
<b>V.</b>	<b>Acknowledgements</b>	<b>114</b>

## **General introduction**

Two main modes of sex determination exist among gonochoristic vertebrates; genotypic sex determination (GSD) and environmental sex determination (ESD).

Among the ESD systems, wide varieties of environmental factors have been displayed to influence sex determination. However, most prominent is the temperature-dependent sex determination (TSD), which is prevalent among the reptiles and is found in all studied crocodylians, tuataras, and in many of turtles and lizard species as well (Bull 1980, Kohno, Parrott et al. 2014). Although the main difference between the two lies in the initial activation trigger, temperature-dependent disruption of GSD and sex reversal can also take place in some lizard and fish species as well (Nakamura 2010). Incubation temperature of the developing embryo during specific temperatures sensitive period (TSP) is able to direct the individual's sexual fate, and initiate gonadal sex differentiation to either ovary or testis. Ever since the initial discovery of TSD, its mechanism of action has been questioned and although multiple theories have been suggested, it remains elusive.

Vertebrate gonadal sexual development follows a conserved pattern (Yao and Capel 2005), in which the onset of bipotential genital ridge formation during embryonic period is accompanied by sex determination period shortly after. During this period the aforementioned systems (GSD/ESD) are activated in various ways, and determine the gonadal sex of the individual by initiating specific gene cascade associated with ovary- or testis-differentiation. While the specific upstream ovarian- or testis-determining trigger may widely vary depending on species, the downstream genetic action and its

complex networks are fairly conserved in each cascade and utilize mostly similar gene sets, which result in similar sex-specific cell differentiation and regulation of sex steroid hormones (Sinclair, Smith et al. 2002). These gonadal transformations later influence the sex of the individual on the endocrine, behavioral and physiological level. Several sex-determining factors have been uniquely identified in many of the organisms with GSD. In contrast, the TSD mechanism still remains unclear and the identification of the initial activation mechanism in TSD system are being widely sought after.

Research for elucidation of TSD has undergone considerable history and progress since its first discovery. In 1966, while studying African lizards species, Charnier first documented TSD in reptiles (Charnier 1966), and which led to the foundation of modern vertebrate TSD studies. During the initial discovery, TSD was met with harsh skepticism and were suspected to be due to temperature-dependent differential mortality, which later were proven untrue and subsequent discovery and proof of TSD naturally taking place in other reptiles, such as turtles and crocodilians, further cemented validity of TSD in wildlife (Bull 1980, Ferguson and Joanen 1982). Single- and double-temperature shift experiments at various developmental stages established TSD temperature range, patterns and TSP in many of the species.

Although no clear model organism is established for reptiles, gonadogenesis has been extensively studied in only a very few reptile species, including the American alligator *Alligator mississippiensis*, and red-eared sliders *Trachemys scripta* (Smith and Joss 1993, Kohno, Parrott et al. 2014). Much of the early works focused on the sex steroid hormone effect upon the sex determination. Sex steroid hormone levels were



manipulated via administration of pharmacological reagents directly onto the eggshell, and the developing embryos successfully displayed altered sexual development (Crews 1994, Lance 2009). As more genes-related to sexual development was identified in model organisms, later studies focused on expressions of key genes related to sex differentiation, such as *SOX9*, *AMH*, and *CYP19A1*. Although these comparative studies were able to characterize the key gene expression movement in the downstream cascade, much of the upstream gene cascade still remained a mystery. Species that display TSD are commonly thought to lack heteromorphic sex chromosomes (Wang, Pascual-Anaya et al. 2013, Green, Braun et al. 2014). Instead, TSD is believed to be triggered by thermosensitive factor in the gonad, as turtle gonad organ culture experiments were able to demonstrate endogenous thermosensitivity (Moreno-Mendoza, Harley et al. 2001, Shoemaker-Daly, Jackson et al. 2010). These major findings provided the foundation for the current research presented, and now, using *Alligator mississippiensis* as experimental organism, further insights on TSD mechanisms have been achieved. In this thesis, several new findings in TSD research using *Alligator mississippiensis* is documented, including identification of potential thermosensitive trigger (Chapter 1) and comprehensive characterization of transcriptome during initial phases of sex determination (Chapter 2), and I provide a novel model for TSD mechanism based on obtained results.

## **Chapter 1.**

**TRPV4 associates environmental temperature and  
sex determination in the American alligator**

## Introduction

Highly diverse modes of sex determination have been observed among vertebrates. In most cases, sex is determined genetically (genotypic sex determination; GSD), which has been characterized by the presence of a key sex-determining gene. In contrast, in many reptiles including crocodylians, select chelonians and squamates, differential sexual outcomes have been identified under varying incubation temperatures during a critical temperature sensitive period (TSP) in the developing embryo (temperature-dependent sex determination; TSD) (Charnier 1966, Bull 1980, Rhen and Schroeder 2010). As an alternative to the GSD system, in which the heritable traits dictate subsequent gonadal differentiation, all species studied to date that exhibit TSD appear to lack sexually heteromorphic chromosomes (Wang, Pascual-Anaya et al. 2013, Green, Braun et al. 2014), and sexual development is assumed to be initiated mostly by environmental cues, independent of the individual's genetic background. However, genetic researches in reptiles are particularly hindered by lack of available genetic manipulation techniques, compared to other vertebrate species, and much of the sex determination mechanism in this pivotal vertebrate clade is yet to be understood.

American alligators, *Alligator mississippiensis*, display TSD, and the developing embryo detects a thermal stimulus that apparently directs the sexual fate of the bipotential gonad; this critical range of incubation temperatures is shared among all other crocodylians studied to date (Ferguson and Joanen 1982, Lang and Andrews 1994, Deeming 2004). Eggs incubated at a constant temperature of 33°C yields 100% male offspring, whereas incubation temperatures below 30°C lead to female biased offspring sex ratio during TSP (Ferguson stages 21 to 24) (Ferguson 1985). Downstream sexual differentiation processes in alligators follows a fairly similar pattern often shared among

vertebrates. Male producing temperatures (MPT) facilitates the medullary supporting cells to enlarge and proliferate, which in turn initiates their arrangement into distinct seminiferous cords by hatching (stage 27), and eventual testicular morphogenesis (Smith and Joss 1993). Dynamic anti-Müllerian hormone (*AMH*) upregulation and ensuing SRY-box 9 (*SOX9*) upregulation are observed during the sex determination phase (Urushitani, Katsu et al. 2011). At female producing temperatures (FPT), however, primordial germ cell proliferation occurs in the thickened cortex while the medulla undergoes extensive fragmentation (Smith and Joss 1993, Moore, Uribe-Aranzábal et al. 2008). By developmental stage 27, irreversible female commitment occurs with the eventual onset of estradiol-17 $\beta$  synthesis by aromatase (*CYP19A1*), thus completing ovarian morphogenesis (Moore, Uribe-Aranzábal et al. 2008).

However, it remains elusive how incubation temperature during the TSP triggers TSD and the subsequent differentiation cascade. Transformation of the initial environmental temperature signal to a biochemical signaling in TSD is not understood in any species, including species with temperature-dependent sex reversal (Nakamura 2010). Isolated gonads from a TSD reptile, *Trachemys scripta*, have been demonstrated to be directly receptive to thermal stimuli, suggesting that the initial reception of environmental cues can be triggered through an endogenous sensory mechanism (Shoemaker-Daly, Jackson et al. 2010). This mechanism hypothesized to be shared among TSD reptiles, including in the alligator as well.

Various mechanisms of thermal detection have been reported in the past, these include protein conformational changes, structural shifts in nucleic acid, and membrane property changes. In eukaryotes especially, several multi-pass

transmembrane ion channels have been the focus for thermal sensing (Cho, Yang et al. 2012, Sengupta and Garrity 2013), most prominent of which is the transient receptor potential (TRP) cation channel superfamily. The channels in this superfamily have been the most extensively characterized among vertebrates. The TRP channels in this superfamily mostly function as environmental sensors primarily through  $\text{Ca}^{2+}$  signaling, uniquely activated by various internal or external cues including osmolarity, pH, pressure, and temperature (Gees, Owsianik et al. 2012). At present, 10 thermosensitive TRP channels have been identified in humans and rodents: TRPV1, TRPV2, TRPV3, TRPV4, TRPM2, TRPM3, TRPM4, TRPM5, TRPM8, and TRPA1. Many of the thermosensitive TRP channels possess well-defined ranges of activation as well as wide diversification in physiological and functional properties (Vay, Gu et al. 2012), and are an ideal candidate as potential thermosensor within TSD mechanism, particularly the TRPV4 since the mammalian TRPV4 channel is known to be activated by moderate heat (33-34°C) (Guler, Lee et al. 2002, Heller and O'Neil 2007).

Here, we report the involvement of *A. mississippiensis* TRPV4 (AmTRPV4) ortholog in temperature-dependent sex determination. Electrophysiological analysis reveals AmTRPV4 functions as a molecular thermal sensor at a threshold near the range observed in TSD for this species, and pharmacological manipulation of channel activity affects the sexual differentiation processes in spite of incubation temperature during development. This is the first demonstration of a link between a well-described thermo-sensory mechanism, TRP channel, and regulation of TSD, shedding light on the elusive TSD molecular mechanism.

## **Results**

### *Expression and cloning of AmTRPV4*

To examine the presence of thermosensitive TRP channels in the gonad during the sex determination period in the American alligator, expression for orthologs of the mammalian thermosensitive TRP channels was screened at the onset of TSP and sex determination (Ferguson stage 21) using RT-PCR. Gene expression was limited to 5 TRP ion channels: *TRPV2*, *TRPV4*, *TRPM3*, and faintly from *TRPA1* and *TRPM8* (Figure 1-1A). Of the 5 confirmed TRP channels expressed in the gonad, *TRPV4* expression was of particular interest due to ideal predicted activation temperature. Thus, AmTRPV4 was deemed noteworthy for further investigation. Quantitative RT-PCR analysis for *TRPV4* was conducted during various developmental stages; at the bipotential stage (stage 19), onset of TSP and sex determination (stage 21), end of TSP and onset of sexual differentiation (stage 24), and latent stages of sex differentiation (stage 27) at both MPT and FPT. The time series revealed a sexually dimorphic expression patterns in the gonad, with suppression at the FPT (Figure 1-1B). *AmTRPV4* expression was also examined in the chorioallantoic membrane, as well as in the epidermal tissues, and its expression was confirmed, although a sexually dimorphic pattern was not observed (Figure 1-2A and B).

AmTRPV4 clone (857 aa) was amplified, slightly shorter in comparison to other reported reptilian TRPV4 orthologs, and phylogenetic analysis showed the AmTRPV4 to be more closely related to birds and other reptilian TRPV4 orthologs, when compared to mammalian TRPV4s (Figure 1-3). An evolutionary comparison of various TRPV4 orthologs seemingly points toward overall sequence conservation among the higher vertebrates (Figure 1-4). Overall similarity in amino acid sequences were observed between alligator TRPV4 and mouse (*Mus musculus*; 86%), human

(*Homo sapiens*; 85%), chicken (*Gallus gallus*; 87%), lizard (*Takydromous tachydromoides*; 88%), and snake (*Elaphe quadrivirgata*; 88%) (Liedtke, Choe et al. 2000, Nagai, Saitoh et al. 2012, Saito and Tominaga 2014). Aside from the proline rich domain (PRD), major domains in the TRPV4 channel structure shared high amino acid sequence identity among higher vertebrate orthologs, and hence, we expected a similar temperature-induced channel activation pattern in AmTRPV4 as observed from mammalian TRPV4 channel activation.

#### *AmTRPV4 is a potential candidate in TSD initiation*

At present, very little of the TRPV4 channel thermosensitivity properties have been well characterized in non-mammalian vertebrate species, and hence, characterization of AmTRPV4 was essential before further investigation. Following AmTRPV4 isolation, ion channel functional properties and activation threshold against thermal stimulus were assessed using the *Xenopus laevis* oocyte expression system (Saito, Banzawa et al. 2014). Administration of mammalian TRPV4-specific agonist elicited a clear response in cRNA-injected oocytes, and not in negative control (water injected oocyte), indicating successful expression in the oocyte. Furthermore, thermal sensitivity was also confirmed and heat stimulation successfully elicited clear inward current (Figure 1-5A and B). *Xenopus* oocytes subjected to water (mock) injection showed no heat-induced current, suggesting specific heat activity by AmTRPV4. An Arrhenius plot analysis indicated an average temperature threshold as  $37.30 \pm 0.54^{\circ}\text{C}$  (n=17), revealing a warm temperature threshold (Figure 1-5C).

Chemical responsiveness to mammalian TRPV4-specific agonists and antagonist administration was examined. AmTRPV4-expressing oocytes displayed

current flow with perfusion of GSK1016790A, a potent TRPV4 specific agonist (Thorneloe, Sulpizio et al. 2008, Vincent and Duncton 2011), at a dose of 50 nM (Figure 1-5D). In addition, RN1734, a known TRPV4-specific antagonist (Vincent and Duncton 2011), was able to partially and reversibly inhibit AmTRPV4 activated by GSK1016790A (Figure 1-5E). Furthermore, RN1734 also was able to inhibit temperature-induced currents in AmTRPV4-expressing oocytes in a reversible manner (Figure 1-5F).

AmTRPV4 was next expressed in HEK293 cells and  $\text{Ca}^{2+}$  imaging experiments were performed to examine whether activation of AmTRPV4 is capable of increasing intracellular  $\text{Ca}^{2+}$  concentration ( $[\text{Ca}^{2+}]_i$ ).  $[\text{Ca}^{2+}]_i$  increased during a heat stimulation above room temperature, as well as after administration of GSK1016790A (Figure 1-5G). In contrast, mock-transfected HEK293 cells showed only faint responses to both stimuli (Figure 1-5H), suggesting that the  $\text{Ca}^{2+}$  influx was specifically mediated by the AmTRPV4 channel activation. These results confirmed the sensitivity of AmTRPV4 to warm temperatures, and its responses to chemicals (an agonist and antagonist) were found to be similar to that described for mammalian TRPV4.

#### *Inhibition of AmTRPV4 during sex determination alter male determination and differentiation-related gene expression*

Marked expression of AmTRPV4 in the gonad during TSP, as well as heat-dependent channel activation at a temperature proximate to temperature range involved with alligator TSD provide strong evidence for a possible role of AmTRPV4 in TSD. In order to assess the role of AmTRPV4 during TSD, the channel was evaluated via pharmacological manipulation. Alligator eggs were given a single



administration of the chemical agonist GSK1016790A or antagonist RN1734 *in ovo* at stage 19 (bipotential gonad stage), using two different concentrations (0.005 µg/g/egg, and 0.5 µg/g/egg). These doses should be considered as nominal, as we lack information concerning the chemicals' permeation of the eggshell and half-life *in vivo*. Also, by dosing AmTRPV4 agonist and antagonist to the whole embryo via *in ovo* exposure, we were able to observe potential full body effects following activation or inhibition of AmTRPV4, replicating an elevated or low thermal effect. The eggs were incubated under MPT (33.5°C) or FPT (30.0°C) conditions and subsequent effects were examined at stage 27 (stage prior to hatching), focusing on various sex differentiation related genes, and specifically on *AMH*, *SOX9*, and *CYP19A1* gonadal gene expression as sexual markers (Figure 1-6A, B and C, Figure 1-7A and B).

Quantitative RT-PCR analysis revealed that two genes (*AMH* and *SOX9*) related to testicular differentiation were significantly down-regulated by administration of the AmTRPV4 antagonist RN1734 at MPT conditions in a dose-dependent manner (Figure 1-6A and B). Recorded body weights of the embryos were similar among all experimental groups, and the differential expressions were not due to delayed embryonic development (Smith and Joss 1993) (Figure 1-8). Similarly, expression levels assessed by *in situ* hybridization on the differentiated gonads also reflected the results from quantitative RT-PCR, and the lowered gene expression level of *AMH* was confirmed (Figure 1-6D). Administration of an AmTRPV4 agonist, GSK1016790A, at FPT did not result in a significant change in gene expression levels based on quantitative RT-PCR, possibly due to sexually dimorphic *AmTRPV4* expression (reduced expression at female generating temperatures) as reported above (Figure 1-1B, 1-6A, B, and C). Interestingly, upon closer inspection, the immunohistochemistry

revealed an ectopic upregulation of *SOX9* in agonist-treated FPT gonads, indicating that AmTRPV4 activation initiated expression of one of the genes required for male sex differentiation (Figure 1-6E). It should be noted, however, that administration of GSK1016790A at the higher dosage induced high mortality; necropsy data indicated premature embryo death that occurred shortly after drug administration. Hence, only low dosage results were available for analysis of the TRPV4 agonist exposure group. In contrast to the genes primarily associated with testicular differentiation, expression levels for *CYP19A1* was unaffected regardless of altered AmTRPV4 channel activity with differing thermal environments (Figure 1-6C). As a result, due to a lack of significantly altered *CYP19A1* expression, feminization of RN1734-treated embryos incubated at MPT was very limited: that is, we were not able to induce a feminized gene expression pattern in the gonad following inhibition of AmTRPV4 suggesting that this channel is not effective in the ovarian pathway.

Histological analysis (Figure 1-9A and B) revealed that while there were instances of complete feminization following exposure to RN1734, over all both RN1734- and GSK10016790A-treated samples were histologically and morphologically similar to their respective control groups despite significantly lowered *AMH* and *SOX9* gene expression levels in the RN1734-treated groups. However, RN1734-treated groups displayed an increase in prominent Müllerian ducts in a dosage-dependent manner, consistent with lowered *AMH* expression (Figure 1-9A and D). In some of these individuals, the ducts showed remarkable signs of regression, namely the reduction in the mesosalpinx (Austin 1989). Although the AmTRPV4 targeted treatment did not yield statistically significant phenotypic changes, it did result in a rise of individuals

with an abnormal sexual phenotype, with both male-like (testis-like gonad) and female-like (developed Müllerian duct) characteristics.

In summary, manipulation of AmTRPV4 activity impeded induction of the testicular differentiation cascade on a molecular level, but had little effect on the ovarian differentiation cascade, suggesting that TRPV4 does not solely account for thermosensitive trigger mechanism in TSD, but rather, may be part of a larger, more complex mechanism in place.

## **Discussion**

Here, we demonstrate an active involvement of TRPV4 channel during TSD in *A. mississippiensis*, and its possible role for promoting male development in a temperature-dependent manner. This is the first experimental demonstration of a link between a well-described thermo-sensory mechanism, TRPV4 channel, and regulation of TSD. In many of the environmentally sex determination (ESD) models, it is widely accepted that a presence of an environmental sensor-like element is responsible for the initiation of sex determination cascade. Similarly, several candidate factors have been investigated in TSD species in the past, including epigenetic influences (Matsumoto, Buemio et al. 2013, Parrott, Kohno et al. 2014), heat shock proteins (Kohno, Katsu et al. 2010), cold inducible RNA binding protein (Kohno, Katsu et al. 2010, Rhen and Schroeder 2010), and enzymes related to endocrine signaling such as estrogenic (Lance 2009, Cruze, Kohno et al. 2012) and/or glucocorticoid (Hayashi, Kobira et al. 2010, Yamaguchi and Kitano 2012). However, no link between sex determination pathway and temperature sensation could be experimentally demonstrated through these factors

and they remained mostly speculations based on correlative data. Our findings serve as a first step toward shedding a new light on the underlying thermosensitive mechanism.

Our results indicate that while AmTRPV4 channel activity may significantly influence male gonadal sex determination pathway at a molecular level, it alone does not account for the initiation of gonadal sex determination mechanism, as evidenced by lack of significant gonadal sex reversal due to unaltered *CYP19A1* expression, and seemingly independent female gonad sex determination pathway. Rather, TRPV4 is expected to be a component of the much larger framework governing the initiation of TSD. Ambient temperature can broadly influence multiple targets at once and most likely several elements are involved in the TSD mechanism one way or the other, including the potential factors investigated previously. Furthermore, co-regulation of  $\text{Ca}^{2+}$  signaling by multiple TRP channels has been well described before (Cheng, Sun et al. 2010), and other TRP channels observed could also be involved. Although current study employs pharmacological manipulation as a first step to study AmTRPV4's role in TSD, more sophisticated methodology is desired in order to evaluate the relational extent between TRPV4 and TSD in the near future.

Our results also indicate that alligator TRPV4 channel activates at 37.3°C, higher than we had originally anticipated, that is, artificial incubation at a constant temperature of 35°C or higher have been associated with embryonic death in the past studies (Ferguson and Joanen 1982, Lang and Andrews 1994). In the wild however, we regularly recorded nest temperatures in that range from nests that produce viable hatchlings (Figure 1-10). We observed that nest temperature fluctuates daily and during incubation in natural alligator nest, and many nests exhibited elevated temperatures, suggesting thermal patterns during incubation may be critical as well.

Although mammalian TRPV4 activates at 27-34°C, AmTRPV4 showed activation at a relatively higher temperature, near 37°C, based on our results. Evolutionary shift in temperature sensitivity has been observed among thermosensitive TRP channel orthologs from various vertebrate species and would most likely account for the difference observed in AmTRPV4. How much of our results from the *Xenopus* oocyte *in vitro* experiment translates to the actual embryonic environment during TSP are up to debate. Although MPT (33.5°C) is relatively lower than supposed activation temperature, *in ovo* administration experiment showed that inhibiting AmTRPV4 activity was still able to induce significant differential gene expression. Activation temperatures of TRP channels have been reported to shift depending on the cellular environment (Heller and O'Neil 2007). In the case of TRPV4, membrane properties greatly influence thermal sensitivity (Heller and O'Neil 2007, Garcia-Elias, Mrkonjic et al. 2013), and a delicate difference in the membrane environment may account for the 4°C margin of difference in this case.

A relatively small degree of sexual dimorphism in *AmTRPV4* gene expression helps explain why the molecular mechanisms behind TSD are so difficult to identify; unlike GSD, in which dynamic sexually dimorphic gene expression (e.g., mammalian *Sry*, galline *DMRT1*) determines sexual fate, the TSD may not necessary be initiated by dimorphic gene expression alone, as implied from our results with TRPV4 channel activity in alligators. Overdependence on comparative analysis between TSD and GSD models may restrict further discoveries; an independent approach will be required for constructing TSD models in the future. It has been suggested that ‘cumulative discrepancy’ underlies TSD, as implied in many of the TSD reptiles (Quinn, Georges et

al. 2007), and activation of AmTRPV4 during the lengthy TSP may contribute to such cumulative mechanism.

Multiple functions have been attributed to the mammalian TRPV4, a polymodal  $\text{Ca}^{2+}$ -permeable channel, including cell-death induction, alteration of gene expression, channel trafficking, and protein interactions by careful maintenance of  $\text{Ca}^{2+}$  levels (Nilius and Voets 2013). This highly flexible and adaptable nature is suitable for regulating cell fate; TRPV4 plays a crucial role in various cellular differentiations, such as chondrocyte (Muramatsu, Wakabayashi et al. 2007), myofibroblast (Rahaman, Grove et al. 2014), osteoclast (Masuyama, Vriens et al. 2008), and keratinocyte (Sokabe, Fukumi-Tominaga et al. 2010). TRPV4-assisted steady influx of  $\text{Ca}^{2+}$  allows for  $\text{Ca}^{2+}$ /calmodulin (CaM) complex-mediated molecular cascades to take place, such as *Sox9* upregulation in chondrocyte differentiation (Muramatsu, Wakabayashi et al. 2007, Nilius and Voets 2013). Consistent with previous reports, AmTRPV4-mediated  $\text{Ca}^{2+}$  influx through channel activation was confirmed, and the positive relationship observed between AmTRPV4 channel activity and *SOX9* expression from our results resembled the regulatory relationship reported during chondrocyte differentiation. TRPV4's role in gonad morphogenesis is less studied, though  $\text{Ca}^{2+}$  influx is an essential component in mammalian male sex determination (Argentaro, Sim et al. 2003, Hanover, Love et al. 2009). Indeed, CaM is crucial for the nuclear import of SOX9 and its subsequent transcriptional activity in mammals, and the loss of a SOX9-CaM interaction is associated with autosomal sex reversal (SRA) disease in humans (Argentaro, Sim et al. 2003). Additionally, innate male biased sexual dimorphism in TRPV4 channel activity has been reported in several studies involving TRPV4-deficient mouse (Clark, Votta et

al. 2010, van der Eerden, Oei et al. 2013). Interestingly, van der Eerden *et al.* (2013) speculated TRPV4 as a male-specific regulator of osteal cell differentiation.

Crocodylians represent an interesting presence among the reptiles. *Alligator mississippiensis* is believed to display a type II TSD pattern (Lang and Andrews 1994, Deeming 2004), in which the embryo feminization is attained at both low and extreme high temperatures, although 100% male productions at incubation temperatures as high as 36°C have also been previously reported (Ferguson and Joanen 1982). Based on our results, this may even imply a presence of a secondary thermosensitive mechanism, though molecular data concerning high temperature female are scarce, and require more investigation before making further insights. While that, in and of itself, already indicates a complex TSD-triggering mechanism among crocodylians, their sex determination threshold temperature is also substantially higher than majority of TSD reptiles (Lang and Andrews 1994), and the sexual developmental pattern are distinct from other reptile species (e.g., *AMH* expression precedes *SOX9* during testis differentiation) (Western, Harry et al. 1999). Variation in the TSD pattern, as well as inconsistency in the gene expression patterns early on in the sex determination even among other TSD reptiles (Yao and Capel 2005, Shoemaker and Crews 2009, Valenzuela, Neuwald et al. 2013), questions the extent of homogeneity and diversity within TSD mechanisms and potential role of TRPV4 in TSD. Non-mammalian vertebrate TRP channels are only starting to be analyzed, including those in reptiles (Saito, Nakatsuka et al. 2012, Di-Poï and Milinkovitch 2013), and further insight is expected in the near future.

## **Materials and Methods**

### *Animals, tissue collection and chemicals*

Alligator eggs were collected at Lake Woodruff National Wildlife Refuge, Volusia County, FL, were approved by and under permits from the Florida Fish and Wildlife Conservation Commission and the U.S. Fish and Wildlife Service (Permit #: SPGS-10-44). Alligator eggs were collected in June of 2011 to 2013. All works involving alligators were approved by and was performed under the guidelines specified by the Institutional Animal Care and Use Committee at Medical University of South Carolina (Permit #: AR3036). Once the eggs were collected, they were transported to Hollings Marine Laboratory (Medical University of South Carolina; Charleston, SC, USA) where they were incubated in damp sphagnum moss.

Embryonic developmental stage of each clutch was determined using criteria described by Ferguson (1985) (Ferguson 1985). Until embryonic stage 19, the eggs were incubated under FPT (30.0°C), at which point they each underwent random treatments and were separated into two groups, incubated under MPT (33.5°C) or FPT (30.0°C). GSK1016790A, (Sigma-Aldrich, St. Louis, MO, USA) and RN1734 (Tocris Bioscience, Bristol, UK) were dissolved in ethanol for embryonic exposure experiment. 0.005, 0.5 µg/g egg of agonist (GSK1016790A) and antagonist (RN1734) were administered once at stage 19 *in ovo*. Ethanol was administrated as vehicle in control group. The alligator embryonic GAM (gonad adrenal mesonephros complex), chorioallantoic membrane, and epidermal tissues were sampled at stages 19, 21, 24 and 27, and subsequently preserved in either RNAlater (Life Technologies, Carlsbad, CA, USA) or 4% paraformaldehyde until further analysis.

### *Molecular cloning of AmTRPV4 and sequence analysis*



Total RNA was extracted from female neonatal gonad, using RNeasy kit (Qiagen, Valencia, CA, USA). Full coding region of the AmTRPV4 was determined by standard procedure using SmartRACE kit (Takara, Ohtsu, Japan), and finally full-length AmTRPV4 was cloned with KOD+ polymerase (Toyobo, Osaka, Japan). The amplified full-length AmTRPV4 cDNA product was then subcloned into pOX+ vector (Saito, Banzawa et al. 2014) for electrophysiological analysis. Primer information is reported in Table 1-1.

Multiple sequence alignment for vertebrate TRPV4 homologues was performed using the CLUSTAL W (Thompson, Higgins et al. 1994). Phylogenetic relationships of TRPV4 were then examined using TRPV4 amino acid sequences derived from GenBank/EMBL database. The TRPV4 genes and species used are summarized in Table 1-2. Based on TRPV4 conserved sites, which include the ankyrin repeat domains and transmembrane domains (652 residues in AmTRPV4), with all the alignment gap sites were eliminated, minimum-evolution methods (Rzhetsky and Nei 1993) was applied to construct an evolutionary tree, using MEGA 5 software (Tamura, Peterson et al. 2011). The statistical confidence was then computed by bootstrap method with 1000 replications.

### *Oocyte electrophysiology*

The alligator TRPV4 channel was expressed in the oocytes of the African clawed frog *Xenopus laevis*, and ionic currents were recorded using the two-electrode voltage-clamp method as described previously (Saito, Banzawa et al. 2014). cRNA of the full length AmTRPV4 channel clone inserted between *X. laevis*  $\beta$ -globin 5' and 3' UTR in the pOX+ vector was synthesized using mMessage mMachine kit (Life

Technologies) according to the manufacturer's protocol, and was injected into *Xenopus* oocytes (4, 10 ng/ $\mu$ l) and ionic currents were recorded 2-5 days post-injection using a heat perfusion system. ND96 solution, which consists of 96 mM NaCl, 2 mM KCl, 1.8 mM CaCl<sub>2</sub>, 1 mM MgCl<sub>2</sub>, and 5 mM 2-[4-(2-Hydroxyethyl)-1-piperazinyl]ethanesulfonic acid (HEPES), was used as bath solution after adjusted to pH 7.4. The oocytes were voltage-clamped at -60 mV. All chemicals used for assay were diluted into ND96 bath solution, and applied to the AmTRPV4 expressing oocytes through perfusion. Likewise, heated thermal stimulations were applied to the oocytes by heated ND96 bath solution perfusion. Temperature threshold for activation was determined by Arrhenius plot, using Origin software (OriginLab, Northhampton, MA, USA). All procedures involving the care and use of the frogs were approved by Institutional Animal Care and Use Committee of National Institutes of Natural Sciences, Japan.

#### *Ca<sup>2+</sup>-imaging experiments*

Alligator TRPV4 was expressed in HEK293 cells, and Ca<sup>2+</sup>-imaging experiments were performed using methods previously described (Saito, Banzawa et al. 2014). HEK293 was cotransfected with AmTRPV4 recombinant pcDNA3.1+ vector and DsRed containing pCMV vector using Effectene Transfection Reagent (QIAGEN) following manufacturer's protocol. The transfected cells were incubated at 33 °C and then used for Ca<sup>2+</sup>- imaging experiments after incubation lasting ~24 h. Fura-2 was loaded into cells by incubating at 33°C for 1h with fura-2 acetoxymethyl ester. During recording, the fura-2-loaded cells were placed in a recording chamber filled with bath solution (140 mM NaCl, 5 mM KCl, 10 mM HEPES, 2 mM MgCl<sub>2</sub>, 2 mM CaCl<sub>2</sub>, 10 mM glucose, pH 7.4). Heated bath solution was perfused for thermal stimulation. For

chemical stimulation, GSK1016790A (50 nM) or ionomycin (2.5  $\mu$ M) were dissolved in bath solution and perfused.  $[Ca^{2+}]_i$  in transfected cells were measured under light at 340 nm and 380 nm, while fluorescent signals at 500 nm were recorded and their ratios (F340/F380) were calculated. The cells expressing DsRed were used for analysis as AmTRPV4 expressing cells. For negative control experiments, HEK293 cells were cotransfected with pcDNA3.1 and DsRed containing pCMV vectors.

#### *Nest Temperature data*

One hundred and eighty TidbiT v2 programmable temperature data loggers (Onset Computer, Bourne, MA, USA) were deployed in 48 alligator nests during the 2010-2014 nesting seasons to determine actual nest temperatures within wild American alligator nests. The loggers were placed within the nest touching eggs at the bottom, middle and top of the nest throughout the incubation process. A fourth temperature logger was also placed on the outside of the nest hanging in the air above to collect ambient air temperature. The thermistors were programmed to record the temperature every five min and were picked up either when the nest hatched, or after 75 days of deployment time (whichever came first). Once retrieved, data from the thermistors were downloaded to examine temperature profiles throughout the incubation period as well as during the period of sexual determination.

For thermister deployment, a vertical 25 cm channel next to the nest chamber was dug out on one side of the eggs within the nest. A rebar or wooden stake with all of the thermistors tied to it was inserted into the thermistor chamber farthest away from the eggs as possible to keep the thermistors at the nest site during the removal of the neonates. Starting from the bottom of the eggs in the nest a thermister would be placed

touching the bottom egg, with the serial number and depth of placement noted on the data sheet. The nesting material would then be placed on that thermister until the middle of the egg chamber where the second thermister would be placed touching an egg. This process was replicated with the third and/or top thermister. The top of the nest was covered with the natural nesting material and left alone until thermistors were recovered. To verify temperature accuracy, the loggers were placed into an incubator with set temperature shifts to verify the accuracy of all loggers. The last calibration had variability within all of the sensors of 0.16 of a degree of true calibration. Out of the 48 nests in which thermistors were deployed, 32 nests hatched, 10 nests were dead, and 6 were depredated (3 hogs, 1 raccoon and 2 fire ants).

#### *Expression profiling and statistical methods*

Gonadal tissues were carefully dissected from the GAM samples stored in RNAlater. Total RNAs were then extracted from gonadal, chorioallantoic membrane, and epidermal tissues, using SV Total RNA Isolation System (Promega, Madison, WI, USA). Template cDNA was synthesized from purified total RNA with iScript cDNA synthesis kit (Bio-Rad, Hercules, CA, USA). Primers used for TRP expression profiling was validated by confirming TRP expression in various tissues with 35 PCR reaction cycles. Real-time quantitative PCR reactions were performed using ABI Prism 7000 (Life Technologies) using the SYBR-Green PCR core reagents kit (Life Technologies), in the presence of appropriate primers, with *RPL8* as a housekeeping gene. Primers used were constructed based on previously reported sequences (Mochizuki, Sokabe et al. 2009, Parrott, Kohno et al. 2014). Primer information is reported in Table 1-1. Each gene was assayed in triplicate samples with relative standard curve method under the

following conditions: 2 min at 50 °C and 10 min at 95 °C, followed by 40 two-temperature cycles (15 sec at 95 °C and 1 min at 60 °C). Data acquisition and analyses were performed by ABI Prism 7000 SDS software ver 1.1 (Life Technologies). The average individual gene expressions were normalized to each average *RPL8* mRNA expression level. The quantitative RT-PCR results are presented as mean  $\pm$  SEM. Two-way ANOVA was performed for comparisons among temperature responses at different developmental stages in TRPV4 channel expression profiling. Multigroup comparisons between MPT experimental groups were performed using one-way ANOVA, followed by stepwise Tukey-Kramer post hoc adjustments. Comparison between FPT experimental groups was performed using Student's *t*-test. Statistical analyses were performed using GraphPad Prism (Version 5.0b; GraphPad Software, Inc., San Diego, CA, USA) software. *P*-value lower than 0.05 was considered to be statistically significant.

### *Histological analysis*

After fixation of GAM tissues in 4% paraformaldehyde, they were dehydrated and embedded in paraffin. GAMs were cross-sectioned at 6  $\mu$ m, re-hydrated using reverse ethanol gradient, and stained with hematoxylin and eosin for standard HE staining. Morphological changes were assessed using Pearson's chi-square test of independence. For *in situ* hybridization analysis, Alligator *AMH* riboprobe, using design by Western *et al.* (1999), was hybridized *in situ* to sections following standard protocols using species-specific digoxigenin-labeled antisense riboprobes at 65°C. Primer information is reported in Table 1-1. For immunohistochemistry, sections of deparaffinized GAMs were washed twice in PBS, microwaved in citrate buffer for 10

min. Samples were then incubated with blocking solution consisting of 0.5% Boehringer Blocking reagent (Roche), 10% heat-inactivated fetal bovine serum (FBS), 3% bovine serum albumin (BSA), and 0.2% Triton-X-100 in PBS for 30 min. Sections were incubated with anti-SOX9 antibody (Chemicon AB5535) which was reportedly compatible with turtle SOX9 (Barske and Capel 2010) as primary antibody in fresh blocking solution overnight at 4 °C at 1:1000. The samples were then washed three times in fresh blocking solution (as described above, with the exception of using 1% FBS instead) for 30 min, and then blocked for an additional hour with anti-rabbit secondary antibody label Alexa Fluor 488 (Life Technologies) at 1:200 at room temperature. The DNA was stained with Hoechst at 1:1000.

### **Figure legends**

**Figure 1-1.** Developmental expression profile of American alligator TRP channels in gonad during sexual development. (A) The mRNA levels of various thermosensitive TRP channels were assessed in gonads at the onset of TSP (stage 21) incubated under MPT and FPT conditions. Gene expressions of 5 AmTRP ion channels (AmTRPV2, AmTRPV4, AmTRPA1, AmTRPM3, AmTRPM8) were observed in varying expression levels. (B) Quantitative RT-PCR analysis was performed for AmTRPV4 at various key sexual developmental stages including bipotential (stage 19; n=13), sex determination (stage 21; n=14, 14), sex differentiation (stage 24; n=14, 15), and pre-hatching (stage 27; n=14, 15) stages at both FPT and MPT temperature conditions respectively;  $\pm$  SEM. Temperature sensitive period is indicated in gray.

**Figure 1-2.** TRPV4 channels expression in chorioallantoic membrane and epidermal tissues during sexual development. Quantitative RT-PCR analysis was performed for AmTRPV4 at various key sexual developmental stages including bipotential (stage 19), sex determination (stage 21), sex differentiation (stage 24), and pre-hatching (stage 27) stages at both temperature conditions, in (A) chorioallantoic membrane tissue and (B) abdominal epidermal tissues;  $\pm$  SEM. Temperature sensitive period is indicated in gray.

**Figure 1-3.** Phylogenetic tree of vertebrate TRPV4. Phylogenetic relationship among TRPV4 amino acid sequences for selected higher vertebrate species is shown. Phylogenetic tree was constructed based on conservative domains including ankyrin repeat and transmembrane domain, using minimum evolution method with Jones-Taylor-Thornton model. Bootstrap value is indicated beside the respective branch (Bootstrap values below 70 percent not shown). Database accession numbers of genes used is tabulated in Table 1-2. Zebrafish TRPV4 was used as outgroup, and Western clawed frog TRPV4b, c, d, e, f is omitted for simplicity.

**Figure 1-4.** Vertebrate TRPV4 amino acid alignment and identity. (A) Alignment of TRPV4 amino acid sequences from various vertebrates TRPV4; overall similarity in amino acid sequences were observed between alligator TRPV4 and mouse (*Mus musculus*; 86%), human (*Homo sapiens*; 85%), chicken (*Gallus gallus*; 87%), lizard (*Takydromous tachydromoides*; 88%), and snake (*Elaphe quadrivirgata*; 88%) TRPV4. Major channel structures are indicated with a bar, including proline-rich domain (PRD), ankyrin repeat domain (ARD), transmembrane region (TM), pore loop (PL), TRP domain (TRP), and calmodulin binding domain (CaMBD). Numbers indicate amino

acid residue position. The alignment was created using ClustalW. (B) Schematic for the major functional structure, and amino acid identity (%) for each of the selected vertebrate TRPV4, in comparison to AmTRPV4.

**Figure 1-5.** AmTRPV4 is a thermosensitive TRP channel that activates near alligator TSD temperature range. (A) A representative trace of the current (upper) activated in response to corresponding changes in bath solution temperature (lower) in the *Xenopus* oocytes expressing AmTRPV4 using a two-electrode voltage-clamp method. (B) A representative temperature-response profile for AmTRPV4 activation by heat. (C) A representative Arrhenius plot for heat-induced AmTRPV4 activation. The average threshold for activation was  $37.30 \pm 0.54^\circ\text{C}$ ; n=17. (D) A representative trace of the AmTRPV4 current in the oocyte activated by a TRPV4 agonist (GSK1016790A indicated in a black bar); n=4. (E) A representative trace of AmTRPV4 current in the oocyte activated by administration of a specific TRPV4 agonist (GSK1016790A indicated by a black bar) and subsequently inhibited by TRPV4 specific antagonist (RN1734 indicated by a gray bar); n=4. (F) A representative current trace of AmTRPV4 expressing oocyte activated by heat stimulus and subsequently inhibited by a specific TRPV4 antagonist (RN1734 indicated by a gray bar); n=4. (G) A representative averaged changes of  $[\text{Ca}^{2+}]_i$  in AmTRPV4-expressing HEK293 cells (n= 75) under both heat and chemical stimulation.  $[\text{Ca}^{2+}]_i$  changes in AmTRPV4-expressing cells (indicated as an average trace  $\pm$  SE; left y-axis) were observed along with temperatures (indicated by open circle trace; right y-axis). Applications of a TRPV4 agonist (GSK1016790) and ionomycin are shown with a black and gray bars, respectively. (H) Representative  $[\text{Ca}^{2+}]_i$  and temperature changes in mock transfected HEK293 cells (n =36).



**Figure 1-6.** Pharmaceutical activation and inhibition of AmTRPV4 during sex determination alters male differentiation. Stage 19 embryos were administered AmTRPV4 antagonist RN1734 (0.5, 0.005  $\mu\text{g/g}$  egg) or agonist GSK1016790A (0.5, 0.005  $\mu\text{g/g}$  egg) *in ovo* and incubated under MPT and FPT conditions, respectively, until stage 27. (A-E) The mRNA levels of major sex differentiation genes, (A) *AMH*, (B) *SOX9*, and (C) *CYP19A1* in the gonad at stage 27 were examined using quantitative RT-PCR analysis for each treatment: MPT control (n=12), 0.005 RN (n=13), 0.5 RN (n=12), FPT control (n=13), 0.005 GSK (n=15). Asterisks indicate statistically significant change in expression;  $\pm$  SEM; \*  $P \leq 0.05$ ; \*\*  $P \leq 0.01$ . Markedly lower mRNA expression was observed for *AMH* and *SOX9*, both involved with male differentiation cascade. (D) *In situ* hybridization was performed on gonadal cross sections using *AMH* antisense riboprobe. White bar indicates 100  $\mu\text{m}$ . (E) Immunohistochemistry for *SOX9* and Hoechst was performed on gonad cross sections. White bar indicates 100  $\mu\text{m}$ .

**Figure 1-7.** Expression levels of major sexually differentiation genes, *DMRT1* and *FOXL2*. The mRNA levels of major genes related to sexual development, (A) Doublesex and mab-3 related transcription factor 1 (*DMRT1*), and (B) Forkhead box protein L2 (*FOXL2*), were also examined using quantitative RT-PCR analysis. Trend similar to dosage-dependent down regulation was observed for *DMRT1*, gene involved with male differentiation.

**Figure 1-8.** Comparison of embryo body weights. Embryonic body weight at the time of sampling (Ferguson stage 27) was recorded for all experimental groups. Treatment of RN1734, TRPV4 antagonist, or GSK1016790A, TRPV4 agonist, on the embryo at MPT and FPT, respectively, did not alter the final body weight, and the no delay in development rate was observed.

**Figure 1-9.** AmTRPV4 inhibition causes rise in Müllerian duct development in MPT. (A) Histological analysis of sexual development was performed. Cross-sections of HE stained gonad and Müllerian duct at stage 27 for FPT control (n=11), 0.005 GSK (n=15), MPT control (n=13), 0.005 RN (n=11), and 0.5 RN (n=11). Instances of ovarian development were observed in RN1734-treated groups. (B) Graph showing number of individuals with ovarian, testicular, or ambiguous morphology in each treatment groups. (C) Graph showing number of individuals with prominent Müllerian duct in each treatment groups. White bar indicates 100  $\mu$ m.

**Figure 1-10.** Representative alligator nest temperature data from the wild. The thermistors were placed within the nest touching eggs at the bottom, middle and top of the nest throughout the entire incubation process. Many nests exhibited elevated temperatures throughout the course of incubation, and a relatively hot nest temperature of 35°C or higher was regularly recorded, with viable hatchlings.

Figure 1-1

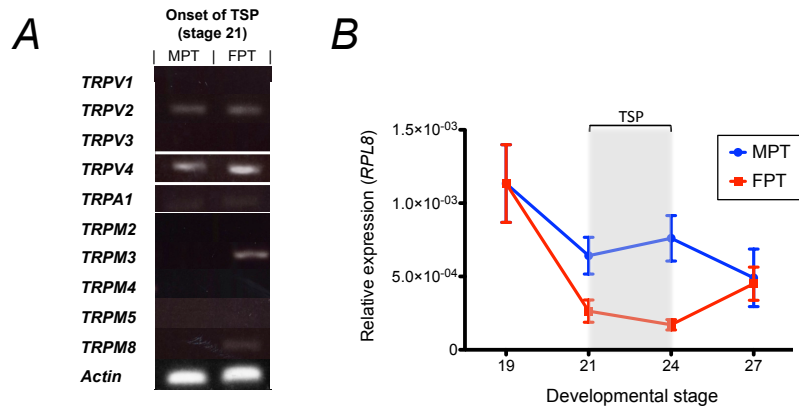
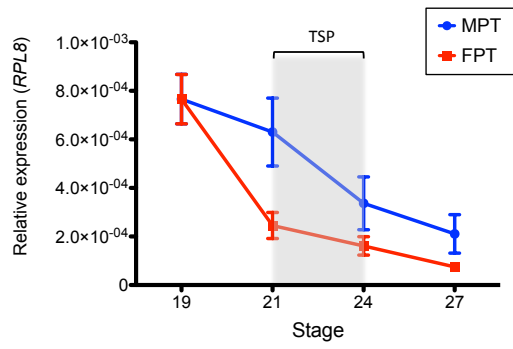


Figure 1-2

A



B

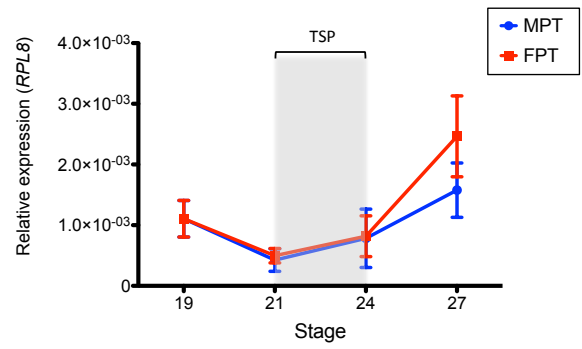


Figure 1-3

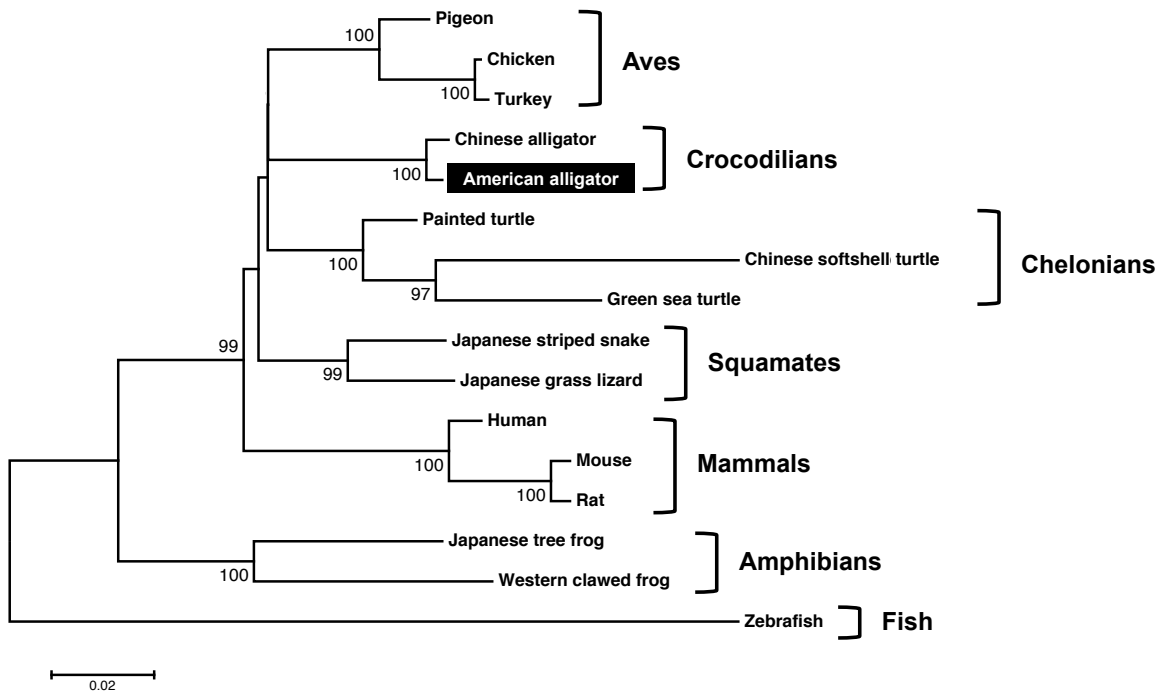


Figure 1-4

A

```

Alligator TRPV4 MTDPEEPQVQVGEPSGQGD-----DAPFLSSLANLFSEEG---VSPPEAARSTPASGDSKQNLRMKFGQAFKRGMPNMDLLESTIYESSVVPAPKAPMDSLDYGYTHHPSD 110
Chicken TRPV4 MADDEDP-----RDAGDVLGD-----DSFPLSSLANLFSEVEDT---PSPAEPRSRGPGAGDQKQNLRMKFGAFKRGPKMELLESTIYESSVVPAPKAPMDSLDYGYTHHPSD 105
Snake TRPV4 HANLEDAHAHSPSESTESSEEL-SPQNDSPFLSSLANLFENEDG---APAAEAARTPGAGDQKQNLRMKFGAFKRGVPMMDLLESTIYESSVVPKAPMDSLDYGYTHHPSD 116
Lizard TRPV4 HANLEDAHAHSPSESTESSEEL-SPQNDSPFLSSLANLFENEDG---APAAEAARTPGAGDQKQNLRMKFGAFKRGVPMMDLLESTIYESSVVPKAPMDSLDYGYTHHPSD 116
Human TRPV4 MADSSGPRAGGEVAELPGDESGTGGAEAPFLSSLANLFEGEDGSLSPADASR-PAGPGDGRPNLRMKFGQAFKRGVPMNIDLESTIYESSVVPKAPMDSLDYGYTHHPSD 119
Mouse TRPV4 MADPGDGPRAAGGEVAELPGDESGTGGAEAPFLSSLANLFEGEGSSLSVADASR-PAGPGDGRPNLRMKFGQAFKRGVPMNIDLESTIYESSVVPKAPMDSLDYGYTHHPSD 119

Alligator TRPV4 NKRRRKRKVEKQVQVGEPSGQGD-----DAPFLSSLANLFSEEG---VSPPEAARSTPASGDSKQNLRMKFGQAFKRGMPNMDLLESTIYESSVVPAPKAPMDSLDYGYTHHPSD 230
Chicken TRPV4 NKRRRKRKVEKQVQVGEPSGQGD-----DAPFLSSLANLFSEVEDT---PSPAEPRSRGPGAGDQKQNLRMKFGAFKRGPKMELLESTIYESSVVPAPKAPMDSLDYGYTHHPSD 225
Snake TRPV4 NKRRRKRKVEKQVQVGEPSGQGD-----DAPFLSSLANLFSEVEDT---PSPAEPRSRGPGAGDQKQNLRMKFGAFKRGPKMELLESTIYESSVVPAPKAPMDSLDYGYTHHPSD 236
Lizard TRPV4 NKRRRKRKVEKQVQVGEPSGQGD-----DAPFLSSLANLFSEVEDT---PSPAEPRSRGPGAGDQKQNLRMKFGAFKRGPKMELLESTIYESSVVPAPKAPMDSLDYGYTHHPSD 236
Human TRPV4 NKRRRKRKVEKQVQVGEPSGQGD-----DAPFLSSLANLFSEVEDT---PSPAEPRSRGPGAGDQKQNLRMKFGAFKRGPKMELLESTIYESSVVPAPKAPMDSLDYGYTHHPSD 239
Mouse TRPV4 NKRRRKRKVEKQVQVGEPSGQGD-----DAPFLSSLANLFSEVEDT---PSPAEPRSRGPGAGDQKQNLRMKFGAFKRGPKMELLESTIYESSVVPAPKAPMDSLDYGYTHHPSD 239

PRD ARD 1 ARD 2
Alligator TRPV4 TALHIAIERCKHYVELLVEKADVHAQARGRFQPKDEGGYFYFGLPLSLAECTNQPHIVYLAEANAKKADLRQDSRGNTVHALVAIADTRENTRKFTKMDLLIKCAKLPD 350
Chicken TRPV4 TALHIAIERCKHYVELLVEKADVHAQARGRFQPKDEGGYFYFGLPLSLAECTNQPHIVYLAEANAKKADLRQDSRGNTVHALVAIADTRENTRKFTKMDLLIKCAKLPD 345
Snake TRPV4 TALHIAIERCKHYVELLVEKADVHAQARGRFQPKDEGGYFYFGLPLSLAECTNQPHIVYLAEANAKKADLRQDSRGNTVHALVAIADTRENTRKFTKMDLLIKCAKLPD 356
Lizard TRPV4 TALHIAIERCKHYVELLVEKADVHAQARGRFQPKDEGGYFYFGLPLSLAECTNQPHIVYLAEANAKKADLRQDSRGNTVHALVAIADTRENTRKFTKMDLLIKCAKLPD 356
Human TRPV4 TALHIAIERCKHYVELLVEKADVHAQARGRFQPKDEGGYFYFGLPLSLAECTNQPHIVYLAEANAKKADLRQDSRGNTVHALVAIADTRENTRKFTKMDLLIKCAKLPD 359
Mouse TRPV4 TSLHIAIERCKHYVELLVEKADVHAQARGRFQPKDEGGYFYFGLPLSLAECTNQPHIVYLAEANAKKADLRQDSRGNTVHALVAIADTRENTRKFTKMDLLIKCAKLPD 359

ARD 3 ARD 4 ARD 5
Alligator TRPV4 TNLEALLNDGSLPLMAAKTKIGIQHIIIRREVDEARHLRKRFDWAYGPVYSSLDLSDTCGEVSVLELVVNSKMNREHMLAVEPINELLDKWRKFGAVSFYINVSYL 470
Chicken TRPV4 TNLEALLNDGSLPLMAAKTKIGIQHIIIRREVDEARHLRKRFDWAYGPVYSSLDLSDTCGEVSVLELVVNSKMNREHMLAVEPINELLDKWRKFGAVSFYINVSYL 465
Snake TRPV4 TNLEALLNDGSLPLMAAKTKIGIQHIIIRREVDEARHLRKRFDWAYGPVYSSLDLSDTCGEVSVLELVVNSKMNREHMLAVEPINELLDKWRKFGAVSFYINVSYL 476
Lizard TRPV4 TNLEALLNDGSLPLMAAKTKIGIQHIIIRREVDEARHLRKRFDWAYGPVYSSLDLSDTCGEVSVLELVVNSKMNREHMLAVEPINELLDKWRKFGAVSFYINVSYL 476
Human TRPV4 SNLEALLNDGSLPLMAAKTKIGIQHIIIRREVDEARHLRKRFDWAYGPVYSSLDLSDTCGEVSVLELVVNSKMNREHMLAVEPINELLDKWRKFGAVSFYINVSYL 479
Mouse TRPV4 SNLEALLNDGSLPLMAAKTKIGIQHIIIRREVDEARHLRKRFDWAYGPVYSSLDLSDTCGEVSVLELVVNSKMNREHMLAVEPINELLDKWRKFGAVSFYINVSYL 479

ARD 6 TM 1
Alligator TRPV4 CAMIIFTLIAYRPLEGTPPYPTTIDYLRAGEVITLFTGVLFNFKIDLFMKKCPGVNSFFIDGSPQLLYFIYSVLVITAGLVAGIEAYLAVMVFALVGMNLYFTRGLKLT 590
Chicken TRPV4 CAMIIFTLIAYRPLEGTPPYPTTIDYLRAGEVITLFTGVLFNFKIDLFMKKCPGVNSFFIDGSPQLLYFIYSVLVITAGLVAGIEAYLAVMVFALVGMNLYFTRGLKLT 585
Snake TRPV4 CAMIIFTLIAYRPLEGTPPYPTTIDYLRAGEVITLFTGVLFNFKIDLFMKKCPGVNSFFIDGSPQLLYFIYSVLVITAGLVAGIEAYLAVMVFALVGMNLYFTRGLKLT 596
Lizard TRPV4 CAMIIFTLIAYRPLEGTPPYPTTIDYLRAGEVITLFTGVLFNFKIDLFMKKCPGVNSFFIDGSPQLLYFIYSVLVITAGLVAGIEAYLAVMVFALVGMNLYFTRGLKLT 596
Human TRPV4 CAMIIFTLIAYRPLEGTPPYPTTIDYLRAGEVITLFTGVLFNFKIDLFMKKCPGVNSFFIDGSPQLLYFIYSVLVITAGLVAGIEAYLAVMVFALVGMNLYFTRGLKLT 599
Mouse TRPV4 CAMIIFTLIAYRPLEGTPPYPTTIDYLRAGEVITLFTGVLFNFKIDLFMKKCPGVNSFFIDGSPQLLYFIYSVLVITAGLVAGIEAYLAVMVFALVGMNLYFTRGLKLT 599

TM 2 TM 3 TM 4
Alligator TRPV4 GYSYIMIQIKLFDKLFRLVLLVLFMIGASALVSLNCPSESECSSEDSNCTLPYPSCRDSQTFSTFLDLFLKLTIGMDLMEISAKYGVFVILLVYIITLTVLLMLIALMG 706
Chicken TRPV4 GYSYIMIQIKLFDKLFRLVLLVLFMIGASALVSLNCPSESECSSEDSNCTLPYPSCRDSQTFSTFLDLFLKLTIGMDLMEISAKYGVFVILLVYIITLTVLLMLIALMG 705
Snake TRPV4 GYSYIMIQIKLFDKLFRLVLLVLFMIGASALVSLNCPSESECSSEDSNCTLPYPSCRDSQTFSTFLDLFLKLTIGMDLMEISAKYGVFVILLVYIITLTVLLMLIALMG 716
Lizard TRPV4 GYSYIMIQIKLFDKLFRLVLLVLFMIGASALVSLNCPSESECSSEDSNCTLPYPSCRDSQTFSTFLDLFLKLTIGMDLMEISAKYGVFVILLVYIITLTVLLMLIALMG 716
Human TRPV4 GYSYIMIQIKLFDKLFRLVLLVLFMIGASALVSLNCPSESECSSEDSNCTLPYPSCRDSQTFSTFLDLFLKLTIGMDLMEISAKYGVFVILLVYIITLTVLLMLIALMG 719
Mouse TRPV4 GYSYIMIQIKLFDKLFRLVLLVLFMIGASALVSLNCPSESECSSEDSNCTLPYPSCRDSQTFSTFLDLFLKLTIGMDLMEISAKYGVFVILLVYIITLTVLLMLIALMG 719

TM 5 PL TM 6
Alligator TRPV4 ETVGVSKESKIKWLQWATTILDIERSPFVFRKAFRSGEMVTVGKSDGTFDRRCVFRVDEVNMSHWNQGLIINEDPGKNETYQYGFSGHTVGLRRDRMSVVPVRVLELNKNSQPD 826
Chicken TRPV4 ETVGVSKESKIKWLQWATTILDIERSPFVFRKAFRSGEMVTVGKSDGTFDRRCVFRVDEVNMSHWNQGLIINEDPGKNETYQYGFSGHTVGLRRDRMSVVPVRVLELNKNSQPD 825
Snake TRPV4 ETVGVSKESKIKWLQWATTILDIERSPFVFRKAFRSGEMVTVGKSDGTFDRRCVFRVDEVNMSHWNQGLIINEDPGKNETYQYGFSGHTVGLRRDRMSVVPVRVLELNKNSQPD 836
Lizard TRPV4 ETVGVSKESKIKWLQWATTILDIERSPFVFRKAFRSGEMVTVGKSDGTFDRRCVFRVDEVNMSHWNQGLIINEDPGKNETYQYGFSGHTVGLRRDRMSVVPVRVLELNKNSQPD 836
Human TRPV4 ETVGVSKESKIKWLQWATTILDIERSPFVFRKAFRSGEMVTVGKSDGTFDRRCVFRVDEVNMSHWNQGLIINEDPGKNETYQYGFSGHTVGLRRDRMSVVPVRVLELNKNSQPD 839
Mouse TRPV4 ETVGVSKESKIKWLQWATTILDIERSPFVFRKAFRSGEMVTVGKSDGTFDRRCVFRVDEVNMSHWNQGLIINEDPGKNETYQYGFSGHTVGLRRDRMSVVPVRVLELNKNSQPD 839

TRP CaMBD
Alligator TRPV4 EVVVPLEGMGASQNDRRRFGH-LNGRKECHI* 857
Chicken TRPV4 EVVVPLEGMGASQNDRRRFGH-LNGRKECHI* 852
Snake TRPV4 EVVVPLEGMGASQNDRRRFGH-LNGRKECHI* 868
Lizard TRPV4 EVVVPLEGMGASQNDRRRFGH-LNGRKECHI* 868
Human TRPV4 EVVVPLEGMGASQNDRRRFGH-LNGRKECHI* 871
Mouse TRPV4 EVVVPLEGMGASQNDRRRFGH-LNGRKECHI* 871

```

B

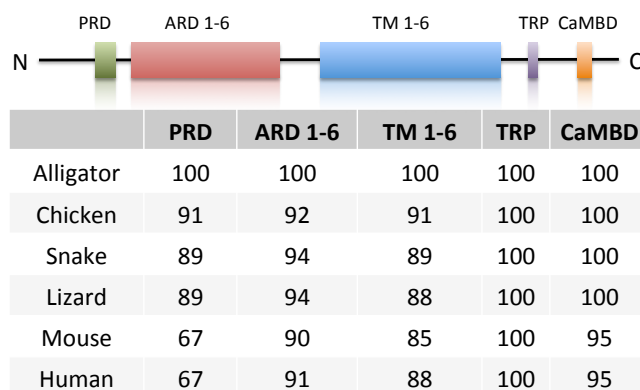


**Figure 1-5**

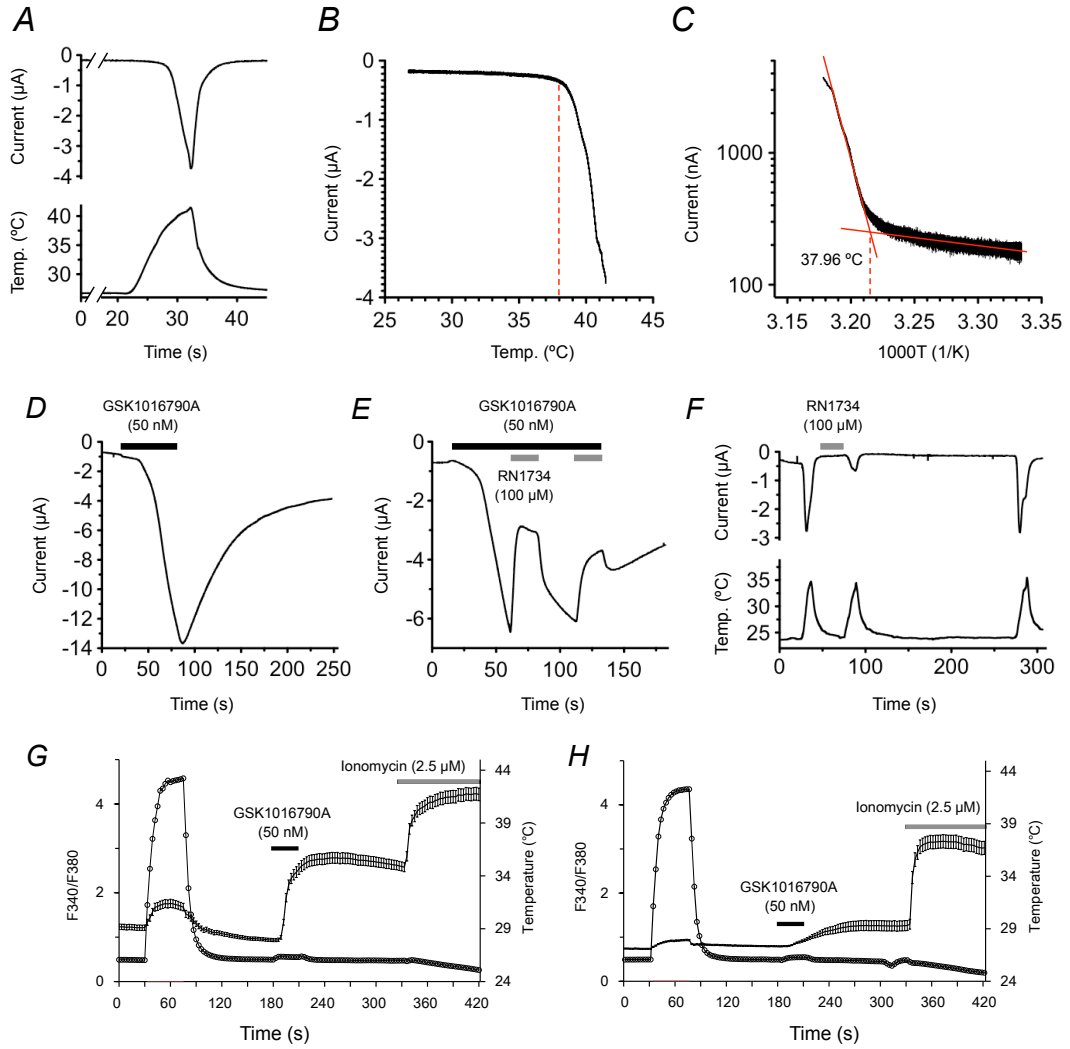
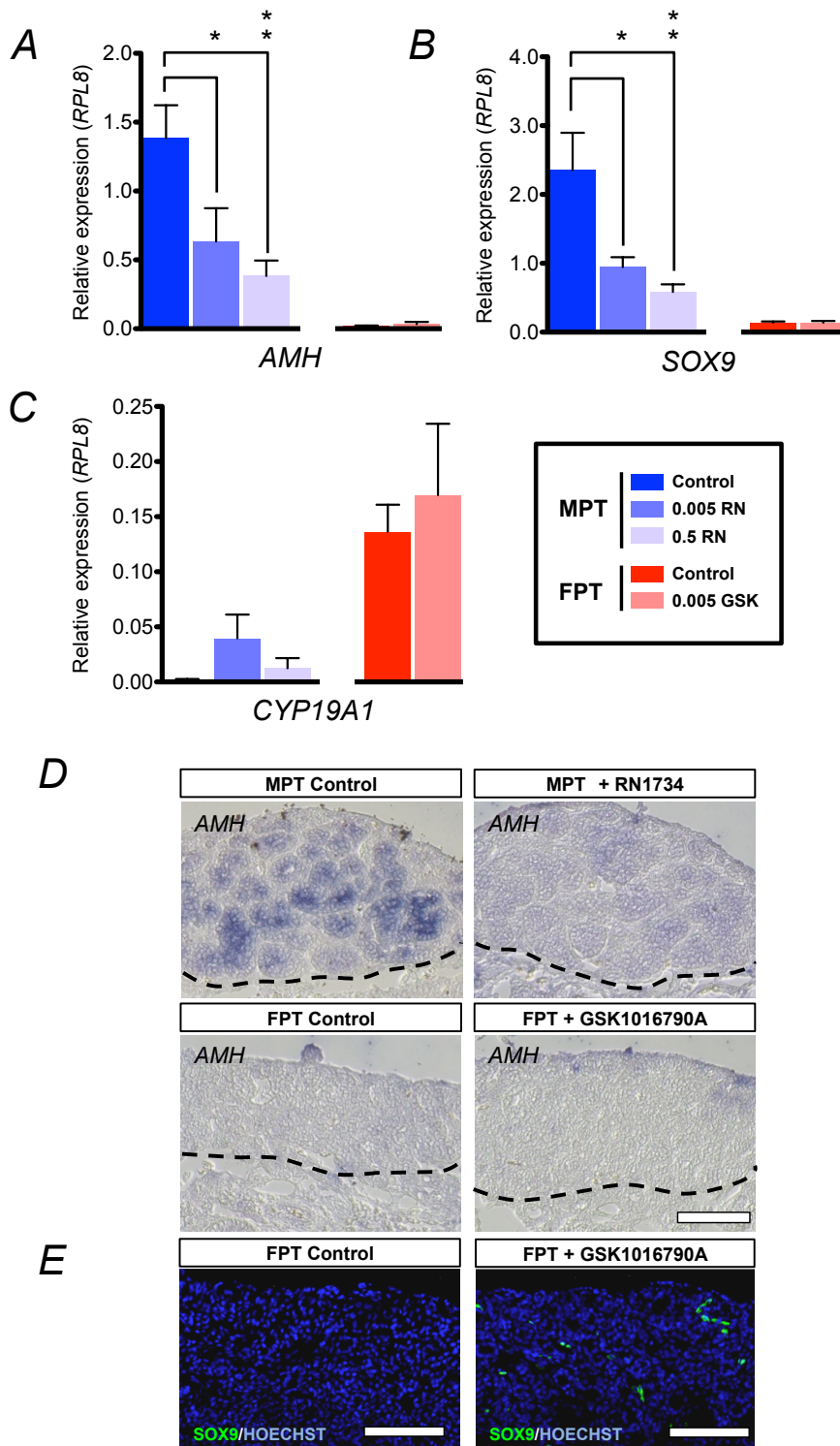
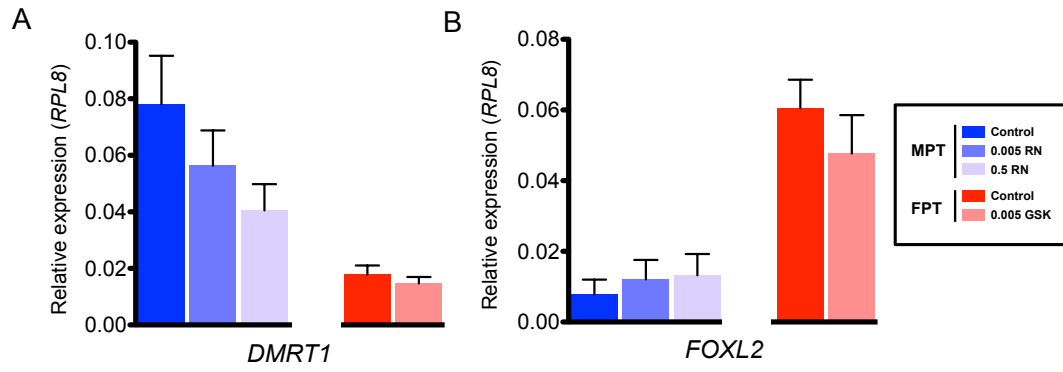


Figure 1-6





**Figure 1-7**



**Figure 1-8**

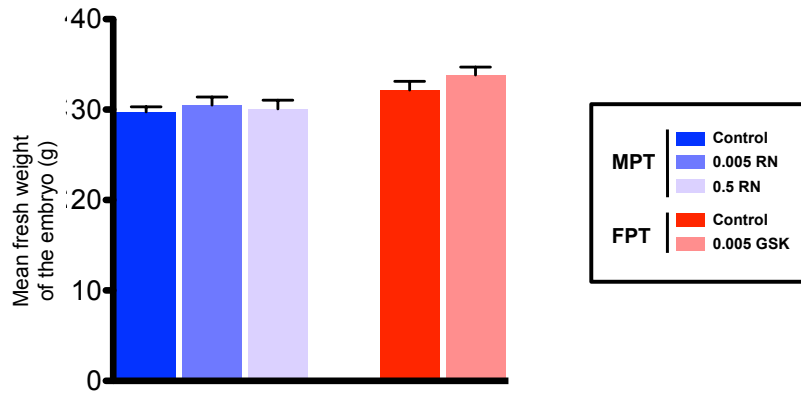


**Figure 1-9**

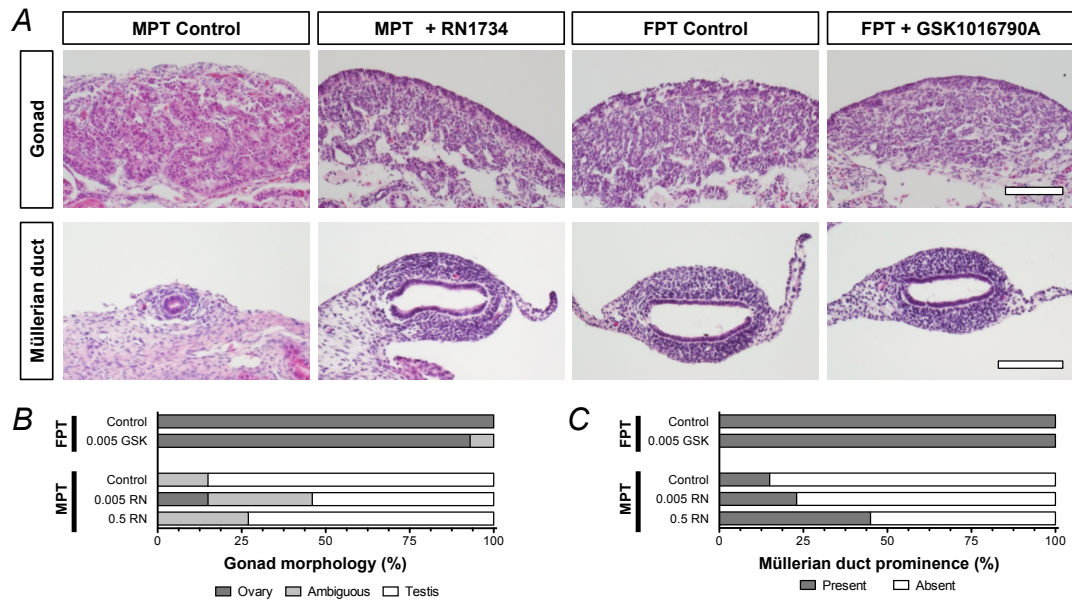
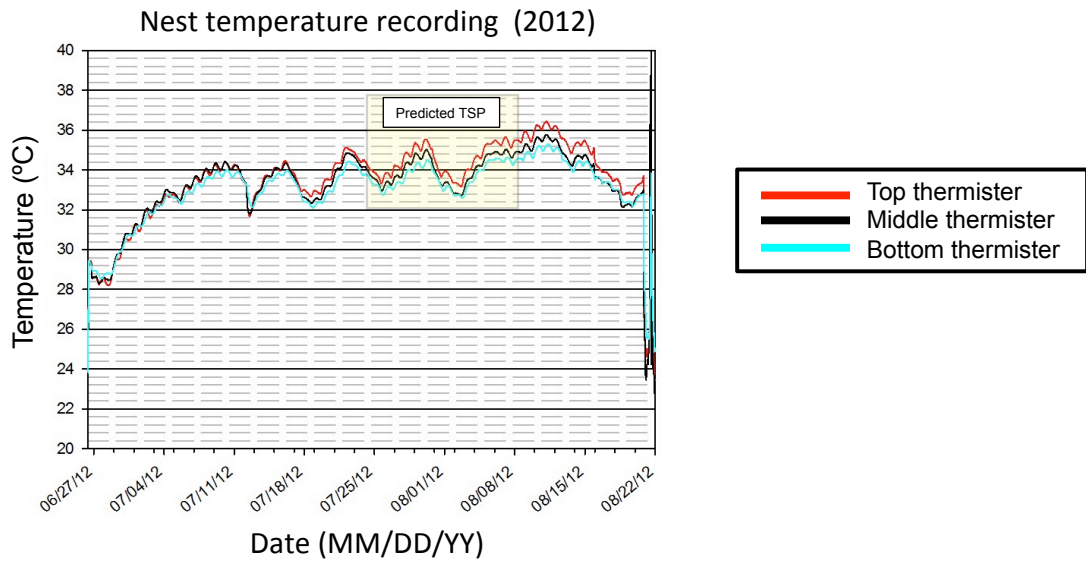


Figure 1-10



**Table 1-1**

Name	Sequence	
<b>TRPV4 cloning and isolation</b>		
aTRPV4-A:	5'-TTYTTYCARCCNAARGAYGARGGN-3'	
aTRPV4-B:	5'-GGNGGNTAYTTYTAYTTYGGNGAR-3'	
aTRPV4-C:	5'-ACYTGNCNACNGTYTCNCCCAT-3'	
aTRPV4-D:	5'-GCCCAYTGNARYTTCCADATRTGYTT-3'	
5'RACE-1	5'-TCCCGGGTGTGTCAGCGATGGCGACC-3'	
5'RACE-2	5'-AGCACGGTGTGCGCGGGAGTCCTGG-3'	
3'RACE-1	5'-GAGACGGTGGGGCAGGTGTCCAAGGAG-3'	
3'RACE-2	5'-ATCTGGAAGCTGCAGTGGGCCACCACC-3'	
Cloning	5'-TGTGTGCTGACCCATAACGCGTGCCAG-3'	5'-CCCGGGAGAGGAGAAACATGGTGCAAG-3'
<b>TRP subtype gene expression RT-PCR</b>		
TRPV1	5'-GAATCTGAAGTCACCGACGAGCA-3'	5'-AAAGATCCTCCTGCGATCATAGTACTTG-3'
TRPV2	5'-CTCAGTCTTTGCCTACCATTGTCCC-3'	5'-AGACCATCAACGGGGTGTAGTATTC-3'
TRPV3	5'-GCTTATGGGCAAGAAACCAAATCCA-3'	5'-CCCTCAGATACTGCCCTGAACAAATA-3'
TRPV4	5'-GAGTCCACCATCTACGAGTCTCC-3'	5'-CAGGTTTCAGCAGTGCCTTGGG-3'
TRPM2	5'-CTTTTCCGGGACACCTATGAGTTCTT-3'	5'-TCACGAACTCAGGCTTGTGGAAAT-3'
TRPM3	5'-GTCATTCCGCATGTTGGAGATGC-3'	5'-GTGCTTTTCCAGTTGTCTACGGAGT-3'
TRPM4	5'-TGCGACTCATCCACATCTTCGC-3'	5'-CGAGGAGGAAGACAACAAGGAGAAC-3'
TRPM5	5'-ATGATGCCTGCAAAGGTTTCTACCA-3'	5'-CGGTCTTCGCTGTTGTGATAACATTC-3'
TRPM8	5'-GAAACACACAAAGGAACTCCCTACTAATG-3'	5'-ACATTCTCCTCGGAAGTCTACTGA-3'
TRPA1	5'-ACAGAAAACGTATAGCAGTCCACTCC-3'	5'-CAATATGGCAGCTTCTTCTAAGTTTGT-3'
<b>Quantitative RT-PCR primer</b>		
<i>RPL8</i>	5'-GGTGTGGCTATGAATCCTGT-3'	5'-ACGACGAGCAGCAATAAGAC-3'
<i>TRPV4</i>	5'-TCACCTTCGTGCTGCTGCTT-3'	5'-AGATCTGCTTGCTCTCCTTG-3'
<i>SOX9</i>	5'-AGTACCCCATCTGCACAAC-3'	5'-CCCCTTCTTCCCGACTTT-3'
<i>AMH</i>	5'-AGCAGCTCAACCTCTCTGAGGA-3'	5'-TAGCAGAAAGCCAGAAGGTGC-3'
<i>CYP19A1</i>	5'-CAGCCAGTTGTGGACTTGATCA-3'	5'-TTGTCCCCTTTTTCACAGGATAG-3'
<i>DMRT1</i>	5'-AGCCCAACTCACTCAACAAG-3'	5'-GATGGAAGGAACATCCTGAA-3'
<i>FOXL2</i>	5'-CATCAGCAAGTCCCTTC-3'	5'-GGGCACCTTGATGAAACAC-3'
<b>In situ probe primer</b>		
<i>amh</i>	5'-GTGTTTCACCAGGATGACGCCGGTGCT-3'	5'-GGCTCCTCCGACTGCACCAGGCGCTCC-3'

**Table 1-2**

**Transient Receptor Potential Vanilloid Receptor subtype 4 homologs in various vertebrates.**

<b>Common name</b>	<b>Scientific name</b>	<b>Accession number</b>
American alligator	<i>Alligator mississippiensis</i>	LC12707
Chinese alligator	<i>Alligator sinensis</i>	XM_006015214.1
Chicken	<i>Gallus gallus</i>	NM_204692.1
Turkey	<i>Meleagris gallopavo</i>	XM_003210979.1
Pigeon	<i>Columba livia</i>	XM_005498200.1
Painted turtle	<i>Chrysemys picta</i>	XM_005298531.1
Chinese softshell turtle	<i>Pelodiscus sinensis</i>	XM_006130238.1
Green sea turtle	<i>Chelonia mydas</i>	XM_007058340.1
Japanese striped snake	<i>Elaphe quadrivirgata</i>	AB_666090.1
Japanese grass lizard	<i>Takydromus tachydromoides</i>	AB_666089.1
Human	<i>Homo sapiens</i>	NM_021625.4
Mouse	<i>Mus musculus</i>	NM_022017.3
Rat	<i>Rattus norvegicus</i>	NM_023970.1
Japanese treefrog	<i>Hyla japonica</i>	AB809362.1
Western clawed frog	<i>Xenopus tropicalis</i>	ENSXETT00000040300 (TRPV4a)
Zebrafish	<i>Danio rerio</i>	NM_001042730.1

## **Chapter 2.**

**RNA-seq analysis of the gonadal transcriptome during *Alligator mississippiensis*  
temperature-dependent sex determination and differentiation**

## Introduction

The intimate interaction between the environment and the organism can be profound; ambient environmental stimuli, such as temperature, are powerful catalysts for biomolecular movement and development that manifest as permanent biological changes. Such is the case for temperature-dependent sex determination (TSD), in which the sexual fates of organisms are seemingly determined not by genotypic factors, but by environmental temperature during a specific embryonic period known as the temperature sensitive period (TSP). In vertebrates, TSD has been observed primarily in reptiles, and the bipotential gonad itself is thought to be receptive to thermal signals (Bull 1980, Bull 1985, Shoemaker-Daly, Jackson et al. 2010). However, mechanistic details of this interaction between environmental temperature and TSD transcriptional profile cascade have remained unclear. While many past reports have focused on conserved genes with known function in sexual differentiation across vertebrates, such as *AMH*, *CYP19A1*, and *SOX9* (Morrish and Sinclair 2002, Valenzuela, Neuwald et al. 2013, Kohno, Parrott et al. 2014), very few other genes have been closely investigated, leading to a limited understanding of overall gene expression throughout TSD. Critical questions, such as how the developing gonad translates temperature cues into specific biochemical signals, remain unanswered.

Several hypotheses accounting for the molecular mechanism underlying TSD have been proposed. Steroid hormone involvement has long been suspected to play a role in TSD, as these molecules are known to play a critical role in sex differentiation in non-mammalian vertebrates (Lance 2009). Furthermore, glucocorticoid has been demonstrated to induce sex reversal in various vertebrate species including reptiles (Warner, Radder et al. 2009, Nakamura 2010), though how the syntheses of steroid



hormones are regulated by temperature remain unanswered. Another major mode of biological response to temperature is epigenetic modification; mounting evidence points toward an involvement of epigenetic modifications in sexual development (Piferrer 2013). Past studies reported sexually dimorphic DNA methylation patterns in promoter regions of major sexual development genes in a temperature specific manner, including TSD organisms (Navarro-Martin, Vinas et al. 2011, Matsumoto, Buemio et al. 2013, Parrott, Kohno et al. 2014). Other factors often associated with temperature stress, such as heat shock proteins (*HSPs*) and cold inducible RNA binding proteins (*CIRBPs*), have also been suggested to play a role in TSD (Kohno, Katsu et al. 2010, Rhen and Schroeder 2010). These varying responses to thermal influences at multiple levels ultimately result in a highly receptive regulatory network that underlies multitudes of cellular processes. Thus, the effect of temperature on the molecular environment can be profound and far-reaching, and consequently, there is crucial need to gain a comprehensive picture in order to fully understand the molecular mechanisms underlying TSD.

Crocodylians are thought to be entirely composed of TSD species (Lang and Andrews 1994), which includes the American alligator, *Alligator mississippiensis* (Ferguson and Joanen 1982). In *A. mississippiensis* TSD, the sexual fates of bipotential gonads are directed in a temperature-dependent manner to differentiate into either testes at a male producing temperature (MPT) at 33.5°C, or into ovaries at female producing temperature (FPT) at 30°C or 34.5°C (Ferguson and Joanen 1983, Lang and Andrews 1994). A recent report shows that sex determination in alligator embryo is thermosensitive as early as stage 15 (Ferguson developmental stage), approximately 18-20 days after oviposition (Ferguson 1985, McCoy, Parrott et al. 2015). Prior to this

report, however, the TSP was defined as occurring during stages 21-24, roughly between 31-46 days after oviposition. It is during this later period (stages 21-24) that temperature effects are reflected in the gonadal development, and many of the key sex determination/differentiation genes acquire sexually dimorphic expression patterns (Lang and Andrews 1994, Morrish and Sinclair 2002, Valenzuela, Neuwald et al. 2013, Kohno, Parrott et al. 2014, McCoy, Parrott et al. 2015). The timing of developmental stages and whole-body morphological growth is also greatly influenced by temperature during embryogenesis in the long term (Deeming and Ferguson 1989). Unfortunately, an effective method to perform gene manipulation is not currently feasible in alligators, and options are limited for detailed studies. This holds true with many of other reptiles and hence, much of the sex determination mechanisms studies in this evolutionary pivotal clade has been primarily resolved through comparative analyses with mammalian or avian sex determination mechanisms.

With rapidly emerging next generation sequencing technologies, global transcriptome studies such as high-throughput RNA sequencing (RNA-seq) is becoming readily available for non-model organisms (Smith, Bernatchez et al. 2013, Sun, Liu et al. 2013). In addition, a number of reptilian genomes have become publicly available (St John, Braun et al. 2012, Shaffer, Minx et al. 2013, Wan, Pan et al. 2013), and comprehensive annotated crocodylian genome assemblies have been released on the National Center for Biotechnology Information (NCBI) (Wan, Pan et al. 2013, Green, Braun et al. 2014). As one of the first TSD species with a published genome, the alligator *A. mississippiensis* is an ideal species for studying molecular signaling cascades and gene expression networks during sex determination in TSD species.

In this study, RNA-seq analyses were performed on developing alligator embryonic gonads incubated under MPT or FPT conditions and sampled at various time points to assess transcriptome changes related to each temperature condition during gonadal differentiation. We present an initial investigation into the sexual development cascade within the alligator TSD system, and provide descriptive data on expression patterns during early sexual development, with the emphasis on the identification of novel candidate genes that might account for alligator sex determination. To our knowledge, this is the first whole transcriptome analysis performed on a TSD organism. These results should allow for insights into the early progression of testis and ovarian fate, and provide a foundation for better understanding the genetic programs driving vertebrate TSD.

## **Results and discussion**

### *Experimental design and sequence assembly*

For sample preparation for transcriptome analyses, field collected *A. mississippiensis* eggs were transported to the laboratory and incubated under FPT (30°C) until Ferguson developmental stage 19 (Ferguson 1985), a period in which the gonads are still bipotential and morphologically indistinguishable. At stage 19, a subset of eggs was shifted to MPT (33.5°C) while the remaining eggs were maintained at FPT for the subsequent incubation period (Figure 2-1). Incubations at high FPT (34.5 °C) were not performed in the current study. Tissues comprising the developing gonad were carefully dissected at multiple time points after stage 19; at Day 0, 3, 6, and 12 post-stage 19 for analysis on sex determination cascade. The samples represent the bipotential gonad prior to incubation temperature shift (Day 0), post temperature shift (Day 3), and during

sexual fate commitment and differentiation (Day 6, 12). Although the embryos are incubated under different temperatures, the embryonic staging indicate that at least until Day 12 the embryos at respective time points are at within same developmental stage, and confounding variables by differential temperature effects are minimized (Kohno and Guillette 2013). In addition to Day 0-12 (sex determination phase), gonads from Day 18, 24, 30, and 36 post-stage 19 were also sampled (sex differentiation phase), although Day 36 was sampled in FPT only (Figure 2-2). Illumina HiSeq2500 sequencing produced a total of 375.2 million paired-end reads (2 x 101 bp) and were assessed for quality. The reads were mapped to the alligator genome assembly (allMis0.2), using the latest NCBI annotation available at the time (NCBI *Alligator mississippiensis* Annotation Release 100). The average mapping rates was 88.3%, among which 94.8% of the mapped reads were single hits, indicating an overall relatively good quality of reads.

#### *Transcriptome characterization of alligator gonadal development*

Differentially expressed gene (DEG) analysis was performed using Cuffdiff workflow (ver 2.2.1) (Trapnell, Williams et al. 2010, Trapnell, Roberts et al. 2012) to screen DEGs with false discovery rate (FDR) adjusted  $p$ -value  $<0.01$ . To evaluate differential expression across development for embryos incubated at the same temperature, multiple comparisons of the fold differences were conducted between temporally adjacent time points under each incubation condition (MPT/FPT). Development-dependent DEG analysis revealed extensive gene expression kinetics during the course of gonadal morphogenesis, and were profiled (Figure 2-3a, b; Figure 2-4a, Table 2-1). Overall, at MPT, Day 0-12 showed 788 DEGs, of which 158 (20.1%)

displayed expression movement at multiple occasions. At FPT, Day 0-12 showed 555 total DEGs, of which 113 DEGs (20.3%) also displayed expression movement at multiple occasions. Several noteworthy gene expression patterns were observed; under both MPT and FPT conditions, the transition from Day 3 to 6 accounted for the majority of DEGs, and nearly half of the total DEGs (460 and 250, respectively) were specific to Day 3-6. This timing corresponds to the onset of morphological differentiation in which the enlargement of presumptive Sertoli cells are observed in the medulla at MPT (Stage 21), and might be an indication of the activation of male and female cascade and gonadal fate commitment (Smith and Joss 1993).

Increases in the magnitude of sexually dimorphic gene expression profiles were then examined in detail. Sex-dependent DEG analysis between MPT and FPT samples were conducted at each corresponding time points in respective groups for intergroup comparisons (Figure 2-3c, Figure 2-4b, Table 2-2). Day 0-12 intersex comparisons revealed a total of 457 DEGs. MPT biased gene expression in each time point gradually increased with the progression of sexual development (68, 97, and 137 DEGs at Day 3, 6, and 12, respectively). However, similar to intrasexual development-dependent DEGs, a majority of sexually dimorphic gene expression was time point specific. Ten genes were consistently sexually dimorphic at all 3 time points (*AMH*, *EIF4A2*, *IFRD1*, *JARID2*, *KDM6B*, *KRT10*, *LOC102561378*, *LOC102574081*, *UCP2*).

#### *Identification of immediate temperature-responsive genes*

Cross-comparisons between Day 0 FPT embryos and Day 3 at MPT and FPT were performed to evaluate for the MPT-specific immediate temperature-responsive

gene expression (Figure 2-5). In order to assess the impact of the temperature shift between Day 0 FPT and Day 3 MPT on gene expression, as well as to account for the shared gene expression movement between Day 0-3 FPT and Day 0-3 MPT, significant male-specific differential expressions between Day 0 FPT and Day 3 MPT with resulting sexual dimorphism between Day 3 embryos were identified. The analysis generated 131 MPT specific DEGs (Figure 2-5a), of which 41 were also found to be sexually dimorphic between Day 3 MPT and Day 3 FPT as well (Figure 2-5b). Seventeen genes with significant upregulation at MPT (*UCP2*, *GALNT5*, *EIF4A2*, etc.) and 24 with significant downregulation (*KDM6B*, *LOC102562106*, *CSRP2*, etc.) were detected, and are likely candidates for immediate temperature-responsive genes (Table 3). While the current study focused upon FPT-to-MPT shift, a complementary MPT-to-FPT study would be ideal to fully identify potential upstream temperature-responsive genes in both male and female sex determination cascades.

Oxidative stress responsive-gene uncoupling protein-2 (*UCP2*) displayed the most prominent up-regulation, and suggests the presence of oxidative stress signaling in gonads incubated at MPT (Chan, Wu et al. 2009). Oxidative stress can be induced by number of factors including the thermosensitive cation channel *TRPV4*, which incidentally is also tightly co-localized with *UCP2* in mammals (Guler, Lee et al. 2002, Cohen, Brown et al. 2011, Bubolz, Mendoza et al. 2012). Interestingly, *TRPV4* has also recently been observed to potentially be involved with alligator TSD (Yatsu, Miyagawa et al. 2015) and may partially account for the immediate temperature-responsive DEGs identified in the current study. Interestingly, other DEGs identified in this study (e.g. *UPK3A*, *C/EBPA*, *ESPN*, etc.) are also co-expressed with *TRPV4* in other mammalian tissues, and may share a functional pathway (Homma, Nomiya et al. 2013, Ovrevik,

Refsnes et al. 2015). However, the relationship shared between these genes and *TRPV4* during the alligator gonadal sex determination is yet to be elucidated.

Gene ontology (GO) analysis was performed on the temperature-responsive transcripts. Interestingly, ‘Regulation of transcription, DNA-dependent’ was one of the highest biological process terms highlighted, and several transcriptional regulators were detected (Figure 2-5c). Most were downregulated by the temperature shift to MPT, such as *KDM6B* and *JARID2*. The roles of chromatin remodelers such as *Cbx2* and *Jmjc1* have been well documented in mammalian sex determination (Katoh-Fukui, Tsuchiya et al. 1998, Kuroki, Matoba et al. 2013), which prompt us to speculate that similar chromatin modification might occur during alligator TSD. Further analysis using Chromatin Immunoprecipitation (ChIP) techniques may help elucidate the chromatin state in alligator gonads during TSD. *WNT11*, which is expressed in mammalian granulosa cells, was also downregulated by shifts to MPT (Harwood et al., 2008). Transcription factor CCAAT/enhancer binding protein  $\alpha$  (*C/EBPA*) was upregulated by shifting incubation temperature to MPT. *C/EBPA* is observed to be active in a wide array of cell differentiation cascades, including mammalian germ cell sex differentiation (Ewen, Jackson et al. 2010). Because the current study did not distinguish between cell types, gene expression specific to somatic and primordial germ cell sex development is unclear. Vertebrate somatic and germ cell sex determination cascades are distinct. Thus, resolving the spatial expression patterns for these genes in alligators will further aid in characterizing their roles and functions during TSD.

*Characterization of known sexual development genes*

Although vertebrate upstream sex determination mechanisms differ by species, downstream sex differentiation genes appear to be highly conserved by comparison (Morrish and Sinclair 2002), and expression pattern of genes that have been well characterized in alligator sex differentiation were investigated (Figure 2-6). Overall, our RNA-seq data was in accordance with the previous reports, based mostly on studies utilizing RT-PCR and *in situ* hybridization techniques. Although, a few surprising discrepancies were revealed by the precise transcript level measurements afforded by RNA-seq analysis (Western, Harry et al. 1999, Western, Harry et al. 2000, Parrott, Kohno et al. 2014). For example, the timing of sexual dimorphism in *AMH* expression was earlier than previously thought, and was observed as early as Day 3. There was a significant upregulation of *AMH* under both MPT and FPT conditions between Day 0 and Day 3; however, the degree of upregulation was far greater at MPT (approximately a 7-fold increase) and continued upregulation was observed at later time points, whereas up-regulation in FPT diminished (Figure 2-6). Expression of *AD4BP/SFI*, a nuclear receptor involved in gonadogenesis and steroidogenic cell differentiation, was reportedly dynamic in alligator during and after sex determination, though depending on the literature, contradicting expression patterns were also reported (Western, Harry et al. 2000, Valenzuela, Neuwald et al. 2013). Here, our results indicate that *AD4BP/SFI* is initially fairly stable at both temperatures and only later shows an increase in expression, but does not show significant sexual dimorphism at any time point examined. Expression patterns of *FOXL2*, *FGF9*, *LHX9*, *WNT4*, and *RSPO1* were also characterized, last of which was not sexually dimorphic at any time point during Day 0-12. Species differences in the expression pattern of *RSPO1* during ovarian differentiation have been noted in the past (Smith, Shoemaker et al. 2008, Matsumoto,



Hannigan et al. 2014), and similar to the pattern observed during *Trachemys scripta* gonad sex differentiation (Matsumoto, Hannigan et al. 2014), there may be a brief female-biased expression between Day 12 and 18 in the alligator.

#### *Characterization of candidate sexual development genes*

Next, we investigated expression patterns that might provide insight into those genes with central roles in alligator sex determination. Cross-comparative analyses of development-dependent DEGs and sex-dependent DEGs were performed. Differentially expressed genes between sequential time points that also showed sexually dimorphic expression were considered to be potentially critical for gonadal sex determination. This criterion was employed to screen out significant gene expression movement in each MPT and FPT cascades that resulted in sexual dimorphism. With this criterion, 74 female and 172 male upregulated gene candidates (230 genes total) for sexual development were identified (Figure 2-7, Table 2-4), including *SOX9*, *AMH*, and *FOXL2*. Genes screened for Day 3 MPT were overall identical to the genes categorized as immediate temperature-responsive genes, with 4 additional genes identified (*AMH*, *FAP*, *COL8A2*, and *COL11A1*). The number of candidate genes increased greatly between Day 3 and Day 6 at MPT, corresponding with the expression of genes involved in testis determination, while only a few candidate genes were identified between Day 3 and Day 6 at FPT.

At MPT, candidate genes identified between Day 3 and Day 6 contained many of the genes with known roles in vertebrate male sexual development, and were profiled for the first time in alligators. These include upregulation of *DMRT3*, *TEX11*, in addition to previously reported *SOX9*. *PIWILI* and *TDK*, which are essential for

mammalian spermatogenesis (Saxe, Chen et al. 2013), were also observed to be up-regulated at MPT during this time. These observations provide details into the transcriptional pathway underlying male fate commitment in alligator, and also reveal genes with potentially crucial roles in somatic and germ cell sex determination/differentiation.

In both the MPT and FPT cascade, several DEG involved with steroid biosynthesis and metabolism were identified, including *HSD17B1*, *STAR*, and *HSD3B2*. Also, some genes expression patterns appeared to have reversed sexually dimorphism between alligator and model organisms. For example, *HEMGN*, a gene critical for male chicken testis development (Nakata, Ishiguro et al. 2013), was up-regulated at FPT. *ARX*, a gene involved in mammalian testis development (Kitamura, Yanazawa et al. 2002) was downregulated on Day 12 at MPT and remained so at later time points. The implications of these gene expression patterns in alligator sex determination are yet to be determined. Finally, 7 uncharacterized transcripts were found to be differentially expressed at various time points. Interestingly, six of these transcripts were identified as ncRNAs (e.g., *LOC102575456*, *LOC102563416*, *LOC102573435*), though their functions and roles during alligator sexual development are yet to be defined. The presence of these ncRNAs may have significant consequences on alligator sex determination as ncRNA (*MHM*) regulation of *DMRT1* plays a pivotal role in *Gallus gallus* sex determination (Teranishi, Shimada et al. 2001). These observations during the early stages of alligator sexual development highlight both conserved elements and divergences from sex determining mechanisms found in other vertebrates.

*Inference of regulatory network*

Gene ontology analyses of the candidate genes for sexual development recognized 25 genes with putative transcriptional regulatory functions, among which 9 were transcription factors (Table 2-5, Figure 2-8). The gene expression patterns were further characterized as long-term, short-term, or ambiguous depending on the duration of continuous sexual dimorphism during Day 0-12 and Day 18-36. Network modeling of genes from both male and female cascades were performed using the *NetGenerator* tool (Weber, Henkel et al. 2013) (see Materials and Methods) (Figure 2-9). The predicted expression patterns based on the modeling overall fit the interpolated expression pattern (Figure 2-9a,b), and more than half of the total modeled interactions satisfied the robustness test. The regulatory network model at MPT consisted of 33 edges, 12 robust putative gene-to-gene interactions, and 7 robust putative influences from MPT (Figure 2-9c). At FPT, 10 putative edges were constructed with 5 robust putative influences of FPT and 3 robust gene-to-gene interactions (Figure 2-9d). As expected, the temperature influences on the regulatory genes were predicted to be widespread in both conditions. In the MPT cascade, *SOX9*, and *ARX* were predicted to be responsible for regulating a number of genes while in the FPT cascade, *FOXL2* was predicted to regulate the phosphatase, *EYAI*, and *FABP4*. Currently, these inferred networks are based on gene expression correlation and generic gene interactions. *In vitro* techniques such as reporter assays will be useful to evaluate such interactions and provide greater insight into the functional relationships between genes in this putative network.

## **Conclusion**

Here, we present the first RNA-seq analysis of gonadal sex determination in a TSD organism. Our analysis clearly shows the dynamic influence of incubation temperature on gene expression, providing insights regarding the state of the gonad at MPT. Differential expression of *UCP2*, *WNT11*, and *KDM6B* highlight the presence of oxidative stress, regulation of Wnt signaling pathway, and chromatin modification on testis development. Furthermore, the global view of gene expression patterns in the gonad during sex determination identified candidate genes that may be integral for the alligator sex determination cascade. Use of network modeling allowed further prediction of the underlying TSD genetic pathway and provides a conceptual framework for empirical tests probing the function of these pathways. These findings, along with the gene expression profiles, will aid future researches on TSD species, and in turn contribute toward further understanding of the vertebrate sex determination mechanisms.

## **Methods**

### *Tissue collection and experimental design*

Alligator eggs were collected from five clutches in June of 2010 at Lake Woodruff National Wildlife Refuge, Volusia County, FL, USA under permits from Florida Fish and Wildlife Conservation Commission and the U.S. Fish and Wildlife Service (Permit #: SPGS-10-44). All work involving alligators was performed under the guidelines specified by the Institutional Animal Care and Use Committee at the Medical University of South Carolina (Permit #: 3069). After the eggs were collected from nests, they were transported to the Medical University of South Carolina (Charleston, SC, USA) and incubated under previously established conditions (Milnes, Bermudez et al.

2005, Urushitani, Katsu et al. 2011). Rate of embryonic development was predicted based on previous data, and staged according to criteria described by Ferguson (Ferguson 1985, Kohno and Guillette 2013). All eggs were incubated under FPT (30°C) conditions until embryonic stage 19, at which point eggs were split into two incubating temperatures, MPT (33.5°C) and FPT, and sampled over the course of 36 days. This design was adopted to account for any potential sexual dimorphism present prior to stage 19, and to differentiate between temperature-responsive and developmental genes during the alligator TSD mechanism. The alligator embryos were sampled at various time points starting at stage 19, and 3rd, 6th, 12th, 18th, 24th, and 30th days post-stage 19. Additionally, FPT embryos at 36 days post-stage 19 were also sampled.

#### *RNA extraction and Illumina library preparation*

Gonad-adrenal mesonephros (GAM) complex was first sampled from the alligator embryos and preserved in RNAlater (Ambion/Thermo Fisher Scientific, Waltham, MA, USA) at -20°C, and later, the gonadal tissue was further dissected from the GAM complex under a dissecting microscope. Total RNA from each individual gonad was extracted using ISOGEN reagent (Nippon Gene, Toyama, Japan) and was purified with Promega SV Total RNA Isolation system (Promega, Madison, WI, USA) according to the manufacturer's instructions. Qubit RNA assay kit (Life Technologies, Carlsbad, CA, USA), dsDNA HS assay kit (Life Technologies), and Agilent 2100 Bioanalyzer RNA pico kit assay (Agilent Technologies, Santa Clara, CA, USA) was used to assess concentration, DNA contamination, and overall quality. Triplicates were selected from each time point and temperature condition between Day 0 to Day 12 (total of 21 individuals), and single samples were selected from each time point and

temperature between Day 18 and Day 36 (total of 7 individuals). Our primary analyses were conducted on the initial phases of sexual determination/differentiation, while single samples taken from Day 18-36 were used to provide an overview for general gene expression kinetics in latter stages. 500 ng of total RNA from each gonad samples was then used for library preparation with Illumina TruSeq RNA sample preparation v2 kit (Illumina, San Diego, CA, USA), following the manufacturer's instructions. The libraries were then evaluated by using KAPA library quantification kit (Kapa Biosystems, Woburn, MA USA) and 2100 Bioanalyzer High Sensitivity DNA assay (Agilent Technologies). Finally, the multiplexed libraries were pooled into three groups, and sequenced using Illumina HiSeq2500 instrument (Illumina) at National Institute for Basic Biology in Okazaki, Japan. Sequencing was performed as 101 bp, paired-end reads in three lanes. The RNA-seq reads are available through DRA under the accession number: DRA004128-41.

#### *Differential gene expression analysis*

Initial FASTQ files were subjected to quality assessment using FastQC tool (<http://www.bioinformatics.bbsrc.ac.uk/projects/fastqc/>). Raw reads were then mapped and assembled using the Tuxedo pipeline (Tophat software: ver. 2.0.12; Cufflinks software: ver.2.2.1) (Trapnell, Pachter et al. 2009, Trapnell, Williams et al. 2010, Trapnell, Roberts et al. 2012). Individual paired-end sequence reads from each sample were aligned to publicly available alligator genome assembly (NCBI database; Assembly name: allMis0.2; Assembly accession: GCF\_000281125.1) with supplement gene model annotation (NCBI *Alligator mississippiensis* Annotation Release 100), and directed to report best possible alignment found with '-read-realign-edit-dist' option.

The mapping rates for each experimental group were assessed using Samtools ‘flagstat’ command (Li, Handsaker et al. 2009). Differential expression between each condition was tested following the Cufflinks workflow (ver. 2.2.1), and Cuffdiff software. The significance of initial differential expression was tested at significance level  $\alpha = 0.05$ , adjusted with allowed FDR at 0.05 following Benjamini-Hochberg correction. DEGs were further screened by FDR at 0.01.

### *Gene ontology mapping*

Contigs were blasted against the NCBI nr database using blastx program, with a minimum E-value score set to 1.0E-06. Successful blast hit results were then imported to Blast2GO program (ver. 3.1.3) where they were functionally mapped and annotated (Conesa, Gotz et al. 2005). Cut-off threshold was set to 55 and the GO level weighting set to 5. Additionally, InterPro IDs from InterProScan were merged to the annotation for further accuracy. ‘Make combined graph’ analysis was performed to score and evaluate the GO distribution in defined gene sets, and top 10 GO terms with highest node scores were selected.

### *Statistical analysis and network inference*

Basic statistical analysis and graph constructions were conducted using Microsoft Excel, R, and GraphPad Prism software (Version 5.0b; GraphPad Software, Inc., San Diego, CA, USA). Log<sub>2</sub> transformed FPKM+1 values were used for both the MA plot and hierarchical clustering heatmap. The NetGenerator tool (ver. 2.4) (Weber, Henkel et al. 2013) was used to perform network inference analysis with time-series log<sub>2</sub> fold change from select candidate DEGs (Table 2-5) under each incubation

temperature condition. NetGenerator offers modeling gene regulatory network from time series data, based on linear differential expression intensities with consideration of influences from external stepwise input signals. Network analysis and robustness analysis was conducted using modified protocol from Schulze et al (2015). In current analysis, input signal was defined as the environmental temperature (MPT or FPT). Prior-knowledge gene-to-gene coexpression data was based on *Mus musculus* (confidence score=0.25) as obtained from Genemania (<http://genemania.org/data/>) and was implemented in the analysis (Moggs, Tinwell et al. 2004, Gallardo, John et al. 2007, Hernandez-Novoa, Bishop et al. 2008, Lattin, Schroder et al. 2008, Thorrez, Van Deun et al. 2008, Schreiner, Bell et al. 2009)(Jacobs et al., 2010; Zapala et al., 2005; Akerblad et al., 2005). Several parameters were tested and ‘allowedError’ was adjusted at 0.01. Robustness of the network was tested using two methods. In the first test, the inference analysis was repeated 1000 times with artificial Gaussian noise (mean=0; standard deviation=0.05) distributed to the expression data to test for susceptibility to perturbations. In second test, the inference analysis was repeated 1000 times with 10% of the total prior knowledge randomly omitted to test for dependency of the interactions on prior knowledge. Interactions that were predicted more than 50% of the time in both tests were considered robust.

### **Figure legends**

**Figure 2-1.** Experimental design. Experimental design of the RNA-seq analysis is illustrated. Bipotential, sex fate commitment and sex differentiation period are indicated, with temperature sensitive period (TSP; indicated in light brown). The dotted line represents the end of the TSP. Eggs were first incubated under female producing



temperature (FPT; indicated in red) until just prior to the onset of sexual differentiation (stage 19; Day 0), which were then either shifted to male producing temperature (MPT; indicated in blue) or kept at FPT. Gonadal regions were sampled from individuals at several subsequent time points (Day 3, 6, 12) with corresponding approximate developmental stage (Ferguson) displayed in the bottom table. Day 0-12 represents the timing of sexual differentiation, and three individuals per temperature condition per time points are used.

**Figure 2-2.** Additional experimental design. Experimental design of the additional RNA-seq analysis during sex differentiation period is illustrated. The dotted line represents the close of the TSP. The eggs were first incubated at female producing temperature (FPT; indicated in red) until just prior to sexual differentiation (stage 19; Day 0), at which point groups of eggs were either shifted to male producing temperature (MPT; indicated in blue) or kept at FPT. Gonadal regions were sampled from individuals at several subsequent time points (Day 18, 24, 30, 36) with corresponding approximate developmental stage (Ferguson) displayed in the bottom table. Day 18-36 represents sex differentiation group, and one individual per temperature condition per time points are used.

**Figure 2-3.** Overlap of development-dependent and sex-dependent differentially expressed genes. Venn diagram of differentially expressed genes (DEGs) in (a) Day 0 to Day 12 MPT (indicated in blue) conditions and (b) Day 0 to Day 12 FPT (indicated in red) conditions based on genome mappings of Tophat. (c) Venn diagram for number of DEGs between Day 0 to Day 12 MPT and FPT conditions at respective time points,

based on genome mapping using Tophat. Number values in blue indicate the number of genes with MPT-biased expression, while values in red indicate the number of genes with FPT-biased expression. All DEGs were determined based on statistical significance ( $FDR < 0.01$ ) using Cuffdiff software. Further details are available in Table 2-1 and 2-2.

**Figure 2-4.** Development-dependent DEGs and Sex-dependent DEGs in alligator transcriptomic profiles. (a) MA plot, with gene expression values expressed as  $\log_2$ FPKM and fold change expressed as  $\text{Log}_2$ FC, is constructed using differential expression analysis between each time point (Day 0-3, Day 3-6, Day 6-12). (b) MA plot, with gene expression values expressed as  $\log_2$ FPKM and fold change expressed as  $\text{Log}_2$ FC, is constructed using differential expression analysis results between FPT and MPT ( $30^\circ\text{C}$  vs  $33.5^\circ\text{C}$ ) for Day 3 FPT vs Day 3 MPT, Day 6 FPT vs Day 6 MPT, and Day 12 FPT vs Day 12 MPT. For both MA plot, 20,181 genes, based on NCBI genome annotation, were examined for differential expression. Red dots indicate significantly up- or down-regulated genes at  $FDR < 0.01$ .

**Figure 2-5.** Candidate temperature-responsive differential gene expression.

(a) Venn diagrams show the number of DEGs between Day 0 and Day 3 incubated either under MPT (indicated in blue) or FPT (indicated in red). 131 genes (indicated in bold) were found to have MPT-specific gene expression movement, possibly in response to changes in incubation temperature. (b) 41 out of 131 genes were found to have been up- or down-regulated significantly enough to be sexually dimorphic. 17 genes displayed MPT-biased expression and 24 genes displayed FPT-biased expression.

Red, blue, and grey indicate FPT-, MPT- or non-bias, respectively. (c) Top 10 biological process gene ontology terms mapped to the candidate temperature-responsive genes with highest node score, based on Blast2GO program.

**Figure 2-6.** Expression profiles of major genes involved in sex differentiation.

Expression profiles of various major genes involved in gonadal sex determination in model organisms are displayed based on FPKM values from RNA-seq analysis under FPT conditions (indicated in red) and MPT conditions (indicated in blue). Predicted onset of sexual differentiation is indicated in orange background; \* FDR  $\leq 0.01$ .

**Figure 2-7.** Candidate potential critical genes central for sex determination. (a) Cross comparison between development- and sex-dependent DEGs (FDR < 0.01; Fig. 2) was performed among Day 0 to Day 12, and a total of 230 genes were identified as candidate genes for *A. mississippiensis* sex determination. Green and orange arrows indicate up- and down-regulation, respectively, with number of corresponding genes indicated. The majority of gene expression dynamics associated with development was observed to be MPT-specific. Further information is available in Table 4 (b) Hierarchical clustering analysis of sexual dimorphism (M-F log<sub>2</sub>FC) in the candidate genes at Day 3, 6, and 12. Red color indicates high *z*-score (female biased expression) while blue indicates a low *z*-score (male biased expression).

**Figure 2-8.** Expression profiles of candidate transcription factors involved in sex differentiation. Expression profiles of candidate transcription factors involved in gonadal sex determination are displayed based on FPKM values from RNA-seq analysis

under FPT conditions (indicated in red) and MPT conditions (indicated in blue).

Predicted onset of sexual differentiation is indicated in orange background; \* FDR  $\leq 0.01$ .

**Figure 2-9.** NetGenerator derived model prediction of MPT and FPT cascade.

(a-b) Interpolated expression (dotted line; dots indicate actual recorded fold change) and inferred patterns derived from the predicted NetGenerator model (solid line) of putative transcriptional regulatory genes over the course of sex differentiation at both (a) MPT and (b) FPT. (c-d) Inferred network model at both (c) MPT and (d) FPT. Robust (solid line) and non-robust (dotted line) predicted interactions are displayed as gene-gene interactions (black), and temperature-gene interactions (MPT:blue; FPT:red). Thickened lines indicate interaction with high robustness (80% or above). Following genes names were modified for inference network: LOC102562106 (*JARID2-1*), LOC102561337 (*JARID2-2*), LOC102569158 (*WNT11*), LOC102560544 (*EEF1A1*), LOC102577358 (*DMRT3*), LOC102573123 (*SOX9*), LOC102576325 (*PAK1*), LOC102559361 (*EDNRB*), LOC102563625 (*PDE2A*), and LOC102577040 (*FOXL2*)

Figure 2-1

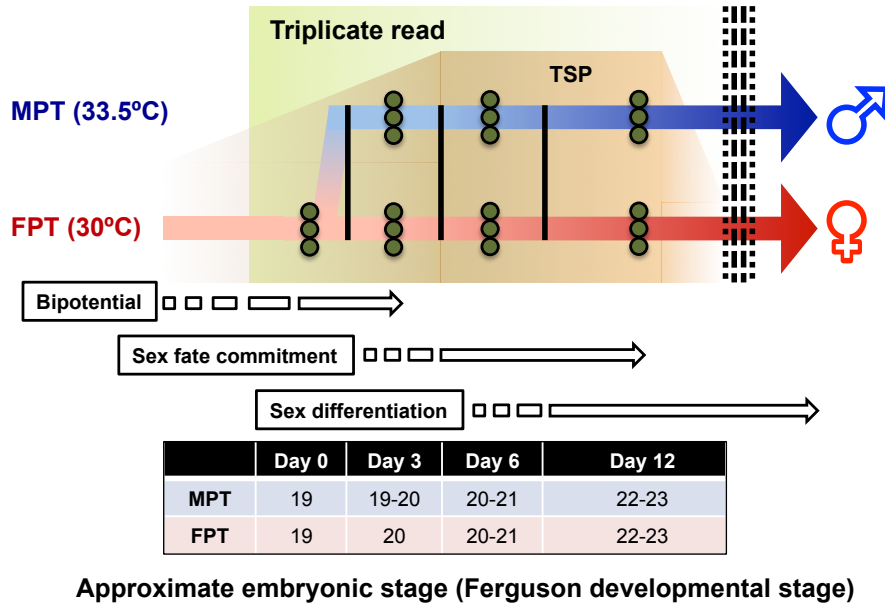
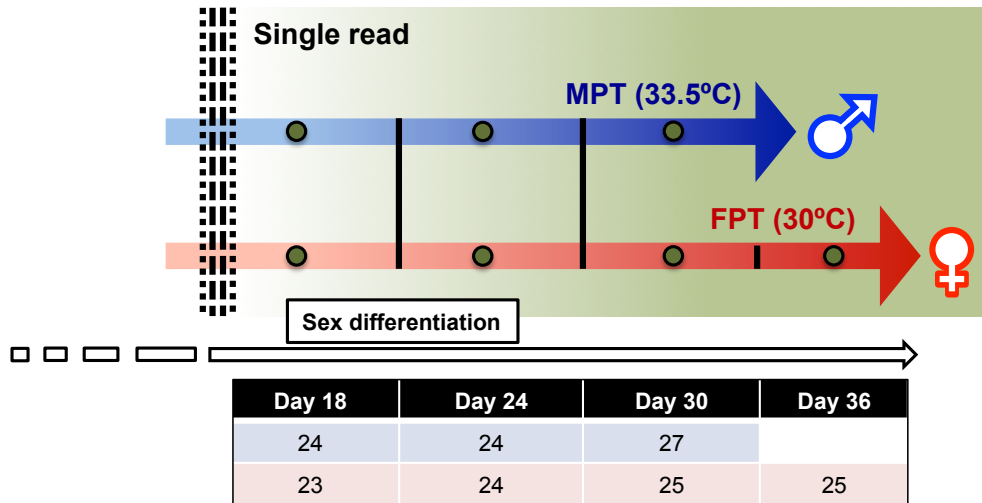


Figure 2-2



Approximate embryonic stage (Ferguson developmental stage)

**Figure 2-3**

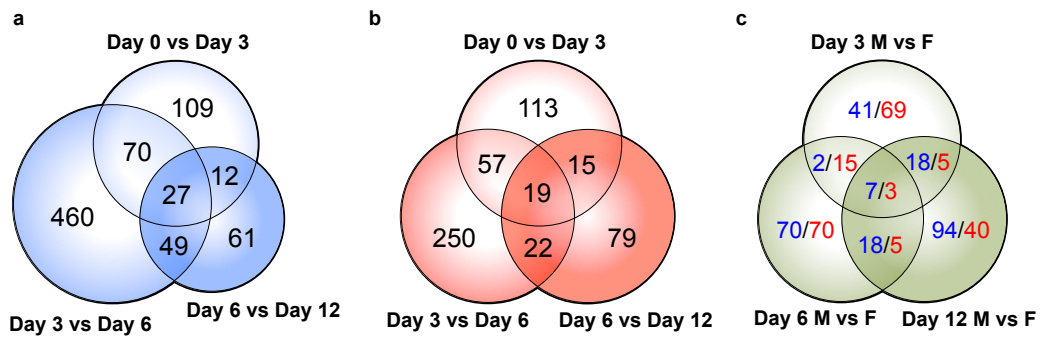
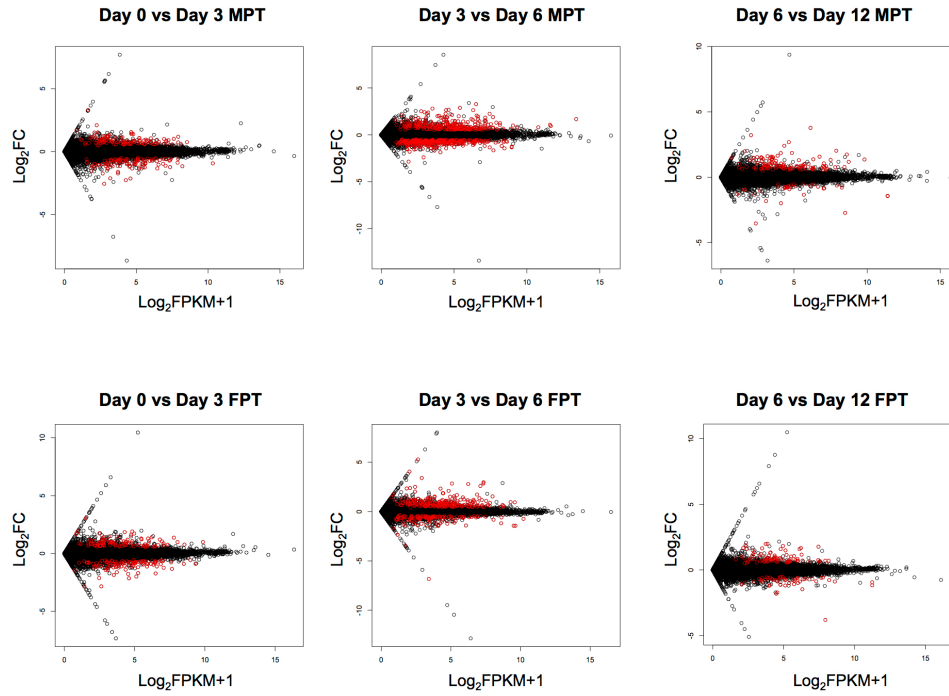


Figure 2-4

**a**



**b**

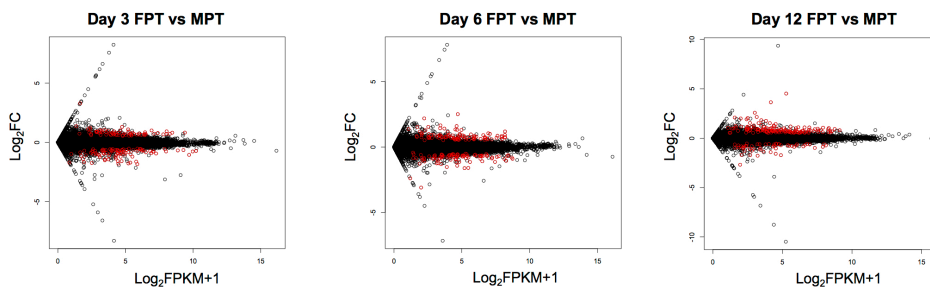




Figure 2-5

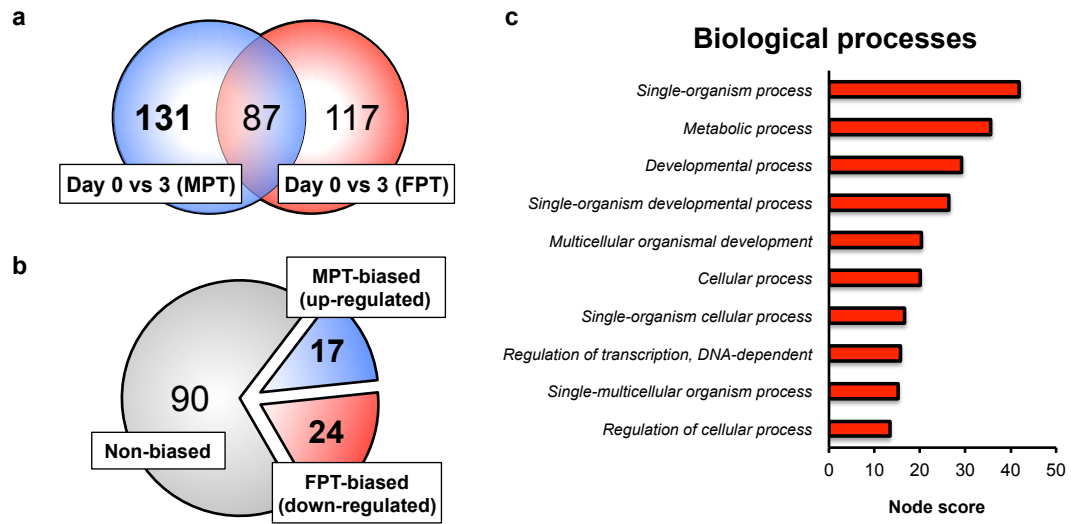


Figure 2-6

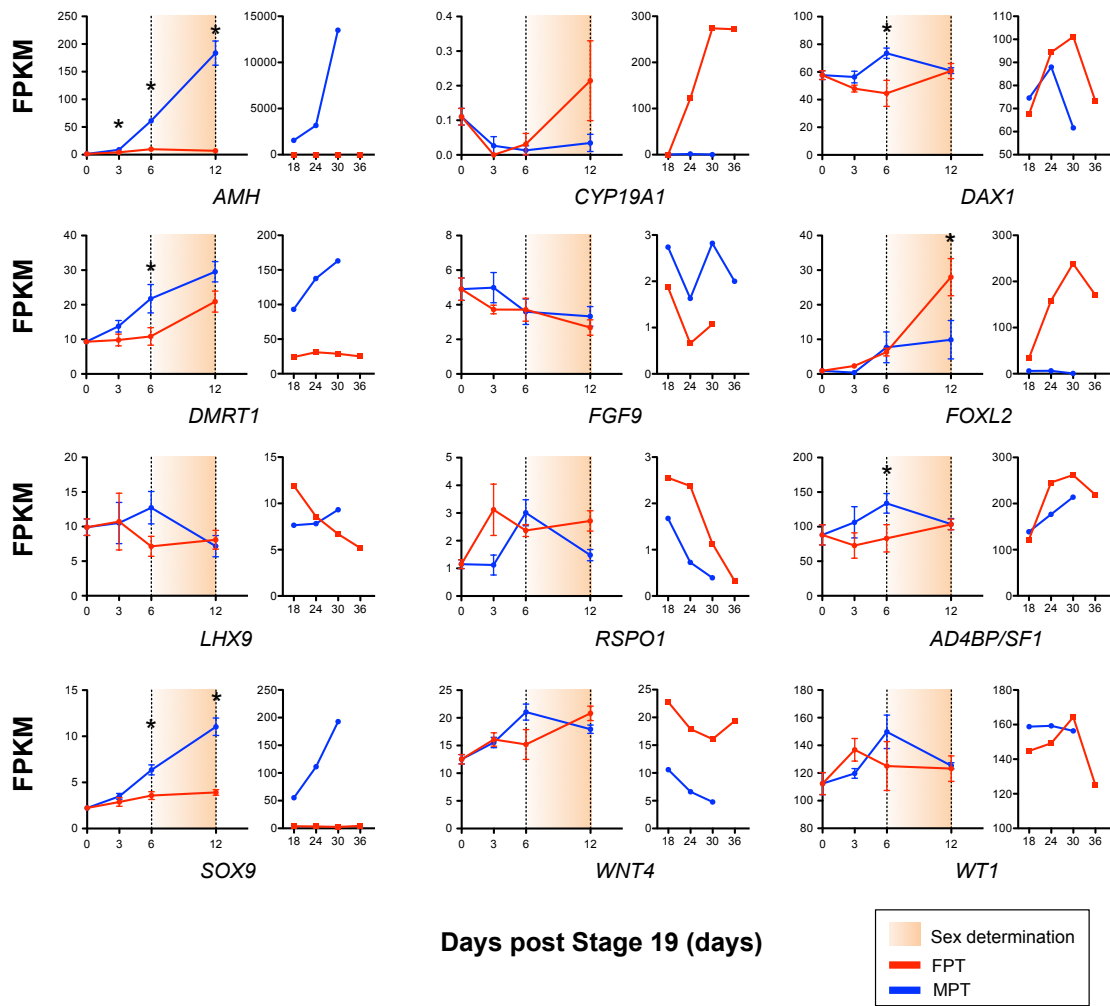


Figure 2-7

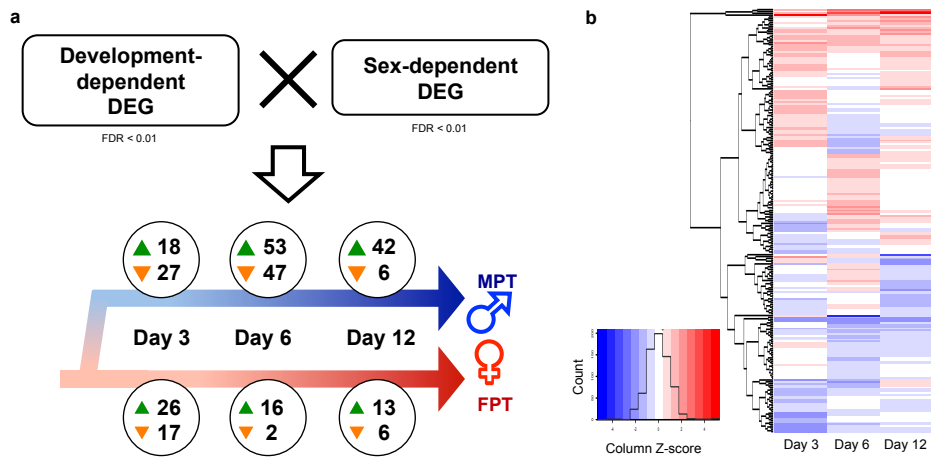


Figure 2-8

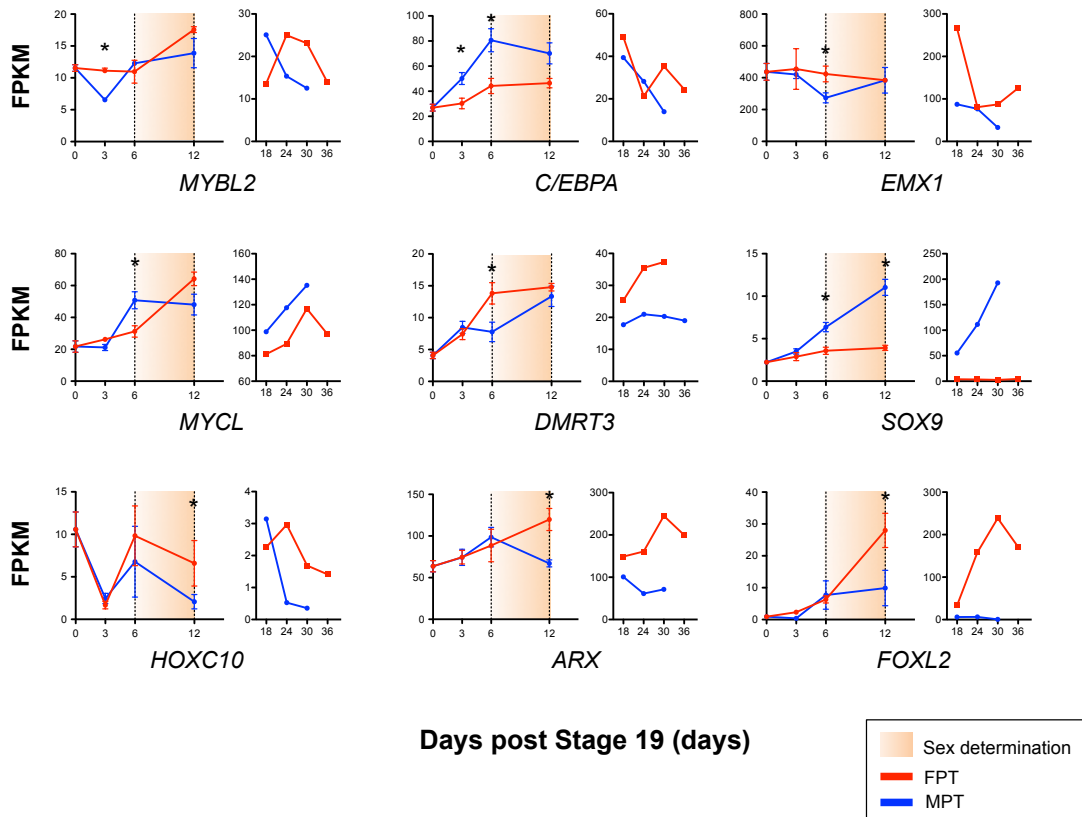
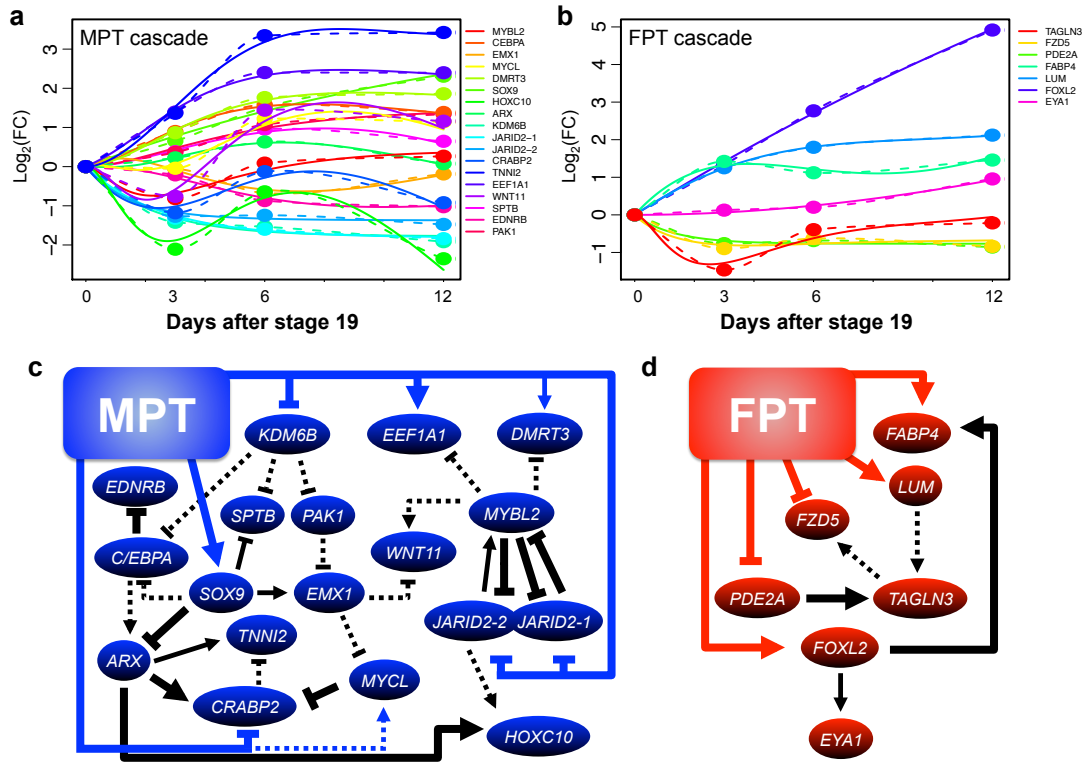


Figure 2-9

















XLOC_012336	SPTB	0.57	2.63E-03	XM_006270827.1	spectrin, beta, erythrocytic, transcript variant X1	XLOC_003833	MYO7B	-0.66	2.63E-03	XM_006261792.1	myosin VIIb
XLOC_010044	PLK1	0.57	8.24E-03	XM_006268449.1	polo-like kinase 1	XLOC_017810	NDRG1	-0.66	2.63E-03	XM_006276526.1	N-myc downstream regulated 1
XLOC_010436	MCM4	0.57	8.24E-03	XM_006268816.1	minichromosome maintenance complex component 4	XLOC_018228	LOC102559361	-0.66	4.73E-03	XM_006276953.1	endothelin B receptor-like
XLOC_001671	RRM1	0.55	9.85E-03	XM_006259539.1	ribonucleotide reductase M1	XLOC_002569	CBS	-0.66	4.73E-03	XM_006260475.1	cystathionine-beta-synthase, transcript variant X3
XLOC_013672	FBL	0.55	9.85E-03	XM_006272275.1	fibrinogen	XLOC_010069	PKD1	-0.65	4.73E-03	XM_006268435.1	polycystic kidney disease 1 (autosomal dominant)
XLOC_003241	LOC102558609	0.55	9.85E-03	XM_006261193.1	matrix metalloproteinase-14-like	XLOC_008408	CALB1	-0.65	2.63E-03	XM_006266690.1	calbindin 1, 28kDa
XLOC_004287	NFIX	0.54	9.85E-03	XM_006262319.1	nuclear factor I/X (CCAAT-binding transcription factor), transcript variant X3	XLOC_009610	LOC102564364	-0.65	2.63E-03	XM_006267961.1	ornithine decarboxylase 2-like
XLOC_017183	HDFG	0.54	8.24E-03	XM_006275864.1	hepatoma-derived growth factor	XLOC_018099	NEFL	-0.65	6.57E-03	XM_006276810.1	neurofilament, light polypeptide
						XLOC_007156	TSPAN9	-0.65	4.73E-03	XM_006265390.1	tetraspanin 9, transcript variant X1
						XLOC_001384	LOC102573310	-0.65	2.63E-03	XM_006259209.1	prostaglandin reductase 1-like
						XLOC_007714	LOC102570482	-0.64	6.57E-03	XM_006265963.1	cytochrome P450 3A21-like
						XLOC_007617	CUBN	-0.64	8.24E-03	XM_006265866.1	cubilin (intrinsic factor-cobalamin receptor)
						XLOC_006400	DIP2B	-0.64	2.63E-03	XM_006264640.1	DIP2 disco-interacting protein 2 homolog B (Drosophila)
						XLOC_004405	FDXR	-0.63	2.63E-03	XM_006262447.1	ferredoxin reductase
						XLOC_009853	SLC37A3	-0.63	6.57E-03	XM_006268207.1	solute carrier family 37, member 3
						XLOC_017667	CGBL2	-0.63	2.63E-03	XM_006276369.1	cysteine conjugate-beta lyase 2
						XLOC_018826	NPC1	-0.63	4.73E-03	XM_006277553.1	Niemann-Pick disease, type C1
						XLOC_005431	ALDH1A3	-0.62	2.63E-03	XM_006263543.1	aldehyde dehydrogenase 1 family, member A3, transcript variant X2
						XLOC_010535	NNT	-0.62	2.63E-03	XM_006268917.1	nicotinamide nucleotide transhydrogenase
						XLOC_007455	LRR8D	-0.62	2.63E-03	XM_006265697.1	leucine rich repeat containing 8 family, member D
						XLOC_009422	MTMR12	-0.62	8.24E-03	XM_006267762.1	myotubularin related protein 12
						XLOC_003353	EMX1	-0.62	2.63E-03	XM_006261299.1	empty spiracles homeobox 1
						XLOC_006464	CELSR1	-0.62	6.57E-03	XM_006264688.1	cadherin, EGF LAG seven-pass G-type receptor 1
						XLOC_006522	ITIH5	-0.61	2.63E-03	XM_006264736.1	inter-alpha-trypsin inhibitor heavy chain family, member 5
						XLOC_000958	ARHGGEF28	-0.61	4.73E-03	XM_006258764.1	Rho guanine nucleotide exchange factor (GEF) 28
						XLOC_005632	GSTZ1	-0.61	4.73E-03	XM_006263770.1	glutathione S-transferase zeta 1, transcript variant X2
						XLOC_016720	SELENBP1	-0.61	4.73E-03	XM_006275408.1	selenium binding protein 1
						XLOC_008886	LOC102577065	-0.61	4.73E-03	XM_006267219.1	eukaryotic translation initiation factor 3 subunit A-like
						XLOC_011596	AGXT2	-0.61	8.24E-03	XM_006270044.1	alanine-glyoxylate aminotransferase 2
						XLOC_002618	GPLD1	-0.61	8.24E-03	XM_006260536.1	glycosylphosphatidylinositol specific phospholipase D1
						XLOC_016042	LOC102564628	-0.61	6.57E-03	XM_006274734.1	succinyl-CoA:3-ketoacid coenzyme A transferase 1, mitochondrial-like
						XLOC_000021	LOC102559447	-0.60	2.63E-03	XM_006257749.1	carbonic anhydrase 2-like
						XLOC_009417	AMACR	-0.60	2.63E-03	XM_006267758.1	alpha-methylacyl-CoA racemase
						XLOC_001823	ARHGGEF12	-0.60	4.73E-03	XM_006259693.1	Rho guanine nucleotide exchange factor (GEF) 12
						XLOC_003428	KIAA1239	-0.60	8.24E-03	XM_006261374.1	KIAA1239 ortholog
						XLOC_011011	LOC102566228	-0.60	2.63E-03	XM_006269424.1	interferon gamma receptor 1-like
						XLOC_011785	TST	-0.60	2.63E-03	XM_006270248.1	thiosulfate sulfurtransferase (rhodanese)
						XLOC_013776	PEAK1	-0.60	9.85E-03	XM_006272401.1	pseudopodium-enriched atypical kinase 1, transcript variant X1
						XLOC_017425	ESPNL	-0.60	4.73E-03	XM_006276123.1	espin-like
						XLOC_014131	FUK	-0.60	8.24E-03	XM_006272777.1	fucokinase
						XLOC_014459	UROC1	-0.60	4.73E-03	XM_006273094.1	urocanate hydratase 1
						XLOC_004496	ASAH1	-0.60	2.63E-03	XM_006262540.1	N-acylsphingosine amidohydrolase (acid ceramidase) 1
						XLOC_016454	GLYCTK	-0.60	6.57E-03	XM_006275130.1	glycerate kinase
						XLOC_007186	IPMK	-0.59	9.85E-03	XM_006265421.1	inositol polyphosphate multikinase
						XLOC_008084	RREB1	-0.59	2.63E-03	XM_006266346.1	ras responsive element binding protein 1, transcript variant X3
						XLOC_004242	LOC102564038	-0.58	4.73E-03	XM_006262282.1	uncharacterized LOC102564038
						XLOC_005148	LOC102558477	-0.58	4.73E-03	XM_006263235.1	UDP-glucuronosyltransferase 1-6-like
						XLOC_013100	PDK4	-0.58	6.57E-03	XM_006271681.1	pyruvate dehydrogenase kinase, isozyme 4
						XLOC_008091	PPFIBP2	-0.57	9.85E-03	XM_006266353.1	PTPRF interacting protein, binding protein 2 (liprin beta 2), transcript variant X3
						XLOC_015907	RCOR1	-0.57	4.73E-03	XM_006274592.1	REST corepressor 1
						XLOC_016043	LOC102565081	-0.57	8.24E-03	N/A	low-density lipoprotein receptor-related protein 2-like
						XLOC_017046	PCBD1	-0.57	8.24E-03	XM_006275727.1	pterin-4 alpha-carbinolamine dehydratase/dimerization cofactor of hepatocyte nuclear factor 1 alpha
						XLOC_009448	LOC102562567	-0.57	8.24E-03	XM_006267800.1	major histocompatibility complex class I-related gene protein-like
						XLOC_010297	PTPRQ	-0.57	9.85E-03	XM_006268681.1	protein tyrosine phosphatase, receptor type, Q
						XLOC_007514	SUCLG2	-0.57	9.85E-03	XM_006265758.1	succinate-CoA ligase, GDP-forming, beta subunit
						XLOC_002665	LOC102567357	-0.57	8.24E-03	XM_006260586.1	probable proline dehydrogenase 2-like
						XLOC_003044	SIPA1L1	-0.56	6.57E-03	XM_006260980.1	signal-induced proliferation-associated 1 like 1
						XLOC_016841	LOC102563541	-0.56	6.57E-03	XM_006275525.1	arginine-glutamic acid dipeptide repeats protein-like
						XLOC_001486	AHCYL1	-0.56	8.24E-03	XM_006259321.1	adenosylhomocysteinase-like 1, transcript variant X1
						XLOC_017584	SORD	-0.56	4.73E-03	XM_006276283.1	sorbitol dehydrogenase
						XLOC_004275	LOC102563808	-0.55	4.73E-03	XM_006262281.1	Na(+)/H(+) exchange regulatory cofactor NHE-RF3-like
						XLOC_014217	IFT80	-0.54	4.73E-03	XM_006272855.1	intraflagellar transport 80 homolog (Chlamydomonas), transcript variant X1



XLOC_011397	HSD11B2	0.93	2.63E-03	XM_006269835.1	hydroxysteroid (11-beta) dehydrogenase 2
XLOC_010513	SLC23A1	0.91	2.63E-03	XM_006268887.1	solute carrier family 23 (ascorbic acid transporter), member 1
XLOC_001686	RET	0.91	4.73E-03	XM_006259549.1	ret proto-oncogene
XLOC_001517	LOC102568516	0.90	2.63E-03	XM_006259359.1	glycine amidinotransferase, mitochondrial-like
XLOC_002973	DBH	0.89	2.63E-03	XM_006260879.1	dopamine beta-hydroxylase (dopamine beta-monoxygenase)
XLOC_005942	GAP43	0.89	2.63E-03	XM_006264120.1	growth associated protein 43
XLOC_008690	SLC5A1	0.88	2.63E-03	XM_006266970.1	solute carrier family 5 (sodium/glucose cotransporter), member 1, transcript variant X1
XLOC_006416	LOC102561391	0.88	4.73E-03	XM_006264660.1	peripherin-like
XLOC_005818	PTPRR	0.87	2.63E-03	XM_006263984.1	protein tyrosine phosphatase, receptor type, R
XLOC_001463	LOC102574572	0.87	2.63E-03	XM_006259299.1	somatostatin-2-like
XLOC_008095	G6PC	0.86	2.63E-03	XM_006266359.1	glucose-6-phosphatase, catalytic subunit
XLOC_019823	LOC102564018	0.85	2.63E-03	XM_006278540.1	cysteine-rich venom protein helothermine-like
XLOC_006802	LOC102573570	0.85	2.63E-03	XM_006265015.1	solute carrier family 22 member 6-A-like
XLOC_014833	SRGN	0.84	2.63E-03	XM_006273478.1	serglycin
XLOC_017872	PCK1	0.84	2.63E-03	XM_006276591.1	phosphoenolpyruvate carboxykinase 1 (soluble)
XLOC_011267	LOC102572104	0.82	2.63E-03	XM_006269693.1	reticulon-1-A-like, transcript variant X3
XLOC_014075	SLC5A10	0.82	2.63E-03	XM_006272714.1	solute carrier family 5 (sodium/sugar cotransporter), member 10, transcript variant X1
XLOC_007107	UPK3A	0.81	2.63E-03	XM_006265339.1	uroplakin 3A
XLOC_018099	NEFL	0.81	2.63E-03	XM_006276810.1	neurofilament, light polypeptide
XLOC_011483	MBNL3	0.81	4.73E-03	XM_006269919.1	muscleblind-like splicing regulator 3, transcript variant X1
XLOC_015057	LOC102568110	0.80	2.63E-03	XM_006273705.1	acyl-coenzyme A synthetase ACSM4, mitochondrial-like
XLOC_008706	CADPS	0.80	2.63E-03	XM_006267004.1	Ca <sup>++</sup> -dependent secretion activator
XLOC_013828	LOC102573123	0.80	2.63E-03	XM_006272455.1	transcription factor SOX-9-like
XLOC_019137	C7	0.79	2.63E-03	XM_006277876.1	complement component 7
XLOC_001658	APOA1	0.79	2.63E-03	XM_006259520.1	apolipoprotein A-I
XLOC_011453	LOC102576383	0.79	6.57E-03	XR_363324.1	uncharacterized LOC102576383
XLOC_004662	SLC18A2	0.78	9.85E-03	XM_006262699.1	solute carrier family 18 (vesicular monoamine transporter), member 2
XLOC_003127	TMEM27	0.77	2.63E-03	XM_006261086.1	transmembrane protein 27
XLOC_017473	UHMK1	0.76	2.63E-03	XM_006276174.1	U2AF homology motif (UHM) kinase 1
XLOC_003591	DOT1L	0.76	2.63E-03	XM_006261554.1	DOT1-like histone H3K79 methyltransferase, transcript variant X1
XLOC_005579	SERINC5	0.75	2.63E-03	XM_006263715.1	serine incorporator 5
XLOC_002556	CALML4	0.74	2.63E-03	XM_006260456.1	calmodulin-like 4
XLOC_002692	LOC102575737	0.74	2.63E-03	XM_006260622.1	cytochrome P450 11B, mitochondrial-like
XLOC_010738	LOC102575314	0.73	2.63E-03	XM_006269131.1	steroid 21-hydroxylase-like
XLOC_001313	LOC102575660	0.73	2.63E-03	XM_006259135.1	dimethylaniline monoxygenase [N-oxide-forming] 1-like, transcript variant X3
XLOC_010742	LOC102576539	0.73	2.63E-03	XM_006269136.1	zona pellucida sperm-binding protein 3-like
XLOC_007888	STAR	0.72	2.63E-03	XM_006266133.1	steroidogenic acute regulatory protein
XLOC_007714	LOC102570482	0.71	2.63E-03	XM_006265963.1	cytochrome P450 3A21-like
XLOC_018173	FKBP5	0.69	2.63E-03	XM_006276891.1	FK506 binding protein 5
XLOC_002016	SLC25A15	0.69	6.57E-03	XM_006259877.1	solute carrier family 25 (mitochondrial carrier; ornithine transporter) member 15
XLOC_008171	ARG2	0.68	8.24E-03	XM_006266445.1	arginase 2
XLOC_018203	CLCNKB	0.68	2.63E-03	XM_006276925.1	chloride channel, voltage-sensitive Kb
XLOC_015376	LOC102571448	0.66	2.63E-03	XM_006274041.1	cytochrome P450 4B1-like
XLOC_005967	LOC102577145	0.65	4.73E-03	XM_006264145.1	D-beta-hydroxybutyrate dehydrogenase, mitochondrial-like
XLOC_013605	SLC4A4	0.65	2.63E-03	XM_006272210.1	solute carrier family 4 (sodium bicarbonate cotransporter), member 4
XLOC_011994	EHHADH	0.63	4.73E-03	XM_006270453.1	enoyl-CoA, hydratase/3-hydroxyacyl CoA dehydrogenase
XLOC_008801	LOC102572026	0.63	9.85E-03	XM_006267109.1	GDNF family receptor alpha-4-like
XLOC_008160	LOC102567071	0.62	8.24E-03	XM_006266432.1	pleckstrin-2-like
XLOC_010986	TUBB3	0.61	2.63E-03	XM_006269387.1	tubulin, beta 3 class III
XLOC_007156	TSPAN9	0.61	6.57E-03	XM_006265390.1	tetraspanin 9, transcript variant X1
XLOC_016831	FRAS1	0.59	4.73E-03	XM_006275515.1	Fraser syndrome 1
XLOC_014444	CPE	0.59	4.73E-03	XM_006273085.1	carboxypeptidase E
XLOC_015438	LOC102569264	0.58	9.85E-03	XM_006274116.1	cytochrome P450 2D14-like
XLOC_017810	NDRG1	0.58	6.57E-03	XM_006276526.1	N-myc downstream regulated 1
XLOC_001357	TM4SF4	0.57	6.57E-03	XM_006259172.1	transmembrane 4 L six family member 4
XLOC_016580	LOC102558436	inf	2.63E-03	XM_006275267.1	zinc finger protein 184-like



XLOC_008408	CALB1	0.77	2.63E-03	XM_00626690.1	calbindin 1, 28kDa	XLOC_017468	RGS4	-0.81	6.57E-03	XM_006276158.1	regulator of G-protein signaling 4
XLOC_009391	LOC102566850	0.76	2.63E-03	XM_006267730.1	FRAS1-related extracellular matrix protein 2-like	XLOC_002692	LOC102575737	-0.80	2.63E-03	XM_006260622.1	cytochrome P450 11B, mitochondrial-like
XLOC_007825	GPR37L1	0.76	4.73E-03	XM_006266077.1	G protein-coupled receptor 37 like 1	XLOC_002220	LOC102569061	-0.79	2.63E-03	XM_006260099.1	glycine N-acyltransferase-like protein 3-like
XLOC_012236	COL21A1	0.76	2.63E-03	XM_006270716.1	collagen, type XXI, alpha 1	XLOC_015664	GATA5	-0.78	4.73E-03	XM_006274328.1	GATA binding protein 5
XLOC_011791	LOC102566081	0.76	2.63E-03	XM_006270235.1	beta-galactoside-binding lectin-like	XLOC_003145	LOC102572230	-0.78	6.57E-03	XM_006261091.1	transmembrane protein 198-B-like
XLOC_007512	LOC102559932	0.75	2.63E-03	XM_006265755.1	collagen alpha-1(XXVI) chain-like	XLOC_007178	MYO1A	-0.77	4.73E-03	XM_006265411.1	myosin IA
XLOC_014618	LOC102575170	0.74	2.63E-03	XM_006273256.1	cystatin-B-like	XLOC_002786	SLC25A29	-0.76	2.63E-03	XM_006275682.1	cGMP-dependent 3',5'-cyclic phosphodiesterase-like
XLOC_000177	LOC102561900	0.74	2.63E-03	XM_006257927.1	semaphorin-3D-like	XLOC_017000	LOC102563625	-0.76	2.63E-03	XM_006260708.1	solute carrier family 25 (mitochondrial carnitine/acylcarnitine carrier), member 29
XLOC_002516	HSD17B1	0.72	2.63E-03	XM_006260402.1	hydroxysteroid (17-beta) dehydrogenase 1, transcript variant X2	XLOC_010746	ACTA2	-0.76	2.63E-03	XM_006269140.1	actin, alpha 2, smooth muscle, aorta
XLOC_010256	LOC102570029	0.71	2.63E-03	XM_006268638.1	vascular cell adhesion protein 1-like, transcript variant X2	XLOC_008801	LOC102572026	-0.75	8.24E-03	XM_006267109.1	GDNF family receptor alpha-4-like
XLOC_003273	PRELP	0.71	2.63E-03	XM_006261224.1	proline/arginine-rich end leucine-rich repeat protein	XLOC_004684	COL11A1	-0.74	4.73E-03	XM_006262736.1	collagen, type XI, alpha 1, transcript variant X3
XLOC_009174	THBD	0.70	2.63E-03	XM_006267522.1	thrombomodulin	XLOC_016034	OSR2	-0.74	2.63E-03	XM_006274725.1	odd-skipped related transcription factor 2, transcript variant X2
XLOC_016824	GAS2	0.68	4.73E-03	XM_006275507.1	growth arrest-specific 2	XLOC_005987	LOC102577145	-0.73	2.63E-03	XM_006264145.1	D-beta-hydroxybutyrate dehydrogenase, mitochondrial-like
XLOC_015934	S100A10	0.68	2.63E-03	XM_006274615.1	S100 calcium binding protein A10	XLOC_008706	CADPS	-0.73	8.24E-03	XM_006267004.1	Ca++-dependent secretion activator
XLOC_019235	LOC102575186	0.66	2.63E-03	XM_006277977.1	transmembrane protein 47-like	XLOC_011701	OGDHL	-0.72	2.63E-03	XM_006270166.1	oxoglutarate dehydrogenase-like, transcript variant X2
XLOC_013512	GJA1	0.65	2.63E-03	XM_006272096.1	gap junction protein, alpha 1, 43kDa	XLOC_008999	LOC102565364	-0.72	2.63E-03	XM_006267336.1	alanine aminotransferase 2-like
XLOC_001181	ME3	0.65	2.63E-03	XM_006258999.1	malic enzyme 3, NADP(+)-dependent, mitochondrial	XLOC_015306	HSD17B2	-0.72	2.63E-03	XM_006273972.1	hydroxysteroid (17-beta) dehydrogenase 2
XLOC_018761	F3	0.64	2.63E-03	XM_006277486.1	coagulation factor III (thromboplastin, tissue factor)	XLOC_012067	CTGF	-0.71	2.63E-03	XM_006270533.1	connective tissue growth factor
XLOC_005663	LOC102575135	0.63	6.57E-03	XM_006263807.1	ammonium transporter Rh type C-like	XLOC_003407	CHRNA3	-0.69	2.63E-03	XM_006261354.1	cholinergic receptor, nicotinic, alpha 3 (neuronal)
XLOC_017835	HEMGN	0.62	4.73E-03	XM_006276548.1	hemogen, transcript variant X1	XLOC_009930	SLC31A1	-0.68	9.85E-03	XM_006268285.1	solute carrier family 31 (copper transporter), member 1
XLOC_013747	SDPR	0.62	2.63E-03	XM_006272372.1	serum deprivation response	XLOC_006525	LOC102562243	-0.68	6.57E-03	XM_006264740.1	ectonucleotide pyrophosphatase/phosphodiesterase family member 3-like
XLOC_006296	SFRP2	0.60	4.73E-03	XM_006264518.1	secreted frizzled-related protein 2	XLOC_015832	LOC102572203	-0.68	4.73E-03	XM_006274533.1	contactin-1-like
XLOC_018247	LOC102563631	0.55	6.57E-03	XR_363745.1	uncharacterized LOC102563631	XLOC_018173	FKBP5	-0.67	2.63E-03	XM_006276891.1	FK506 binding protein 5
XLOC_001291	LOC102570689	inf	2.63E-03	XM_006259113.1	normin-like	XLOC_008171	ARG2	-0.66	8.24E-03	XM_006266445.1	arginase 2
XLOC_012590	LOC102566935	inf	2.63E-03	XM_006271052.1	collagen alpha-1(I) chain-like	XLOC_018116	SOAT1	-0.66	2.63E-03	XM_006276828.1	sterol O-acyltransferase 1
XLOC_001053	LOC102568912	inf	6.57E-03	XR_362717.1	uncharacterized LOC102568912	XLOC_006677	LOC102574741	-0.65	2.63E-03	XM_006264941.1	homeobox protein meis3-B-like
XLOC_009696	LOC102563028	inf	9.85E-03	XM_006268040.1	histone H2B 1/2/3/4/6-like	XLOC_011181	CTH	-0.63	2.63E-03	XM_006269606.1	cystathionase (cystathionine gamma-lyase)
						XLOC_001112	LOC102563319	-0.63	2.63E-03	XM_006258919.1	dehydrogenase/reductase SDR family member 1-like
						XLOC_019177	HOXB3	-0.61	2.63E-03	XM_006277919.1	homeobox B3
						XLOC_002963	SARDH	-0.58	4.73E-03	XM_006260892.1	sarcosine dehydrogenase
						XLOC_015775	APOA2	-0.57	9.85E-03	XM_006274463.1	apolipoprotein A-II
						XLOC_005771	LOC102563338	-inf	2.63E-03	XM_006263922.1	thioredoxin domain-containing protein 17-like
						XLOC_001066	LOC102573078	-inf	4.73E-03	XM_006258879.1	chromosome unknown open reading frame, human C2orf50







XLOC_014144	DQX1	0.71	3.58E-02	XM_006272784.1	DEAQ box RNA-dependent ATPase 1
XLOC_004875	ECEL1	0.70	2.85E-02	XM_006262936.1	endothelin converting enzyme-like 1
XLOC_006178	LOC102572775	0.70	4.73E-03	XM_006264382.1	mothers against decapentaplegic homolog 4-like
XLOC_008795	SLC34A1	0.69	2.63E-03	XM_006267103.1	solute carrier family 34 (type II sodium/phosphate cotransporter), member 1
XLOC_014042	SLC23A3	0.69	2.63E-03	XM_006272671.1	solute carrier family 23, member 3
XLOC_007534	CAV1	0.69	2.63E-03	XM_006265774.1	caveolin 1, caveolae protein, 22kDa
XLOC_012234	LOC102565383	0.69	2.63E-03	XM_006270714.1	neuronal acetylcholine receptor subunit alpha-7-like
XLOC_019869	LOC102571991	0.69	6.57E-03	XM_006278573.1	polymerase I and transcript release factor-like, transcript variant X2
XLOC_010742	LOC102576539	0.69	3.58E-02	XM_006269136.1	zona pellucida sperm-binding protein 3-like
XLOC_007888	STAR	0.69	1.66E-02	XM_006266133.1	steroidogenic acute regulatory protein
XLOC_003288	PGM5	0.68	4.73E-03	XM_006261237.1	phosphoglucomutase 5
XLOC_002559	LOC102577353	0.68	3.67E-02	XM_006260458.1	fibroblast growth factor 13-like, transcript variant X2
XLOC_006353	PTRF	0.68	2.63E-03	XM_006264575.1	polymerase I and transcript release factor
XLOC_003145	LOC102572230	0.67	3.50E-02	XM_006261091.1	transmembrane protein 198-B-like
XLOC_013799	TH	0.67	4.40E-02	XM_006272424.1	tyrosine hydroxylase
XLOC_000771	FRZB	0.67	2.63E-03	XM_006258581.1	frizzled-related protein
XLOC_006311	HTRA1	0.67	2.63E-03	XM_006264531.1	HtrA serine peptidase 1
XLOC_017186	CRABP2	0.67	4.73E-03	XM_006275867.1	cellular retinoic acid binding protein 2
XLOC_019005	NFKB1B	0.66	4.73E-03	XM_006277754.1	nuclear factor of kappa light polypeptide gene enhancer in B-cells inhibitor, beta
XLOC_006702	AOC1	0.66	6.57E-03	XM_006264919.1	amine oxidase, copper containing 1
XLOC_019900	TIMP1	0.66	2.63E-03	XM_006278610.1	TIMP metalloproteinase inhibitor 1
XLOC_008638	LOC102568241	0.66	2.63E-03	XM_006266925.1	von Willebrand factor-like
XLOC_015832	LOC102572203	0.66	2.63E-03	XM_006274533.1	contactin-1-like
XLOC_019890	CFP	0.66	2.63E-03	XM_006278617.1	complement factor properdin
XLOC_002077	CRIP1	0.66	1.13E-02	XM_006259954.1	cysteine-rich protein 1 (intestinal)
XLOC_015386	AP5B1	0.65	4.40E-02	XM_006274050.1	adaptor-related protein complex 5, beta 1 subunit
XLOC_005818	PTPRR	0.64	3.14E-02	XM_006263984.1	protein tyrosine phosphatase, receptor type, R
XLOC_018350	LOC102569355	0.63	2.63E-03	XM_006277074.1	collagen alpha-1(XI) chain-like
XLOC_003569	CD01	0.63	2.63E-03	XM_006261528.1	cysteine dioxygenase type 1
XLOC_000149	BLVRB	0.63	2.63E-03	XM_006257898.1	biliverdin reductase B (flavin reductase (NADPH))
XLOC_014654	ADAMTSL4	0.62	8.24E-03	XM_006273298.1	ADAMTS-like 4
XLOC_006827	HSD17B11	0.62	2.65E-02	XM_006265040.1	hydroxysteroid (17-beta) dehydrogenase 11, transcript variant X2
XLOC_012770	OLFML2A	0.62	2.63E-03	XM_006271324.1	olfactomedin-like 2A
XLOC_011913	PRNP	0.62	1.27E-02	XM_006270385.1	prion protein
XLOC_016538	JPH2	0.61	2.85E-02	XM_006275231.1	junctophilin 2, transcript variant X1
XLOC_014143	AUP1	0.61	1.54E-02	XM_006272782.1	ancient ubiquitous protein 1
XLOC_009005	LOC102569324	0.61	6.57E-03	XM_006267352.1	vitamin D3 hydroxylase-associated protein-like
XLOC_017215	EMLIN1	0.61	2.63E-03	XM_006275898.1	elastin microfibril interlacer 1
XLOC_002134	ASS1	0.60	6.57E-03	XM_006260002.1	argininosuccinate synthase 1
XLOC_004612	LOC102574966	0.60	1.41E-02	XM_006262659.1	1,25-dihydroxyvitamin D(3) 24-hydroxylase, mitochondrial-like
XLOC_002748	SLC5A12	0.60	4.73E-03	XM_006260672.1	solute carrier family 5 (sodium/monocarboxylate cotransporter), member 12
XLOC_015712	CLEC11A	0.59	2.94E-02	XM_006274395.1	C-type lectin domain family 11, member A
XLOC_003617	MYH11	0.59	8.24E-03	XM_006261582.1	myosin, heavy chain 11, smooth muscle
XLOC_000591	DMTN	0.58	3.75E-02	XM_006258386.1	dematin actin binding protein, transcript variant X1
XLOC_014047	TUBA4A	0.58	1.27E-02	XM_006272667.1	tubulin, alpha 4a
XLOC_014444	CPE	0.58	1.27E-02	XM_006273085.1	carboxypeptidase E
XLOC_002902	SALL2	0.56	9.85E-03	XM_006260826.1	spalt-like transcription factor 2
XLOC_015382	LOC102572890	0.56	4.73E-03	XM_006274047.1	solute carrier family 22 member 6-A-like
XLOC_010951	LOC102568868	0.56	1.41E-02	XM_006269351.1	rho-related GTP-binding protein RhoB-like
XLOC_008568	TREH	0.56	4.72E-02	XM_006266854.1	trehalase (brush-border membrane glycoprotein)
XLOC_003724	ALPL	0.55	2.46E-02	XM_006261695.1	alkaline phosphatase, liver/bone/kidney
XLOC_007477	NUPR1	0.55	3.58E-02	XM_006265711.1	nuclear protein, transcriptional regulator, 1
XLOC_018173	FKBP5	0.54	2.85E-02	XM_006276891.1	FK506 binding protein 5
XLOC_004287	NFIX	0.54	1.27E-02	XM_006262319.1	nuclear factor I/X (CCAAT-binding transcription factor), transcript variant X3
XLOC_005418	ADAMTS2	0.54	3.58E-02	XM_006263538.1	ADAM metalloproteinase with thrombospondin type 1 motif, 2
XLOC_012939	LOC102557733	0.54	2.01E-02	XM_006271508.1	fibrillin-2-like
XLOC_014691	CELSR3	0.54	4.16E-02	XM_006273334.1	cadherin, EGF LAG seven-pass G-type receptor 3
XLOC_006860	LOC102569158	0.53	3.14E-02	XM_006265079.1	protein Wnt-11-like, transcript variant X2
XLOC_006801	LOC102573333	0.53	2.56E-02	XM_006265014.1	solute carrier family 22 member 6-A-like
XLOC_008746	EEF1A2	0.53	2.01E-02	XM_006267053.1	eukaryotic translation elongation factor 1 alpha 2
XLOC_003005	LOC102574190	0.53	4.33E-02	XR_362827.1	uncharacterized LOC102574190
XLOC_011804	ERF	0.53	3.75E-02	XM_006270269.1	Ets2 repressor factor
XLOC_007478	SULT1A1	0.51	2.94E-02	XM_006265713.1	sulfotransferase family, cytosolic, 1A, phenol-preferring, member 1
XLOC_013775	LINGO1	0.51	3.14E-02	XM_006272399.1	leucine rich repeat and Ig domain containing 1, transcript variant X3
XLOC_003774	LOC102571925	0.50	1.90E-02	XM_006261728.1	tyrosine-protein kinase receptor Tie-1-like
XLOC_002042	APSS2	0.50	3.67E-02	XM_006259906.1	adaptor-related protein complex 3, sigma 2 subunit
XLOC_019742	ITGA5	0.49	3.75E-02	XM_006278464.1	integrin, alpha 5 (fibronectin receptor, alpha polypeptide)
XLOC_006411	CACNB3	0.49	4.16E-02	XM_006264650.1	calcium channel, voltage-dependent, beta 3 subunit
XLOC_000158	LTBP4	0.48	4.08E-02	XM_006257901.1	latent transforming growth factor beta binding protein 4
XLOC_000369	NCAM	0.47	2.56E-02	XM_006258155.1	melanoma cell adhesion molecule
XLOC_018524	JAG1	0.47	4.87E-02	XM_006277242.1	jagged 1
XLOC_006023	CPXM1	0.47	4.64E-02	XM_006264207.1	carboxypeptidase X (M14 family), member 1

XLOC_002679	SERPINF1	0.47	4.79E-02	XM_006260604.1	serpin peptidase inhibitor, clade F (alpha-2 antiplasmin, pigment epithelium derived factor), member 1
XLOC_000048	LOC102564090	0.47	4.40E-02	XM_006257769.1	tropomyosin alpha-4 chain-like, transcript variant X4
XLOC_015969	CLU	0.47	4.79E-02	XM_006274651.1	clusterin
XLOC_000387	TAC1	inf	2.63E-03	XM_006258170.1	tachykinin, precursor 1, transcript variant X2
XLOC_019004	LOC102558904	inf	2.63E-03	XM_006277748.1	synaptosomal-associated protein 25-like
XLOC_003232	LOC102575047	inf	3.41E-02	XR_362840.1	uncharacterized LOC102575047
XLOC_020082	LOC102569673	inf	3.50E-02	XR_363878.1	uncharacterized LOC102569673

---



XLOC_015352	LOC102567023	0.65	2.63E-03	XM_006274023.1	smoothelin-like protein 2-like
XLOC_003129	PIR	0.64	2.63E-03	XM_006261077.1	pirin (iron-binding nuclear protein)
XLOC_001463	LOC102574572	0.64	2.63E-03	XM_006259299.1	somatosatin-2-like
XLOC_001658	APQA1	0.62	6.57E-03	XM_006269520.1	apolipoprotein A-1
XLOC_004506	SALL1	0.62	2.63E-03	XM_006262552.1	spalt-like transcription factor 1, transcript variant X4
XLOC_002641	GPX3	0.58	9.85E-03	XM_006260571.1	glutathione peroxidase 3 (plasma)
XLOC_011119	MSH6	0.57	2.63E-03	XM_006269539.1	mutS homolog 6



XLOC_001261	LOC102563321	-0.73	2.63E-03	XM_006259088.1	hemoglobin subunit epsilon-like
XLOC_004704	EDNRA	-0.72	2.63E-03	XM_006262752.1	endothelin receptor type A, transcript variant X1
XLOC_003288	PGM5	-0.70	4.73E-03	XM_006261237.1	phosphoglucomutase 5
XLOC_017597	SCG5	-0.69	9.85E-03	XM_006276292.1	secretogranin V (7B2 protein), transcript variant X1
XLOC_006833	TGFB2	-0.69	4.73E-03	XM_006265048.1	transforming growth factor, beta 2
XLOC_003617	MYH11	-0.69	6.57E-03	XM_006261582.1	myosin, heavy chain 11, smooth muscle
XLOC_010256	LOC102570029	-0.69	2.63E-03	XM_006268638.1	vascular cell adhesion protein 1-like, transcript variant X2
XLOC_017835	HEMGN	-0.68	2.63E-03	XM_006276548.1	hemogen, transcript variant X1
XLOC_006538	LOC102565592	-0.68	2.63E-03	XM_006264753.1	BPTIKunitz domain-containing protein-like
XLOC_017724	FN1	-0.67	9.85E-03	XM_006276433.1	fibronectin 1, transcript variant X4
XLOC_001036	LRIG3	-0.67	2.63E-03	XM_006258847.1	leucine-rich repeats and immunoglobulin-like domains 3
XLOC_006984	RINT1	-0.67	4.73E-03	XM_006265209.1	RAD50 interactor 1, transcript variant X1
XLOC_004684	COL11A1	-0.67	8.24E-03	XM_006262736.1	collagen, type XI, alpha 1, transcript variant X3
XLOC_001309	LOC102576189	-0.66	2.63E-03	XM_006259136.1	dimethylamine monooxygenase [N-oxide-forming] 3-like
XLOC_013855	LOC102560862	-0.66	6.57E-03	XM_006272484.1	ribonucleoside-diphosphate reductase subunit M2-like
XLOC_009126	LOC102560553	-0.65	2.63E-03	XM_006267475.1	protein S100-A11-like
XLOC_004860	LOC102574734	-0.64	2.63E-03	XM_006262895.1	procollagen C-endopeptidase enhancer 1-like
XLOC_003054	LSS	-0.62	4.73E-03	XM_006260992.1	lanosterol synthase (2,3-oxidosqualene-lanosterol cyclase)
XLOC_013090	NUAK1	-0.60	6.57E-03	XM_006271673.1	NUAK family, SNF1-like kinase, 1
XLOC_015352	LOC102567023	-0.60	6.57E-03	XM_006274023.1	smoothelin-like protein 2-like
XLOC_010661	BGN	-0.59	2.63E-03	XM_006269028.1	biglycan
XLOC_003940	TNNI3	-0.58	6.57E-03	XM_006261916.1	troponin I type 3 (cardiac)
XLOC_011391	CMTM3	-0.57	9.85E-03	XM_006269831.1	CKLF-like MARVEL transmembrane domain containing 3
XLOC_000678	UCHL1	-0.56	6.57E-03	XM_006258484.1	ubiquitin carboxyl-terminal esterase L1 (ubiquitin thiolesterase)
XLOC_010162	SMAD1	-0.55	9.85E-03	XM_006268534.1	SMAD family member 1
XLOC_012065	MOXD1	-0.53	9.85E-03	XM_006270532.1	monooxygenase, DBH-like 1
XLOC_018826	LOC102563028	-inf	2.63E-03	XM_006268040.1	histone H2B 1/2/3/4/6-like

XLOC_017425	ESPNL	0.58	9.85E-03	XM_006276123.1	espin-like
XLOC_018826	NPC1	0.57	6.57E-03	XM_006277553.1	Niemann-Pick disease, type C1
XLOC_007526	LOC102563416	inf	4.73E-03	XR_363102.1	uncharacterized LOC102563416





XLOC_004380	GSTA4	-0.71	9.85E-03	XM_006262426.1	glutathione S-transferase alpha 4	XLOC_004389	LOC102558544	0.77	2.63E-03	XM_006262429.1	cathelicidin-2-like
XLOC_003367	STEAP4	-0.70	2.63E-03	XM_006261315.1	STEAP family member 4	XLOC_010356	LOC102575076	0.76	2.63E-03	XM_006268737.1	butyrophilin subfamily 1 member A1-like
XLOC_011163	LOC102565377	-0.70	2.63E-03	XM_006269585.1	serotriphin-like	XLOC_013658	PCED1A	0.76	9.85E-03	XM_006272260.1	PC-esterase domain containing 1A
XLOC_008928	ZBTB6	-0.69	2.63E-03	XM_006267251.1	zinc finger and BTB domain containing 6	XLOC_011927	HSP90AA1	0.76	2.63E-03	XM_006270404.1	heat shock protein 90kDa alpha (cytosolic), class A member 1
XLOC_018724	LOC102564013	-0.69	4.73E-03	XM_006277452.1	regucalcin-like	XLOC_014546	LOC102576325	0.74	6.57E-03	XM_006273179.1	serine/threonine-protein kinase PAK 1-like
XLOC_010094	LOC102567929	-0.69	2.63E-03	XM_006268475.1	sulfotransferase 1 family member D1-like	XLOC_014068	MMP23B	0.74	2.63E-03	XM_006259289.1	matrix metalloproteinase 23B
XLOC_014605	DNAH5	-0.69	8.24E-03	XM_006273245.1	dynein, axonemal, heavy chain 5	XLOC_017446	LOC102558523	0.73	9.85E-03	XM_006276142.1	musculin-like
XLOC_009005	LOC102569324	-0.69	2.63E-03	XM_006267352.1	vitamin D3 hydroxylase-associated protein-like	XLOC_014705	AMHR2	0.73	2.63E-03	XM_006273345.1	anti-Mullerian hormone receptor, type II
XLOC_018905	NEFM	-0.68	2.63E-03	XM_006276809.1	neurofilament, medium polypeptide	XLOC_005111	LOC102568149	0.72	2.63E-03	XM_006263192.1	nuclear receptor subfamily 0 group B member 1-like
XLOC_007684	LOC102562558	-0.67	2.63E-03	XM_006265929.1	3-ketoacyl-CoA thiolase B, peroxisomal-like	XLOC_000149	BLVRB	0.71	2.63E-03	XM_006257898.1	biliverdin reductase B (flavin reductase (NADPH))
XLOC_018601	RRM2B	-0.67	2.63E-03	XM_006277330.1	ribonucleotide reductase M2 B (TP53 inducible)	XLOC_017860	LOC102565559	0.70	9.85E-03	XM_006276579.1	lymphocyte antigen 86-like
XLOC_000655	LOC102570455	-0.66	2.63E-03	XM_006258459.1	probable acyl-CoA dehydrogenase 6-like	XLOC_009637	MYCL	0.70	2.63E-03	XM_006267966.1	v-myc avian myelocytomatosis viral oncogene lung carcinoma derived homolog 1
XLOC_008616	GPD2	-0.66	2.63E-03	XM_006266903.1	glycerol-3-phosphate dehydrogenase 2 (mitochondrial)	XLOC_019253	LOC102559669	0.70	4.73E-03	XM_006277993.1	frizzled-10-like
XLOC_007017	SCRN1	-0.66	2.63E-03	XM_006265245.1	secernin 1	XLOC_012763	NR5A1	0.69	2.63E-03	XM_006271311.1	nuclear receptor subfamily 5, group A, member 1
XLOC_015056	LOC102564848	-0.65	2.63E-03	XM_006273691.1	acyl-coenzyme A synthetase ACSM3, mitochondrial-like	XLOC_006205	TPRA1	0.68	2.63E-03	XM_006264421.1	transmembrane protein, adipocyte associated 1
XLOC_013605	SLC4A4	-0.64	8.24E-03	XM_006272210.1	solute carrier family 4 (sodium bicarbonate cotransporter), member 4	XLOC_012997	SLC4A1	0.67	2.63E-03	XM_006271577.1	solute carrier family 4 (anion exchanger), member 1
XLOC_014253	SLC6A19	-0.64	4.73E-03	XM_006272903.1	solute carrier family 6 (neutral amino acid transporter), member 19	XLOC_016032	LOC102561962	0.67	4.73E-03	XM_006274722.1	parvalbumin, muscle-like
XLOC_008854	SPOCK2	-0.63	2.63E-03	XM_006265063.1	sparc/osteonectin, cwcv and kazal-like domains proteoglycan (testican) 2	XLOC_011428	PTPRZ1	0.66	6.57E-03	XM_006269867.1	protein tyrosine phosphatase, receptor-type, Z polypeptide 1
XLOC_003353	EMX1	-0.63	2.63E-03	XM_006261299.1	empty spiracles homeobox 1	XLOC_005256	ENPP2	0.66	2.63E-03	XM_006263351.1	ectonucleotide pyrophosphatase/phosphodiesterase 2, transcript variant X2
XLOC_009514	LOC102561484	-0.62	4.73E-03	XM_006267878.1	potassium-transporting ATPase alpha chain 2-like	XLOC_009636	TRIT1	0.65	2.63E-03	XM_006267965.1	tRNA isopentenyltransferase 1
XLOC_002055	LOC102568673	-0.62	8.24E-03	XM_006259931.1	uncharacterized LOC102568673	XLOC_002515	NAGLU	0.64	2.63E-03	XM_006260415.1	N-acetylglucosaminidase, alpha
XLOC_009610	LOC102564364	-0.62	6.57E-03	XM_006267961.1	ornithine decarboxylase 2-like	XLOC_001582	BOC	0.63	2.63E-03	XM_006259427.1	BOC cell adhesion associated, oncogene regulated
XLOC_006431	NCKAP5L	-0.62	2.63E-03	XM_006264647.1	NCK-associated protein 5-like	XLOC_003589	LOC102566435	0.63	4.73E-03	XM_006261548.1	small EDRK-rich factor 1-like
XLOC_019177	HOXB3	-0.59	2.63E-03	XM_006277919.1	homeobox B3	XLOC_006860	LOC102569158	0.61	6.57E-03	XM_006265079.1	protein Wnt-11-like, transcript variant X2
XLOC_017921	WDR26	-0.59	2.63E-03	XM_006276637.1	WD repeat domain 26	XLOC_007754	TNMD	0.60	2.63E-03	XM_006265998.1	tenomodulin
XLOC_005828	MPI	-0.59	8.24E-03	XM_006264007.1	mannose phosphate isomerase	XLOC_005633	AHSA1	0.59	2.63E-03	XM_006263776.1	AHA1, activator of heat shock 90kDa protein ATPase homolog 1 (yeast)
XLOC_010264	LOC102572032	-0.58	2.63E-03	XM_006268644.1	platelet-derived growth factor D-like	XLOC_010818	ST6GALNAC2	0.59	4.73E-03	XM_006269266.1	ST6 (alpha-N-acetyl-neuraminyl-2,3-beta-galactosyl-1,3)-N-acetylgalactosaminidase
XLOC_018671	THBS2	-0.57	4.73E-03	XM_006277394.1	thrombospondin 2, transcript variant X1	XLOC_009748	LOC102573884	0.59	4.73E-03	XM_006268087.1	cystatin-like
XLOC_018228	LOC102559361	-0.57	4.73E-03	XM_006276953.1	endothelin B receptor-like	XLOC_005629	MST1	0.59	4.73E-03	XM_006263766.1	macrophage stimulating 1 (hepatocyte growth factor-like)
XLOC_001384	LOC102573310	-0.54	9.85E-03	XM_006259209.1	prostaglandin reductase 1-like	XLOC_014289	BRINP2	0.59	6.57E-03	XM_006272949.1	bone morphogenetic protein/retnoic acid inducible neural-specific 2
XLOC_018473	LOC102559751	-0.52	8.24E-03	XM_006277194.1	vitamin K-dependent protein S-like	XLOC_007028	LOC102573251	0.59	4.73E-03	XM_006265256.1	aquaporin-3-like
XLOC_009837	LOC102558436	-inf	2.63E-03	XM_006275267.1	zinc finger protein 184-like	XLOC_019928	LOC102573222	0.57	2.63E-03	XM_0062718652.1, XM_0062718653.1	tensin-like C1 domain-containing phosphatase-like
						XLOC_012336	SPTB	0.57	6.57E-03	XM_006270827.1	spectrin, beta, erythrocytic, transcript variant X1
						XLOC_018338	COLGALT1	0.57	2.63E-03	XM_006277067.1	collagen beta(1-O)galactosyltransferase 1
						XLOC_018060	LOC102575942	0.57	8.24E-03	XM_006276780.1	exostosin-1c-like
						XLOC_009845	LOC102564670	0.55	2.63E-03	XM_006268214.1	3-oxo-5-beta-steroid 4-dehydrogenase-like



99

inide alpha-2,6-sialyltransferase 2

XLOC_002043	ANPEP	0.88	2.63E-03	XM_006259907.1	alanyl (membrane) aminopeptidase
XLOC_014240	LOC102559116	0.88	6.57E-03	XM_006272882.1	chromosome unknown open reading frame, human C10orf90
XLOC_007107	UPK3A	0.88	2.63E-03	XM_006265339.1	uroplakin 3A
XLOC_019890	CFP	0.86	2.63E-03	XM_006278617.1	complement factor properdin
XLOC_013067	CPT1B	0.86	2.63E-03	XM_006271642.1	carnitine palmitoyltransferase 1B (muscle)
XLOC_008388	LOC102566921	0.85	2.63E-03	XM_006266674.1	SPARC-like protein 1-like
XLOC_001938	ACSF3	0.83	2.63E-03	XM_006259815.1	acyl-CoA synthetase family member 3
XLOC_007730	AGMAT	0.83	2.63E-03	XM_006265981.1	agmatine ureohydrolase (agmatinase)
XLOC_005663	LOC102575135	0.82	2.63E-03	XM_006263807.1	ammonium transporter Rh type C-like
XLOC_001313	LOC102575660	0.82	2.63E-03	XM_006259135.1	dimethylaniline monooxygenase [N-oxide-forming] 1-like, transcript variant X3
XLOC_004855	TFR2	0.82	4.73E-03	XM_006262912.1	transferrin receptor 2
XLOC_000025	CA13	0.81	2.63E-03	XM_006257756.1	carbonic anhydrase XIII
XLOC_009566	ELN	0.81	2.63E-03	XM_006267934.1	elastin
XLOC_007228	DDX58	0.81	2.63E-03	XM_006265462.1	DEAD (Asp-Glu-Ala-Asp) box polypeptide 58
XLOC_010370	ALDOB	0.80	2.63E-03	XM_006268753.1	aldolase B, fructose-bisphosphate, transcript variant X2
XLOC_003595	JSRP1	0.80	6.57E-03	XM_006261560.1	junctional sarcoplasmic reticulum protein 1
XLOC_003790	ALDH4A1,LOC10	0.80	2.63E-03	96261753.1, XM_00626	aldehyde dehydrogenase 4 family, member A1, taste receptor type 1 member 2-like
XLOC_017558	AMN	0.79	2.63E-03	XM_006276258.1	amion associated transmembrane protein
XLOC_018070	LOC102574081	0.79	2.63E-03	XM_006276772.1	chromosome unknown open reading frame, human C1orf63
XLOC_003589	LOC102566435	0.78	2.63E-03	XM_006261548.1	small EDRK-rich factor 1-like
XLOC_015976	LOC102567479	0.77	2.63E-03	XM_006274661.1	zinc finger protein 208-like
XLOC_004612	LOC102574966	0.77	2.63E-03	XM_006262659.1	1,25-dihydroxyvitamin D(3) 24-hydroxylase, mitochondrial-like
XLOC_001624	PCYOX1	0.77	2.63E-03	XM_006268735.1	prenylcysteine oxidase 1
XLOC_016914	CLEC18A	0.76	2.63E-03	XM_006259479.1	cytochrome P450 4F22-like
XLOC_004420	PAMR1	0.76	2.63E-03	XM_006275598.1	C-type lectin domain family 18, member A
XLOC_003061	MFSD4	0.76	2.63E-03	XM_006262454.1	peptidase domain containing associated with muscle regeneration 1, transcript variant X1
XLOC_000041	LOC102566578	0.75	6.57E-03	XM_006261001.1	major facilitator superfamily domain containing 4
XLOC_016610	LOC102566253	0.74	6.57E-03	XM_006275296.1	avidin-like
XLOC_003184	P4HA2	0.74	2.63E-03	XM_006261132.1	diamine acetyltransferase 2-like
XLOC_014252	SLC6A18	0.73	2.63E-03	XM_006272902.1	prolyl 4-hydroxylase, alpha polypeptide II, transcript variant X1
XLOC_008408	CALB1	0.72	2.63E-03	XM_006266690.1	solute carrier family 6 (neutral amino acid transporter), member 18
XLOC_004857	GIGYF1	0.72	2.63E-03	XM_006262914.1	calbindin 1, 28kDa
XLOC_003053	FTCD	0.72	2.63E-03	XM_006260991.1	GRB10 interacting GYF protein 1
XLOC_012802	PDZD3	0.71	2.63E-03	XM_006271363.1	formimidoyltransferase cyclodeaminase
XLOC_006538	LOC102565592	0.70	2.63E-03	XM_006264753.1	PDZ domain containing 3
XLOC_014342	AMDHD1	0.70	2.63E-03	XM_006272991.1	BPTI/Kunitz domain-containing protein-like
XLOC_013750	STAT1	0.70	4.73E-03	XM_006272369.1	amidohydrolase domain containing 1
XLOC_014873	ANK1	0.70	9.85E-03	XM_006273519.1	signal transducer and activator of transcription 1, 91kDa
XLOC_000299	GJB1	0.68	8.24E-03	XM_006258059.1	ankyrin 1, erythrocytic
XLOC_016032	LOC102561962	0.68	2.63E-03	XM_006274722.1	gap junction protein, beta 1, 32kDa
XLOC_002205	LOC102567904	0.68	4.73E-03	XM_006260094.1	parvalbumin, muscle-like
XLOC_007714	LOC102570482	0.68	2.63E-03	XM_006265963.1	aspartoacylase-2-like
XLOC_004389	LOC102558544	0.67	2.63E-03	XM_006262429.1	cytochrome P450 3A21-like
XLOC_009584	F13A1	0.67	2.63E-03	XM_006267941.1	cathelicidin-2-like
XLOC_001181	ME3	0.66	2.63E-03	XM_006258999.1	coagulation factor XIII, A1 polypeptide
XLOC_007888	STAR	0.65	4.73E-03	XM_006266133.1	malic enzyme 3, NADP(+)-dependent, mitochondrial
XLOC_019852	IFRD1	0.65	2.63E-03	XM_006278568.1	steroidogenic acute regulatory protein
XLOC_001310	FMO2	0.65	8.24E-03	XM_006259130.1	interferon-related developmental regulator 1, transcript variant X2
XLOC_002641	GPX3	0.64	2.63E-03	XM_006260571.1	flavin containing monooxygenase 2 (non-functional)
XLOC_006702	AOC1	0.64	6.57E-03	XM_006264919.1	glutathione peroxidase 3 (plasma)
XLOC_002679	SERPINF1	0.63	2.63E-03	XM_006260604.1	amine oxidase, copper containing 1
XLOC_007638	LOC102571097	0.63	2.63E-03	XM_006265883.1	serpin peptidase inhibitor, clade F (alpha-2 antiplasmin, pigment epithelium derived factor), member 1
XLOC_007175	LOC102573334	0.62	6.57E-03	XM_006265415.1	poly (ADP-ribose) polymerase 14-like
XLOC_007156	TSPAN9	0.61	6.57E-03	XM_006265390.1	low-density lipoprotein receptor-related protein 1-like
XLOC_004838	LOC102558546	0.61	6.57E-03	N/A	tetraspanin 9, transcript variant X1
XLOC_003127	TMEM27	0.61	2.63E-03	XM_006261086.1	zinc finger protein 850-like
XLOC_016572	MIOX	0.60	2.63E-03	XM_006275260.1	transmembrane protein 27
XLOC_020119	TNNI2	0.60	9.85E-03	XM_006278838.1	myo-inositol oxygenase
XLOC_009465	PM20D1	0.60	2.63E-03	XM_006267821.1	troponin 1 type 2 (skeletal, fast)
XLOC_019094	HIF3A	0.59	4.73E-03	XM_006277828.1	peptidase M20 domain containing 1
XLOC_016611	LOC102559968	0.58	8.24E-03	XM_006275273.1	hypoxia inducible factor 3, alpha subunit
XLOC_010513	SLC23A1	0.57	6.57E-03	XM_006268887.1	diamine acetyltransferase 2-like, transcript variant X1
XLOC_001517	LOC102568516	0.57	4.73E-03	XM_006259359.1	solute carrier family 23 (ascorbic acid transporter), member 1
XLOC_001546	LOC102577042	0.57	8.24E-03	XM_006259394.1	glycine amidinotransferase, mitochondrial-like
XLOC_009799	PHKA1	0.57	8.24E-03	XM_006268154.1	sulfotransferase 6B1-like
XLOC_020135	SLC5A2	0.56	9.85E-03	XM_006278885.1	phosphorylase kinase, alpha 1 (muscle)
XLOC_019480	RENBP	0.56	9.85E-03	XM_006278205.1	solute carrier family 5 (sodium/glucose cotransporter), member 2
XLOC_009845	LOC102564670	0.56	8.24E-03	XM_006268214.1	renin binding protein
					3-oxo-5-beta-steroid 4-dehydrogenase-like

**Table 2-3.** Candidate temperature-responsive genes.

<b>Day 0 – Day 3 MPT: MPT dimorphic (up-regulated)</b>				
<b>Description</b>	<b>RefSeq Accession No.</b>	<b>Log<sub>2</sub>(FC)</b>	<b>FDR</b>	<b>Primary Ontology</b>
uncoupling protein 2 (mitochondrial, proton carrier)	XM_006257947.1	1.47	2.63E-03	P: liver regeneration
UDP-N-acetyl-alpha-D-galactosamine polypeptide N-acetylgalactosaminyltransferase 5	XM_006262802.1	1.46	2.63E-03	C: Golgi membrane
eukaryotic translation initiation factor 4A2	XM_006262029.1	1.18	2.63E-03	F: translation initiation factor activity
uropodin 3A	XM_006265339.1	1.09	2.63E-03	C: integral to membrane
low-density lipoprotein receptor-related protein 1-like	XM_006265415.1	1.09	2.63E-03	P: lipoprotein transport
acyl-coenzyme A synthetase ACSM4, mitochondrial-like	XM_006273705.1	1.01	2.63E-03	F: catalytic activity
solute carrier family 1 (glutamate/neutral amino acid transporter), member 4	XM_006264916.1	0.97	2.63E-03	P: proline transmembrane transport
transient receptor potential cation channel, subfamily C, member 4 associated protein	XM_006258376.1	0.91	2.63E-03	C: Cul4A-RING ubiquitin ligase complex
CCAAT/enhancer binding protein (C/EBP), alpha	XM_006274301.1	0.90	2.63E-03	P: regulation of cell proliferation
methylcrotonoyl-CoA carboxylase beta chain, mitochondrial-like	XM_006273834.1	0.86	2.63E-03	F: ligase activity
myosin XVIIIIB	XM_006261765.1	0.86	2.63E-03	C: nucleolus
chromosome unknown open reading frame, human C1orf63	XM_006276772.1	0.80	2.63E-03	N/A
interferon-related developmental regulator 1, transcript variant X2	XM_006278568.1	0.69	2.63E-03	P: myoblast fate determination
espin-like	XM_006276123.1	0.65	2.63E-03	N/A
prenylcysteine oxidase 1	XM_006268735.1	0.62	9.85E-03	C: lysosome
formimidoyltransferase cyclodeaminase	XM_006260991.1	0.57	6.57E-03	C: cytosol
uncharacterized LOC102563416	XR_363102.1	infinite	4.73E-03	C: cytosol
<b>Day 0 – Day 3 MPT: FPT dimorphic (down-regulated)</b>				
<b>Description</b>	<b>RefSeq Accession No.</b>	<b>Log<sub>2</sub>(FC)</b>	<b>FDR</b>	<b>Primary Ontology</b>
lysine (K)-specific demethylase 6B	XM_006271864.1	-1.42	2.63E-03	P: positive regulation of transcription from RNA polymerase II promoter
protein Jumonji-like	XM_006270621.1	-1.32	2.63E-03	P: negative regulation of transcription from RNA polymerase II promoter
protein Jumonji-like	XM_006270617.1	-1.32	2.63E-03	P: negative regulation of transcription from RNA polymerase II promoter
cysteine and glycine-rich protein 2	XM_006269901.1	-1.31	2.63E-03	P: multicellular organismal development
myeloid protein 1-like	XM_006275897.1	-1.30	2.63E-03	P: granulocyte differentiation
protease, serine, 35	XM_006258407.1	-1.24	2.63E-03	C: extracellular region
ADAM metalloproteinase with thrombospondin type 1 motif, 15	XM_006262089.1	-1.24	2.63E-03	F: metalloendopeptidase activity
cellular retinoic acid binding protein 2	XM_006275867.1	-1.18	2.63E-03	F: retinoic acid binding
angiopoietin-like 1, transcript variant X2	XM_006267260.1	-1.18	2.63E-03	C: extracellular space
transgelin	XM_006278069.1	-1.14	2.63E-03	F: protein binding, bridging
dimethylaniline monooxygenase [N-oxide-forming] 3-like	XM_006259136.1	-1.06	2.63E-03	C: endoplasmic reticulum membrane
elastin	XM_006267934.1	-1.05	2.63E-03	N/A
uncharacterized LOC102575456, transcript variant X1	XR_363216.1	-1.03	2.63E-03	N/A
hematopoietic prostaglandin D synthase	XM_006265263.1	-1.01	4.73E-03	C: cytoplasm
hemoglobin subunit epsilon-like	XM_006259088.1	-0.95	2.63E-03	P: oxygen transport
matrix-remodelling associated 5	XM_006277556.1	-0.94	2.63E-03	C: extracellular region
epidermal retinol dehydrogenase 2-like	XM_006277024.1	-0.90	8.24E-03	P: retinal metabolic process
v-myb avian myeloblastosis viral oncogene homolog-like 2	XM_006276553.1	-0.82	2.63E-03	P: spindle assembly involved in mitosis
protein Wnt-11-like, transcript variant X2	XM_006265079.1	-0.76	4.73E-03	P: positive regulation of apoptotic process
thrombospondin 2, transcript variant X1	XM_006277394.1	-0.73	2.63E-03	C: basement membrane
protein NEL-like	XM_006272242.1	-0.66	2.63E-03	F: kinase activity
platelet-derived growth factor D-like	XM_006268644.1	-0.63	4.73E-03	P: regulation of peptidyl-tyrosine phosphorylation
RAS-like, family 11, member B	XM_006261252.1	-0.63	6.57E-03	P: small GTPase mediated signal transduction
ubiquitin carboxyl-terminal esterase L1 (ubiquitin thiolesterase)	XM_006258484.1	-0.58	4.73E-03	F: cysteine-type endopeptidase activity





**Table 2-5.** Candidate critical genes with putative regulatory functions.

Candidate transcriptional regulator					
Gene ID	Gene symbol	Description	Molecule type	Expression	Timespan
<b>MPT Day 0 vs MPT Day 3</b>					
XLOC_015643	<i>CEBPA</i>	CCAAT/enhancer binding protein (C/EBP), alpha	Transcription factor	Up	Short
XLOC_013275	<i>KDM6B</i>	Lysine (K)-specific demethylase 6B	Transcription regulator	Down	Long
XLOC_012144	<i>LOC102562106</i>	Protein Jumonji-like	Transcription regulator	Down	Long
XLOC_012145	<i>LOC102561337</i>	Protein Jumonji-like	Transcription regulator	Down	Long
XLOC_017186	<i>CRABP2</i>	Cellular retinoic acid binding protein 2	Transporter	Down	Short
XLOC_017840	<i>MYBL2</i>	v-myb avian myeloblastosis viral oncogene homolog-like 2	Transcription factor	Down	Short
XLOC_006860	<i>LOC102569158</i>	Protein Wnt-11-like, transcript variant X2	Other	Down	Short
<b>MPT Day 3 vs MPT Day 6</b>					
XLOC_006860	<i>LOC102569158</i>	Protein Wnt-11-like, transcript variant X2	Other	Up	Short
XLOC_020119	<i>TNNI2</i>	Troponin I type 2 (skeletal, fast)	Enzyme	Up	Short
XLOC_009637	<i>MYCL</i>	v-myc avian myelocytomatosis viral oncogene lung carcinoma derived homolog	Transcription factor	Up	Short
XLOC_006593	<i>LOC102560544</i>	Elongation factor 1-alpha-like	Other	Up	Short
XLOC_003318	<i>LOC102577358</i>	Duplex and mab-3 related transcription factor 3-like	Transcription factor	Up	Long
XLOC_013828	<i>LOC102573123</i>	Transcription factor SOX-9-like	Transcription factor	Up	Long
XLOC_014546	<i>LOC102576325</i>	Serine/threonine-protein kinase PAK 1-like	Protein kinase	Up	Long
XLOC_015643	<i>CEBPA</i>	CCAAT/enhancer binding protein (C/EBP), alpha	Transcription factor	Up	Short
XLOC_012336	<i>SPTB</i>	Spectrin, beta, erythrocytic, transcript variant X1	Other	Up	Short
XLOC_018228	<i>LOC102559361</i>	Endothelin B receptor-like	Receptor	Down	Ambiguous
XLOC_003353	<i>EMX1</i>	Empty spiracles homeobox 1	Transcription factor	Down	Short
<b>MPT Day 6 vs MPT Day 12</b>					
XLOC_013828	<i>LOC102573123</i>	Transcription factor SOX-9-like	Transcription factor	Up	Long
XLOC_019721	<i>HOXC10</i>	Homeobox C10	Transcription factor	Down	Ambiguous
XLOC_001928	<i>ARX</i>	Aristaless related homeobox	Transcription factor	Down	Long
<b>FPT Day 0 vs FPT Day 3</b>					
XLOC_003878	<i>FABP4</i>	Fatty acid binding protein 4, adipocyte	Transporter	Up	Ambiguous
XLOC_000567	<i>LUM</i>	Lumican	Other	Up	Short
XLOC_012101	<i>TAGLN3</i>	Transgelin 3	Other	Down	Short
XLOC_007693	<i>FZD5</i>	Frizzled family receptor 5	Receptor	Down	Short
XLOC_017000	<i>LOC102563625</i>	cGMP-dependent 3',5'-cyclic phosphodiesterase-like	Enzyme	Down	Short
<b>FPT Day 6 vs FPT Day 12</b>					
XLOC_001005	<i>LOC102577040</i>	Forkhead box protein L2-like	Transcription factor	Up	Long
XLOC_006272	<i>EYA1</i>	Eyes absent homolog 1 (Drosophila), transcript variant X1	Phosphatase	Up	Long



## General discussion

In this thesis, integrated use of classical methodology (pharmacological administration experiments) and modern methodology (next generation RNA sequencing analysis) were employed to potentially elucidate and comprehensively characterize molecular mechanism underlying TSD in *Alligator mississippiensis*. In chapter 1, I was able to suggest for potential model of temperature sensation mechanism during TSD in the developing embryo. Expression analysis of the gonad during sex determination period indicated expression of the thermosensitive cation channel TRPV4 (Figure 1-1). Electrophysiological analysis indicated that channel was activated at warm temperatures, near temperature range associated with alligator sex determination, and the channel activation led to intracellular  $Ca^{2+}$  influx (Figure 1-5). By selective activation and inhibition of TRPV4 channel activity using administration of TRPV4-specific pharmacological agents during sex determination period, I was able to demonstrate that TRPV4 channel activity can influence the expression of genes related to testis-determination in the long term. Expression levels of *AMH* and *SOX9*, genes critical for testis formation, were significantly altered several weeks after the chemical administration, and partial feminization was observed at histological level in male producing temperature (Figure 1-6,9). In conclusion, TRPV4 was able to influence genetic cascade related with testicular formation. Hence, for the first time a biomolecule, TRPV4, was able to directly associate temperature and sex determination in TSD species.

In chapter 2, I was able to comprehensively characterize the global transcriptome in the embryonic gonad at female- and male-producing temperature during sex determination using RNA-sequencing (RNA-seq) analysis (Figure 2-1).

RNA-seq data was collected, and I was able to track differentially expressed genes between adjacent time points at same temperature conditions, and also between the two temperature conditions at corresponding time points (Figure 2-3), and by cross-comparison, 230 genes with both development-wise and sex-wise differential expression were screened out (Figure 2-7). Forty-one genes expressions were observed to be temperature-responsive, including jumonji proteins *KDM6B*, *JARID2*, transcription factor *C/EBPA*, and Wnt signaling factor *WNT11* (Table 2-3). Furthermore, twenty-five transcriptional regulators were highly regulated in a sexually dimorphic manner. These include *SOX9*, *FOXL2*, *MYBL2*, *MYCL* and *HOXC10* (Table 2-5). In conclusion, utilization of the high-throughput RNA-seq analysis provided novel insights into the genetic framework underlining alligator TSD, and establishes the much needed gene expression data for future studies.

Two experiments presented in thesis cover the aspect of temperature sensation from both upstream and downstream. TRPV4 channel addresses how temperature, a physical energy, can be translated to chemical signaling via channel activation and  $\text{Ca}^{2+}$  influx. Global transcriptome data presents potential targets, and direct results of the  $\text{Ca}^{2+}$  influx, and also provides short- and long-term gene expression changes during sex determination. Both results from chapter 1 and 2 were not able to explain female sex determination as much as male sex determination, and much of the ovarian sex determination cascade remains unclear. Much of this is only speculation at this stage, however, and more robust evidence is required in the future. Classical methodology such as pharmacological administration experiments can be difficult to provide robust results, unlike modern genome editing and such. However, with advent of modern methodologies such as reporter assays and chromatin immunoprecipitation (ChIP) as

mentioned in chapter 2, as well as organ culture experiments, it would be possible to conduct experiments and validate the role of TRPV4. Additionally, with plethora of observations made in chapter 2 during sex determination, TSD can now be researched from variety of ways, including epigenetic, metabolomics, stress-response.

Sex of species that display GSD is determined at fertilization, and the sexually dimorphic heterochromosomes (XX/XY, ZW/ZZ) have been noted since the beginning of 20th century. However, the molecular mechanisms itself were not identified until the functional characterization of *Sry* gene on the eutherian Y chromosome, almost three decades ago, followed by discovery of many other vertebrate sex determining genes. Generally speaking, in contrast to the binary determination mechanism seen in GSD (presence/absence of heteromorphic sex chromosomes), TSD tends to work in a gradient manner (low to high temperature), meaning screening of sexually dimorphic gene expression alone cannot easily provide clues to elusive sex determining factor.

In the past, several comparative analyses were performed between TSD and GSD organisms, such as mouse, chicken, turtles and alligators. However, the genes in focus were genes found to be crucial in GSD sex determination. This resulted in dependency on GSD model organism for answer to TSD mechanism. When *sry* was first described as master sex determination switch in mammals, reptiles with TSD were immediately theorized to possess thermosensitive *sry* homolog, which later were found to be untrue (Lance, 2009). While comparative analyses are powerful tool, it alone is not enough to study TSD. Furthermore, temperature, in practice, is the measure of particle kinetic energy, and heat radiation. This implies that temperature shift affects the system from the atomic level, rather than specific receptor. In comparison with other

ESD systems, temperature have the ability to influence both specific thermosensors, and non-targets unlike other biotic and physical cues used in ESD such as stress (cortisol level), and photoperiod (photoreceptor) and hence there is greater difficulty in pinpointing the molecular level in which the temperature works during TSD. This is part of reason why so much mechanisms have been theorized, as temperature effects have been observed through DNA bending, RNA stem-loop, protein dimerization, and enzyme efficiency (Sengupta, 2013). Because of temperature's global influence, an alternative method was required.

There is an innate assumption that TSD among reptiles share similar mode of TSD mechanism. In practice, it is necessary to make such assumption, due to relatively limited selection of previous literatures. However, it is becoming increasingly apparent that deep evolutionary division exists among these reptiles; via pattern of gene expression such as timing of *AMH* and *SOX9*, germ cell movement patterns, and pattern of TSD. Current understanding of sex determination indicates that the high diversity is present during the initial activation mechanism, according to researches on GSD organisms. Hence, it should be expected that other reptiles might possess their own unique method of thermosensation, and opens potential for further exotic molecular mechanism of sex determination. Likewise, TRPV4 could not account for all of sex determination in alligator, and another novel element may be present. Therefore, these conclusions only press the further need for more research on TSD. Integration of the classical data with global transcriptomic data, new ideas can be attained. By sharing the RNAseq reads and proposing a novel mechanism of sex determination in alligators, I hope to contribute to the ever-increasing understanding of TSD, and by extension, other ESD systems as well.

## References

- Akerblad P, Månsson R, Lagergren A, Westerlund S, Basta B, Lind U, et al. Gene expression analysis suggests that EBF-1 and PPAR $\gamma$ 2 induce adipogenesis of NIH-3T3 cells with similar efficiency and kinetics. *Physiol Genomics*. 2005;23:206-16.
- Argentaro, A., H. Sim, S. Kelly, S. Preiss, A. Clayton, D. A. Jans and V. R. Harley (2003). "A SOX9 defect of calmodulin-dependent nuclear import in campomelic dysplasia/autosomal sex reversal." *J Biol Chem* 278(36): 33839-33847.
- Austin, H. B. (1989). "Mullerian-Duct Regression in the American Alligator (Alligator-Mississippiensis) - Its Morphology and Testicular Induction." *Journal of Experimental Zoology* 251(3): 329-338.
- Barske, L. A. and B. Capel (2010). "Estrogen represses SOX9 during sex determination in the red-eared slider turtle *Trachemys scripta*." *Dev Biol* 341(1): 305-314.
- Bubolz, A. H., S. A. Mendoza, X. Zheng, N. S. Zinkevich, R. Li, D. D. Gutterman and D. X. Zhang (2012). "Activation of endothelial TRPV4 channels mediates flow-induced dilation in human coronary arterioles: role of Ca<sup>2+</sup> entry and mitochondrial ROS signaling." *Am J Physiol Heart Circ Physiol* 302(3): H634-642.
- Bull, J. J. (1980). "Sex Determination in Reptiles." *Quarterly Review of Biology* 55(1): 3-21.
- Bull, J. J. (1985). "Sex determining mechanisms: an evolutionary perspective." *Experientia* 41(10): 1285-1296.
- Chan, S. H., C. A. Wu, K. L. Wu, Y. H. Ho, A. Y. Chang and J. Y. Chan (2009). "Transcriptional upregulation of mitochondrial uncoupling protein 2 protects against oxidative stress-associated neurogenic hypertension." *Circ Res* 105(9): 886-896.
- Charnier, M. (1966). "[Action of temperature on the sex ratio in the *Agama agama* (Agamidae, Lacertilia) embryo]." *C R Seances Soc Biol Fil* 160(3): 620-622.
- Cheng, W., C. Sun and J. Zheng (2010). "Heteromerization of TRP channel subunits: extending functional diversity." *Protein Cell* 1(9): 802-810.
- Cho, H., Y. D. Yang, J. Lee, B. Lee, T. Kim, Y. Jang, S. K. Back, H. S. Na, B. D. Harfe, F. Wang, R. Raouf, J. N. Wood and U. Oh (2012). "The calcium-activated chloride channel anoctamin 1 acts as a heat sensor in nociceptive neurons." *Nat Neurosci* 15(7): 1015-1021.
- Clark, A. L., B. J. Votta, S. Kumar, W. Liedtke and F. Guilak (2010). "Chondroprotective role of the osmotically sensitive ion channel transient receptor potential vanilloid 4: age- and sex-dependent progression of osteoarthritis in *Trpv4*-deficient mice." *Arthritis Rheum* 62(10): 2973-2983.
- Cohen, R. D., C. L. Brown, C. Nickols, P. Levey, B. J. Boucher, S. E. Greenwald and W. Wang (2011). "Inbuilt mechanisms for overcoming functional problems inherent in hepatic microlobular structure." *Comput Math Methods Med* 2011: 185845.
- Conesa, A., S. Gotz, J. M. Garcia-Gomez, J. Terol, M. Talon and M. Robles (2005). "Blast2GO: a universal tool for annotation, visualization and analysis in functional genomics research." *Bioinformatics* 21(18): 3674-3676.
- Crews, D. (1994). "Temperature, steroids and sex determination." *J Endocrinol* 142(1): 1-8.

- Cruze, L., S. Kohno, M. W. McCoy and L. J. Guillette, Jr. (2012). "Towards an understanding of the evolution of the chorioallantoic placenta: steroid biosynthesis and steroid hormone signaling in the chorioallantoic membrane of an oviparous reptile." *Biol Reprod* 87(3): 71.
- Deeming, D. C. (2004). *Prevalence of TSD in crocodylians. Temperature-dependent sex determination in vertebrates.* N. Valenzuela and V. Lance. Washington, D.C., Smithsonian Books.
- Deeming, D. C. and M. W. J. Ferguson (1989). "Effects of incubation temperature on growth and development of embryos of *Alligator mississippiensis*." *Journal of Comparative Physiology B* 159(2): 183-193.
- Di-Poï, N. and M. C. Milinkovitch (2013). "Crocodylians evolved scattered multi-sensory micro-organs." *Evodevo* 4(1): 19.
- Ewen, K., A. Jackson, D. Wilhelm and P. Koopman (2010). "A male-specific role for p38 mitogen-activated protein kinase in germ cell sex differentiation in mice." *Biol Reprod* 83(6): 1005-1014.
- Ferguson, M. W. and T. Joanen (1982). "Temperature of egg incubation determines sex in *Alligator mississippiensis*." *Nature* 296(5860): 850-853.
- Ferguson, M. W. J. (1985). *The reproductive biology and embryology of crocodylians. Biology of the Reptilia.* 14. Development A. C. Gans, F. Billet and P. F. A. Maderson. New York, John Wiley and Sons.
- Ferguson, M. W. J. and T. Joanen (1983). "Temperature-Dependent Sex Determination in *Alligator-Mississippiensis*." *Journal of Zoology* 200(Jun): 143-177.
- Gallardo, T. D., G. B. John, L. Shirley, C. M. Contreras, E. A. Akbay, J. M. Haynie, S. E. Ward, M. J. Shidler and D. H. Castrillon (2007). "Genomewide discovery and classification of candidate ovarian fertility genes in the mouse." *Genetics* 177(1): 179-194.
- Garcia-Elias, A., S. Mrkonjic, C. Pardo-Pastor, H. Inada, U. A. Hellmich, F. Rubio-Moscardo, C. Plata, R. Gaudet, R. Vicente and M. A. Valverde (2013). "Phosphatidylinositol-4,5-biphosphate-dependent rearrangement of TRPV4 cytosolic tails enables channel activation by physiological stimuli." *Proc Natl Acad Sci U S A* 110(23): 9553-9558.
- Gees, M., G. Owsianik, B. Nilius and T. Voets (2012). "TRP channels." *Compr Physiol* 2(1): 563-608.
- Green, R. E., E. L. Braun, J. Armstrong, D. Earl, N. Nguyen, G. Hickey, M. W. Vandewege, J. A. St John, S. Capella-Gutierrez, T. A. Castoe, C. Kern, M. K. Fujita, J. C. Opazo, J. Jurka, K. K. Kojima, J. Caballero, R. M. Hubley, A. F. Smit, R. N. Platt, C. A. Lavoie, M. P. Ramakodi, J. W. Finger, Jr., A. Suh, S. R. Isberg, L. Miles, A. Y. Chong, W. Jaratlerdsiri, J. Gongora, C. Moran, A. Iriarte, J. McCormack, S. C. Burgess, S. V. Edwards, E. Lyons, C. Williams, M. Breen, J. T. Howard, C. R. Gresham, D. G. Peterson, J. Schmitz, D. D. Pollock, D. Haussler, E. W. Triplett, G. Zhang, N. Irie, E. D. Jarvis, C. A. Brochu, C. J. Schmidt, F. M. McCarthy, B. C. Faircloth, F. G. Hoffmann, T. C. Glenn, T. Gabaldon, B. Paten and D. A. Ray (2014). "Three crocodylian genomes reveal ancestral patterns of evolution among archosaurs." *Science* 346(6215): 1254449.
- Guler, A. D., H. Lee, T. Iida, I. Shimizu, M. Tominaga and M. Caterina (2002). "Heat-evoked activation of the ion channel, TRPV4." *J Neurosci* 22(15): 6408-6414.

- Hanover, J. A., D. C. Love and W. A. Prinz (2009). "Calmodulin-driven nuclear entry: trigger for sex determination and terminal differentiation." *J Biol Chem* 284(19): 12593-12597.
- Harwood BN, Cross SK, Radford EE, Haac BE, De Vries WN. Members of the WNT signaling pathways are widely expressed in mouse ovaries, oocytes, and cleavage stage embryos. *Dev Dyn*. 2008;237;1099-111.
- Hayashi, Y., H. Kobira, T. Yamaguchi, E. Shiraishi, T. Yazawa, T. Hirai, Y. Kamei and T. Kitano (2010). "High temperature causes masculinization of genetically female medaka by elevation of cortisol." *Mol Reprod Dev* 77(8): 679-686.
- Heller, S. and R. G. O'Neil (2007). "Molecular mechanisms of TRPV4 gating." *Molecular mechanisms of TRPV4 gating*.
- Heller, S. and R. G. O'Neil (2007). *Molecular mechanisms of TRPV4 Gating. TRP ion channel function in sensory transduction and cellular signaling cascades*. W. B. Liedtke and S. Heller. Boca Raton, FL, CRC/Taylor & Francis: 467 p.
- Hernandez-Novoa, B., L. Bishop, C. Logun, P. J. Munson, E. Elnekave, Z. G. Rangel, J. Barb, R. L. Danner and J. A. Kovacs (2008). "Immune responses to *Pneumocystis murina* are robust in healthy mice but largely absent in CD40 ligand-deficient mice." *J Leukoc Biol* 84(2): 420-430.
- Homma, Y., A. Nomiya, M. Tagaya, T. Oyama, K. Takagaki, H. Nishimatsu and Y. Igawa (2013). "Increased mRNA expression of genes involved in pronociceptive inflammatory reactions in bladder tissue of interstitial cystitis." *J Urol* 190(5): 1925-1931.
- Jacobs JP, Ortiz-Lopez A, Campbell JJ, Gerard CJ, Mathis D, Benoist C. Deficiency of CXCR2, but not other chemokine receptors, attenuates a murine model of autoantibody-mediated arthritis. *Arthritis Rheum*. 2010;62:1921–1932.
- Katoh-Fukui, Y., R. Tsuchiya, T. Shiroishi, Y. Nakahara, N. Hashimoto, K. Noguchi and T. Higashinakagawa (1998). "Male-to-female sex reversal in M33 mutant mice." *Nature* 393(6686): 688-692.
- Kitamura, K., M. Yanazawa, N. Sugiyama, H. Miura, A. Iizuka-Kogo, M. Kusaka, K. Omichi, R. Suzuki, Y. Kato-Fukui, K. Kamiirisa, M. Matsuo, S. Kamijo, M. Kasahara, H. Yoshioka, T. Ogata, T. Fukuda, I. Kondo, M. Kato, W. B. Dobyns, M. Yokoyama and K. Morohashi (2002). "Mutation of ARX causes abnormal development of forebrain and testes in mice and X-linked lissencephaly with abnormal genitalia in humans." *Nat Genet* 32(3): 359-369.
- Kohno, S. and L. Guillette, Jr. (2013). *Endocrine disruption and reptiles: Using the unique attributes of temperature-dependent sex determination to assess impacts. Endocrine disruptors: Hazard testing and assessment methods*. M. P. Hoboken, N.J., John Wiley & Sons: 245-271.
- Kohno, S., Y. Katsu, H. Urushitani, Y. Ohta, T. Iguchi and L. J. Guillette, Jr. (2010). "Potential contributions of heat shock proteins to temperature-dependent sex determination in the American alligator." *Sex Dev* 4(1-2): 73-87.
- Kohno, S., B. B. Parrott, R. Yatsu, S. Miyagawa, B. C. Moore, T. Iguchi and L. Guillette, Jr. (2014). "Gonadal differentiation in reptiles exhibiting environmental sex determination." *Sex Dev* 8(5): 208-226.
- Kuroki, S., S. Matoba, M. Akiyoshi, Y. Matsumura, H. Miyachi, N. Mise, K. Abe, A. Ogura, D. Wilhelm, P. Koopman, M. Nozaki, Y. Kanai, Y. Shinkai and M.

- Tachibana (2013). "Epigenetic regulation of mouse sex determination by the histone demethylase Jmjd1a." *Science* 341(6150): 1106-1109.
- Lance, V. A. (2009). "Is regulation of aromatase expression in reptiles the key to understanding temperature-dependent sex determination?" *J Exp Zool A Ecol Genet Physiol* 311(5): 314-322.
- Lang, J. W. and H. V. Andrews (1994). "Temperature-Dependent Sex Determination in Crocodylians." *Journal of Experimental Zoology* 270(1): 28-44.
- Lattin, J. E., K. Schroder, A. I. Su, J. R. Walker, J. Zhang, T. Wiltshire, K. Saijo, C. K. Glass, D. A. Hume, S. Kellie and M. J. Sweet (2008). "Expression analysis of G Protein-Coupled Receptors in mouse macrophages." *Immunome Res* 4: 5.
- Li, H., B. Handsaker, A. Wysoker, T. Fennell, J. Ruan, N. Homer, G. Marth, G. Abecasis, R. Durbin and S. Genome Project Data Processing (2009). "The Sequence Alignment/Map format and SAMtools." *Bioinformatics* 25(16): 2078-2079.
- Liedtke, W., Y. Choe, M. A. Marti-Renom, A. M. Bell, C. S. Denis, A. Sali, A. J. Hudspeth, J. M. Friedman and S. Heller (2000). "Vanilloid receptor-related osmotically activated channel (VR-OAC), a candidate vertebrate osmoreceptor." *Cell* 103(3): 525-535.
- Masuyama, R., J. Vriens, T. Voets, Y. Karashima, G. Owsianik, R. Vennekens, L. Lieben, S. Torrekens, K. Moermans, A. Vanden Bosch, R. Bouillon, B. Nilius and G. Carmeliet (2008). "TRPV4-mediated calcium influx regulates terminal differentiation of osteoclasts." *Cell Metab* 8(3): 257-265.
- Matsumoto, Y., A. Buemio, R. Chu, M. Vafae and D. Crews (2013). "Epigenetic control of gonadal aromatase (cyp19a1) in temperature-dependent sex determination of red-eared slider turtles." *PLoS One* 8(6): e63599.
- Matsumoto, Y., B. Hannigan and D. Crews (2014). "Embryonic PCB exposure alters phenotypic, genetic, and epigenetic profiles in turtle sex determination, a biomarker of environmental contamination." *Endocrinology* 155(11): 4168-4177.
- McCoy, J. A., B. B. Parrott, T. R. Rainwater, P. M. Wilkinson and L. J. Guillette, Jr. (2015). "Incubation history prior to the canonical thermosensitive period determines sex in the American alligator." *Reproduction* 150(4): 279-287.
- Milnes, M. R., D. S. Bermudez, T. A. Bryan, M. P. Gunderson and L. J. Guillette, Jr. (2005). "Altered neonatal development and endocrine function in Alligator mississippiensis associated with a contaminated environment." *Biol Reprod* 73(5): 1004-1010.
- Mochizuki, T., T. Sokabe, I. Araki, K. Fujishita, K. Shibasaki, K. Uchida, K. Naruse, S. Koizumi, M. Takeda and M. Tominaga (2009). "The TRPV4 cation channel mediates stretch-evoked Ca<sup>2+</sup> influx and ATP release in primary urothelial cell cultures." *J Biol Chem* 284(32): 21257-21264.
- Moggs, J. G., H. Tinwell, T. Spurway, H. S. Chang, I. Pate, F. L. Lim, D. J. Moore, A. Soames, R. Stuckey, R. Currie, T. Zhu, I. Kimber, J. Ashby and G. Orphanides (2004). "Phenotypic anchoring of gene expression changes during estrogen-induced uterine growth." *Environ Health Perspect* 112(16): 1589-1606.
- Moore, B. C., M. C. Uribe-Aranzábal, A. S. Boggs and L. J. Guillette, Jr. (2008). "Developmental morphology of the neonatal alligator (*Alligator mississippiensis*) ovary." *J Morphol* 269(3): 302-312.



- Moreno-Mendoza, N., V. R. Harley and H. Merchant-Larios (2001). "Temperature regulates SOX9 expression in cultured gonads of *Lepidochelys olivacea*, a species with temperature sex determination." *Dev Biol* 229(2): 319-326.
- Morrish, B. C. and A. H. Sinclair (2002). "Vertebrate sex determination: many means to an end." *Reproduction* 124(4): 447-457.
- Muramatsu, S., M. Wakabayashi, T. Ohno, K. Amano, R. Ooishi, T. Sugahara, S. Shiojiri, K. Tashiro, Y. Suzuki, R. Nishimura, S. Kuhara, S. Sugano, T. Yoneda and A. Matsuda (2007). "Functional gene screening system identified TRPV4 as a regulator of chondrogenic differentiation." *J Biol Chem* 282(44): 32158-32167.
- Nagai, K., Y. Saitoh, S. Saito and K. Tsutsumi (2012). "Structure and hibernation-associated expression of the transient receptor potential vanilloid 4 channel (TRPV4) mRNA in the Japanese grass lizard (*Takydromus tachydromoides*)." *Zoolog Sci* 29(3): 185-190.
- Nakamura, M. (2010). "The mechanism of sex determination in vertebrates-are sex steroids the key-factor?" *J Exp Zool A Ecol Genet Physiol* 313(7): 381-398.
- Nakata, T., M. Ishiguro, N. Aduma, H. Izumi and A. Kuroiwa (2013). "Chicken hemogen homolog is involved in the chicken-specific sex-determining mechanism." *Proc Natl Acad Sci U S A* 110(9): 3417-3422.
- Navarro-Martin, L., J. Vinas, L. Ribas, N. Diaz, A. Gutierrez, L. Di Croce and F. Piferrer (2011). "DNA methylation of the gonadal aromatase (*cyp19a*) promoter is involved in temperature-dependent sex ratio shifts in the European sea bass." *PLoS Genet* 7(12): e1002447.
- Nilius, B. and T. Voets (2013). "The puzzle of TRPV4 channelopathies." *EMBO Rep* 14(2): 152-163.
- Ovrevik, J., M. Refsnes, M. Lag, J. A. Holme and P. E. Schwarze (2015). "Activation of Proinflammatory Responses in Cells of the Airway Mucosa by Particulate Matter: Oxidant- and Non-Oxidant-Mediated Triggering Mechanisms." *Biomolecules* 5(3): 1399-1440.
- Parrott, B. B., S. Kohno, J. A. Cloy-McCoy and L. J. Guillette, Jr. (2014). "Differential incubation temperatures result in dimorphic DNA methylation patterning of the SOX9 and aromatase promoters in gonads of alligator (*Alligator mississippiensis*) embryos." *Biol Reprod* 90(1): 2.
- Piferrer, F. (2013). "Epigenetics of sex determination and gonadogenesis." *Dev Dyn* 242(4): 360-370.
- Quinn, A. E., A. Georges, S. D. Sarre, F. Guarino, T. Ezaz and J. A. Graves (2007). "Temperature sex reversal implies sex gene dosage in a reptile." *Science* 316(5823): 411.
- Rahaman, S. O., L. M. Grove, S. Paruchuri, B. D. Southern, S. Abraham, K. A. Niese, R. G. Scheraga, S. Ghosh, C. K. Thodeti, D. X. Zhang, M. M. Moran, W. P. Schilling, D. J. Tschumperlin and M. A. Olman (2014). "TRPV4 mediates myofibroblast differentiation and pulmonary fibrosis in mice." *J Clin Invest* 124(12): 5225-5238.
- Rhen, T. and A. Schroeder (2010). "Molecular mechanisms of sex determination in reptiles." *Sex Dev* 4(1-2): 16-28.
- Rzhetsky, A. and M. Nei (1993). "Theoretical foundation of the minimum-evolution method of phylogenetic inference." *Mol Biol Evol* 10(5): 1073-1095.

- Saito, S., N. Banzawa, N. Fukuta, C. T. Saito, K. Takahashi, T. Imagawa, T. Ohta and M. Tominaga (2014). "Heat and noxious chemical sensor, chicken TRPA1, as a target of bird repellents and identification of its structural determinants by multispecies functional comparison." *Mol Biol Evol* 31(3): 708-722.
- Saito, S., K. Nakatsuka, K. Takahashi, N. Fukuta, T. Imagawa, T. Ohta and M. Tominaga (2012). "Analysis of transient receptor potential ankyrin 1 (TRPA1) in frogs and lizards illuminates both nociceptive heat and chemical sensitivities and coexpression with TRP vanilloid 1 (TRPV1) in ancestral vertebrates." *J Biol Chem* 287(36): 30743-30754.
- Saito, S. and M. Tominaga (2014). "Functional diversity and evolutionary dynamics of thermoTRP channels." *Cell Calcium*.
- Saxe, J. P., M. Chen, H. Zhao and H. Lin (2013). "Tdrkh is essential for spermatogenesis and participates in primary piRNA biogenesis in the germline." *EMBO J* 32(13): 1869-1885.
- Schreiner, C. M., S. M. Bell and W. J. Scott, Jr. (2009). "Microarray analysis of murine limb bud ectoderm and mesoderm after exposure to cadmium or acetazolamide." *Birth Defects Res A Clin Mol Teratol* 85(7): 588-598.
- Schulze S, Henkel SG, Driesch D, Guthke R, Linde J. Computational prediction of molecular pathogen-host interactions based on dual transcriptome data. *Front Microbiol.* 2015;6:65.
- Sengupta, P. and P. Garrity (2013). "Sensing temperature." *Curr Biol* 23(8): R304-307.
- Shaffer, H. B., P. Minx, D. E. Warren, A. M. Shedlock, R. C. Thomson, N. Valenzuela, J. Abramyan, C. T. Amemiya, D. Badenhorst, K. K. Biggar, G. M. Borchert, C. W. Botka, R. M. Bowden, E. L. Braun, A. M. Bronikowski, B. G. Bruneau, L. T. Buck, B. Capel, T. A. Castoe, M. Czerwinski, K. D. Delehaunty, S. V. Edwards, C. C. Fronick, M. K. Fujita, L. Fulton, T. A. Graves, R. E. Green, W. Haerty, R. Hariharan, O. Hernandez, L. W. Hillier, A. K. Holloway, D. Janes, F. J. Janzen, C. Kandoth, L. Kong, A. P. de Koning, Y. Li, R. Litterman, S. E. McGaugh, L. Mork, M. O'Laughlin, R. T. Paitz, D. D. Pollock, C. P. Ponting, S. Radhakrishnan, B. J. Raney, J. M. Richman, J. St John, T. Schwartz, A. Sethuraman, P. Q. Spinks, K. B. Storey, N. Thane, T. Vinar, L. M. Zimmerman, W. C. Warren, E. R. Mardis and R. K. Wilson (2013). "The western painted turtle genome, a model for the evolution of extreme physiological adaptations in a slowly evolving lineage." *Genome Biol* 14(3): R28.
- Shoemaker, C. M. and D. Crews (2009). "Analyzing the coordinated gene network underlying temperature-dependent sex determination in reptiles." *Semin Cell Dev Biol* 20(3): 293-303.
- Shoemaker-Daly, C. M., K. Jackson, R. Yatsu, Y. Matsumoto and D. Crews (2010). "Genetic network underlying temperature-dependent sex determination is endogenously regulated by temperature in isolated cultured *Trachemys scripta* gonads." *Dev Dyn* 239(4): 1061-1075.
- Sinclair, A., C. Smith and P. Western (2002). "A comparative analysis of vertebrate sex determination." *Novartis Foundation* ....
- Smith, C. A. and J. M. P. Joss (1993). "Gonadal Sex-Differentiation in Alligator-Mississippiensis, a Species with Temperature-Dependent Sex Determination." *Cell and Tissue Research* 273(1): 149-162.

- Smith, C. A., C. M. Shoemaker, K. N. Roeszler, J. Queen, D. Crews and A. H. Sinclair (2008). "Cloning and expression of R-Spondin1 in different vertebrates suggests a conserved role in ovarian development." *BMC Dev Biol* 8: 72.
- Smith, S., L. Bernatchez and L. B. Beheregaray (2013). "RNA-seq analysis reveals extensive transcriptional plasticity to temperature stress in a freshwater fish species." *BMC Genomics* 14: 375.
- Sokabe, T., T. Fukumi-Tominaga, S. Yonemura, A. Mizuno and M. Tominaga (2010). "The TRPV4 channel contributes to intercellular junction formation in keratinocytes." *J Biol Chem* 285(24): 18749-18758.
- St John, J. A., E. L. Braun, S. R. Isberg, L. G. Miles, A. Y. Chong, J. Gongora, P. Dalzell, C. Moran, B. Bed'hom, A. Abzhanov, S. C. Burgess, A. M. Cooksey, T. A. Castoe, N. G. Crawford, L. D. Densmore, J. C. Drew, S. V. Edwards, B. C. Faircloth, M. K. Fujita, M. J. Greenwold, F. G. Hoffmann, J. M. Howard, T. Iguchi, D. E. Janes, S. Y. Khan, S. Kohno, A. J. de Koning, S. L. Lance, F. M. McCarthy, J. E. McCormack, M. E. Merchant, D. G. Peterson, D. D. Pollock, N. Pourmand, B. J. Raney, K. A. Roessler, J. R. Sanford, R. H. Sawyer, C. J. Schmidt, E. W. Triplett, T. D. Tuberville, M. Venegas-Anaya, J. T. Howard, E. D. Jarvis, L. J. Guillette, Jr., T. C. Glenn, R. E. Green and D. A. Ray (2012). "Sequencing three crocodylian genomes to illuminate the evolution of archosaurs and amniotes." *Genome Biol* 13(1): 415.
- Sun, F., S. Liu, X. Gao, Y. Jiang, D. Perera, X. Wang, C. Li, L. Sun, J. Zhang, L. Kaltenboeck, R. Dunham and Z. Liu (2013). "Male-biased genes in catfish as revealed by RNA-Seq analysis of the testis transcriptome." *PLoS One* 8(7): e68452.
- Tamura, K., D. Peterson, N. Peterson, G. Stecher, M. Nei and S. Kumar (2011). "MEGA5: molecular evolutionary genetics analysis using maximum likelihood, evolutionary distance, and maximum parsimony methods." *Mol Biol Evol* 28(10): 2731-2739.
- Teranishi, M., Y. Shimada, T. Hori, O. Nakabayashi, T. Kikuchi, T. Macleod, R. Pym, B. Sheldon, I. Solovei, H. Macgregor and S. Mizuno (2001). "Transcripts of the MHM region on the chicken Z chromosome accumulate as non-coding RNA in the nucleus of female cells adjacent to the DMRT1 locus." *Chromosome Res* 9(2): 147-165.
- Thompson, J. D., D. G. Higgins and T. J. Gibson (1994). "CLUSTAL W: improving the sensitivity of progressive multiple sequence alignment through sequence weighting, position-specific gap penalties and weight matrix choice." *Nucleic Acids Res* 22(22): 4673-4680.
- Thorneloe, K. S., A. C. Sulpizio, Z. Lin, D. J. Figueroa, A. K. Clouse, G. P. McCafferty, T. P. Chendrimada, E. S. Lashinger, E. Gordon, L. Evans, B. A. Misajet, D. J. Demarini, J. H. Nation, L. N. Casillas, R. W. Marquis, B. J. Votta, S. A. Sheardown, X. Xu, D. P. Brooks, N. J. Laping and T. D. Westfall (2008). "N-((1S)-1-{{[4-((2S)-2-{{[(2,4-dichlorophenyl)sulfonyl]amino}}-3-hydroxypropanoyl)-1-piperazinyl]carbonyl}}-3-methylbutyl)-1-benzothiophene-2-carboxamide (GSK1016790A), a novel and potent transient receptor potential vanilloid 4 channel agonist induces urinary bladder contraction and hyperactivity: Part I." *J Pharmacol Exp Ther* 326(2): 432-442.

- Thorrez, L., K. Van Deun, L. C. Tranchevent, L. Van Lommel, K. Engelen, K. Marchal, Y. Moreau, I. Van Mechelen and F. Schuit (2008). "Using ribosomal protein genes as reference: a tale of caution." *PLoS One* 3(3): e1854.
- Trapnell, C., L. Pachter and S. L. Salzberg (2009). "TopHat: discovering splice junctions with RNA-Seq." *Bioinformatics* 25(9): 1105-1111.
- Trapnell, C., A. Roberts, L. Goff, G. Pertea, D. Kim, D. R. Kelley, H. Pimentel, S. L. Salzberg, J. L. Rinn and L. Pachter (2012). "Differential gene and transcript expression analysis of RNA-seq experiments with TopHat and Cufflinks." *Nat Protoc* 7(3): 562-578.
- Trapnell, C., B. A. Williams, G. Pertea, A. Mortazavi, G. Kwan, M. J. van Baren, S. L. Salzberg, B. J. Wold and L. Pachter (2010). "Transcript assembly and quantification by RNA-Seq reveals unannotated transcripts and isoform switching during cell differentiation." *Nat Biotechnol* 28(5): 511-515.
- Urushitani, H., Y. Katsu, S. Miyagawa, S. Kohno, Y. Ohta, L. J. Guillette, Jr. and T. Iguchi (2011). "Molecular cloning of anti-Müllerian hormone from the American alligator, *Alligator mississippiensis*." *Mol Cell Endocrinol* 333(2): 190-199.
- Valenzuela, N., J. L. Neuwald and R. Literman (2013). "Transcriptional evolution underlying vertebrate sexual development." *Dev Dyn* 242(4): 307-319.
- van der Eerden, B. C., L. Oei, P. Roschger, N. Fratzl-Zelman, J. G. Hoenderop, N. M. van Schoor, U. Pettersson-Kymmer, M. Schreuders-Koedam, A. G. Uitterlinden, A. Hofman, M. Suzuki, K. Klaushofer, C. Ohlsson, P. J. Lips, F. Rivadeneira, R. J. Bindels and J. P. van Leeuwen (2013). "TRPV4 deficiency causes sexual dimorphism in bone metabolism and osteoporotic fracture risk." *Bone* 57(2): 443-454.
- Vay, L., C. Gu and P. A. McNaughton (2012). "The thermo-TRP ion channel family: properties and therapeutic implications." *Br J Pharmacol* 165(4): 787-801.
- Vincent, F. and M. A. Duncton (2011). "TRPV4 agonists and antagonists." *Curr Top Med Chem* 11(17): 2216-2226.
- Wan, Q. H., S. K. Pan, L. Hu, Y. Zhu, P. W. Xu, J. Q. Xia, H. Chen, G. Y. He, J. He, X. W. Ni, H. L. Hou, S. G. Liao, H. Q. Yang, Y. Chen, S. K. Gao, Y. F. Ge, C. C. Cao, P. F. Li, L. M. Fang, L. Liao, S. Zhang, M. Z. Wang, W. Dong and S. G. Fang (2013). "Genome analysis and signature discovery for diving and sensory properties of the endangered Chinese alligator." *Cell Res* 23(9): 1091-1105.
- Wang, Z., J. Pascual-Anaya, A. Zadissa, W. Li, Y. Niimura, Z. Huang, C. Li, S. White, Z. Xiong, D. Fang, B. Wang, Y. Ming, Y. Chen, Y. Zheng, S. Kuraku, M. Pignatelli, J. Herrero, K. Beal, M. Nozawa, Q. Li, J. Wang, H. Zhang, L. Yu, S. Shigenobu, J. Wang, J. Liu, P. Flicek, S. Searle, J. Wang, S. Kuratani, Y. Yin, B. Aken, G. Zhang and N. Irie (2013). "The draft genomes of soft-shell turtle and green sea turtle yield insights into the development and evolution of the turtle-specific body plan." *Nat Genet* 45(6): 701-706.
- Warner, D. A., R. S. Radder and R. Shine (2009). "Corticosterone exposure during embryonic development affects offspring growth and sex ratios in opposing directions in two lizard species with environmental sex determination." *Physiol Biochem Zool* 82(4): 363-371.
- Weber, M., S. G. Henkel, S. Vlačić, R. Guthke, E. J. van Zoelen and D. Driesch (2013). "Inference of dynamical gene-regulatory networks based on time-resolved

- multi-stimuli multi-experiment data applying NetGenerator V2.0." *BMC Syst Biol* 7: 1.
- Western, P. S., J. L. Harry, J. A. Graves and A. H. Sinclair (1999).  
"Temperature-dependent sex determination in the American alligator: AMH precedes SOX9 expression." *Dev Dyn* 216(4-5): 411-419.
- Western, P. S., J. L. Harry, J. A. Marshall Graves and A. H. Sinclair (2000).  
"Temperature-dependent sex determination in the American alligator: expression of SF1, WT1 and DAX1 during gonadogenesis." *Gene* 241(2): 223-232.
- Yamaguchi, T. and T. Kitano (2012). "High temperature induces cyp26b1 mRNA expression and delays meiotic initiation of germ cells by increasing cortisol levels during gonadal sex differentiation in Japanese flounder." *Biochem Biophys Res Commun* 419(2): 287-292.
- Yao, H. H. and B. Capel (2005). "Temperature, genes, and sex: a comparative view of sex determination in *Trachemys scripta* and *Mus musculus*." *J Biochem* 138(1): 5-12.
- Yatsu, R., S. Miyagawa, S. Kohno, S. Saito, R. H. Lowers, Y. Ogino, N. Fukuta, Y. Katsu, Y. Ohta, M. Tominaga, L. J. Guillette, Jr. and T. Iguchi (2015). "TRPV4 associates environmental temperature and sex determination in the American alligator." *Sci Rep* 5: 18581.
- Zapala MA, Hovatta I, Ellison JA, Wodicka L, Del Rio JA, Tennant R, et al. Adult mouse brain gene expression patterns bear an embryologic imprint. *Proc Natl Acad Sci USA*. 2005;102:10357–10362.

## **Acknowledgments**

I am especially grateful to my supervisor Professor Iguchi Taisen of SOKENDAI (Graduate University for Advanced Studies) and Okazaki Institute for Integrative Bioscience for all the mentoring and academic advices. I am grateful to my supervisors Assistant professors Dr. Shinichi Miyagawa and Dr. Yukiko Ogino for direct supervisions and all their help. I am grateful to Professor Makoto Tominaga and Assistant professor Shigeru Saito for the help with patch clamp studies, and kind support. I would like to thank the members of Iguchi laboratory, Professor Yoshinao Katsu, Professor Ohta for all their advice and help. I would like to thank late Professor Louis J. Guillette Jr. for this collaboration, and his kind support, as this research would not have been possible without him. I would like to thank Dr. Satomi Kohno, Dr. Benjamin B. Parrott, Mr. Russell H. Lowers, and members of Dr. Guillette laboratory for all advices and help with alligator embryo experiments. I would like to thank my family members for all their support. Finally, I would like to thank Dr. David Crews and members of Crews laboratory for inviting me to field of TSD research and recommending me to Dr. Iguchi.